

Supplementary Information

***In silico* derived small molecules bind the filovirus VP35 protein and inhibit its polymerase co-factor activity**

Craig S. Brown^{a,b,j,1}, Michael S. Lee^{c,d,1}, Daisy W. Leung^{a,1}, Tianjiao Wang^b, Wei Xu^a, Priya Luthra^e, Manu Anantpadma^f, Reed S. Shabman^e, Lisa M. Melito^g, Karen S. MacMillan^g, Dominika M. Borek^{g,h,i}, Zbyszek Otwinowski^{g,h,i}, Parameshwaran Ramanan^{a,k}, Alisha J. Stubbs^{b,j}, Dayna S. Peterson^{b,j}, Jennifer M. Binning^{a,k}, Marco Tonelli^l, Mark A. Olson^d, Rob Davey^f, Joseph M. Ready^g, Christopher F. Basler^e, and Gaya K. Amarasinghe^{a*}

^aDepartment of Pathology and Immunology, Washington University School of Medicine, St Louis, MO 63110; ^b Roy J. Carver Department of Biochemistry, Biophysics and Molecular Biology, Iowa State University, Ames, IA 50011; ^cComputational Sciences and Engineering Branch, US Army Research Laboratory, Aberdeen, MD 21005; ^dIntegrated Toxicology Division, USAMRIID, 1425 Porter St., Ft. Detrick, MD 21702; ^eDepartment of Microbiology, Icahn School of Medicine at Mount Sinai, New York, NY 10029; ^f Department of Virology and Immunology, Texas Biomedical Research Institute, San Antonio, Texas, 78227; ^gDepartment of Biochemistry & ^hDepartment of Biophysics, UT Southwestern Medical Center at Dallas, Dallas, TX 75390; ⁱCenter for Structural Genomics of Infectious Diseases (CSGID), Chicago, Illinois; ^jBiochemistry Undergraduate Program, Iowa State University, Ames, IA 50011; ^kBiochemistry Graduate Program, Iowa State University, Ames, IA 50011; ^lNational Magnetic Resonance Facility at Madison, University of Wisconsin, Madison, 433 Babcock Drive, Madison, WI 53706 USA.

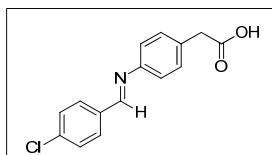
¹These authors made equal contributions.

Supplementary Methods

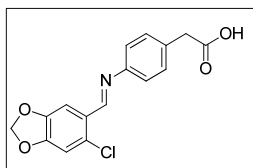
Synthesis of Ligands for VP35

1. General Procedure for Imine synthesis:

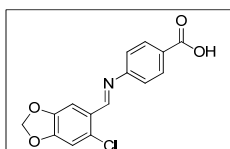
The aldehyde (1 eq.) and aniline (1 eq.) were dissolved in ethanol and stirred at room temperature. When the reaction was complete (0.5-1 h), the mixture was filtered and rinsed with cold ethanol to afford the desired imine.



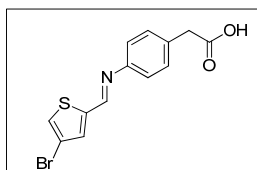
Imine 1: ^1H NMR (500 MHz, CDCl_3) δ 8.42 (s, 1H), 7.84 (d, $J = 8.4$ Hz, 2H), 7.45 (d, $J = 8.4$ Hz, 2H), 7.32 (d, $J = 8.2$ Hz, 2H), 7.19 (d, $J = 8.3$ Hz, 2H), 3.69 (s, 2H).



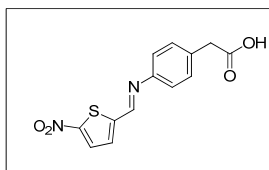
Imine 2: ^1H NMR (500 MHz, CDCl_3) δ 8.79 (s, 1H), 7.70 (s, 1H), 7.31 (d, $J = 7.7$ Hz, 2H), 7.18 (d, $J = 7.6$ Hz, 2H), 6.87 (s, 1H), 6.05 (s, 2H), 3.65 (s, 2H).



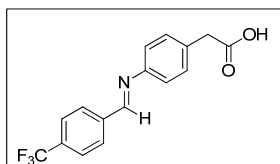
Imine 3 (LM-133-107): ^1H NMR (500 MHz, $\text{DMSO-}d_6$) δ 12.91 (s, 1H), 8.74 (d, $J = 2.3$ Hz, 1H), 7.98 (dd, $J = 8.3, 2.0$ Hz, 2H), 7.59 (d, $J = 2.3$ Hz, 1H), 7.31 (dd, $J = 8.3, 1.9$ Hz, 2H), 7.27 (d, $J = 2.4$ Hz, 1H), 6.20 (s, 2H).



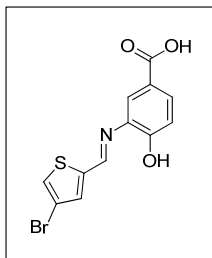
Imine 4: ^1H NMR (500 MHz, CDCl_3) δ 8.49 (s, 1H), 7.38 (d, $J = 5.8$ Hz, 1H), 7.31 (d, $J = 8.1$ Hz, 2H), 7.19 (d, $J = 8.2$ Hz, 2H), 3.68 (s, 2H).



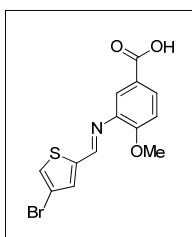
Imine 5: ^1H NMR (500 MHz, CDCl_3) δ 8.54 (s, 1H), 7.92 (d, $J = 4.2$ Hz, 1H), 7.37 (d, $J = 4.2$ Hz, 1H), 7.35 (d, $J = 8.2$ Hz, 2H), 7.25 (d, $J = 8.2$ Hz, 2H), 3.70 (s, 2H).



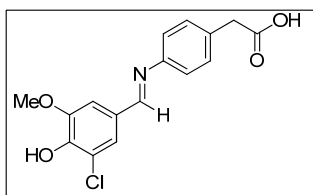
Imine 6: ^1H NMR (500 MHz, CDCl_3) δ 8.50 (s, 1H), 8.01 (d, $J = 7.7$ Hz, 2H), 7.73 (d, $J = 7.7$ Hz, 2H), 7.34 (d, $J = 7.3$ Hz, 2H), 7.22 (d, $J = 7.2$ Hz, 2H), 3.70 (s, 2H).



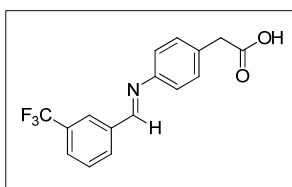
Imine 7: ^1H NMR (400 MHz, $\text{DMSO}-d_6$) δ 12.60 (s, 1H), 10.13 (s, 1H), 8.86 (s, 1H), 7.94 (s, 1H), 7.75 (d, $J = 1.2$ Hz, 1H), 7.71 – 7.64 (m, 2H), 6.97 (d, $J = 8.0$ Hz, 1H).



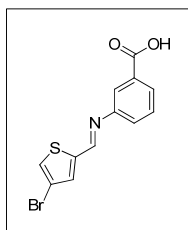
Imine 8: ^1H NMR (500 MHz, CDCl_3) δ 8.58 (s, 1H), 7.99 (d, $J = 8.6$ Hz, 1H), 7.76 (s, 1H), 7.42 (s, 2H), 7.00 (d, $J = 8.7$ Hz, 1H), 3.96 (s, 2H).



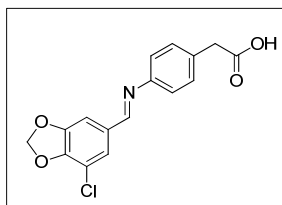
Imine 9: ^1H NMR (400 MHz, $\text{DMSO}-d_6$) δ 12.32 (s, 1H), 8.47 (s, 1H), 7.51 (s, 2H), 7.28 (d, $J = 8.3$ Hz, 2H), 7.18 (d, $J = 8.2$ Hz, 2H), 3.91 (s, 3H), 3.58 (s, 2H).



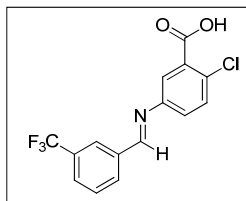
Imine 10: ^1H NMR (400 MHz, CDCl_3) δ 8.50 (s, 1H), 8.19 (s, 1H), 8.07 (d, $J = 7.9$ Hz, 1H), 7.74 (d, $J = 7.4$ Hz, 1H), 7.61 (t, $J = 8.0$ Hz, 1H), 7.34 (d, $J = 7.2$ Hz, 2H), 7.21 (d, $J = 7.8$ Hz, 2H), 3.70 (s, 2H).



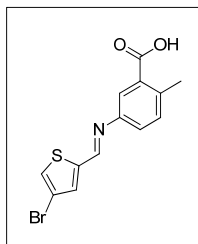
Imine 11: ^1H NMR (500 MHz, CDCl_3) δ 8.55 (s, 1H), 8.00 (d, $J = 7.3$ Hz, 1H), 7.94 (s, 1H), 7.50 (dt, $J = 15.7, 7.8$ Hz, 2H), 7.43 (s, 2H).



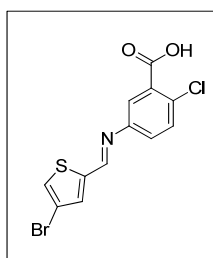
Imine 12: ^1H NMR (400 MHz, $\text{acetone-}d_6$) δ 8.50 (s, 1H), 7.46 (dd, $J = 5.6, 1.3$ Hz, 1H), 7.36 (d, $J = 8.4$ Hz, 2H), 7.21 (d, $J = 8.4$ Hz, 2H), 6.24 (s, 2H), 3.65 (s, 2H).



Imine 13: ^1H NMR (500 MHz, $\text{acetone-}d_6$) δ 8.84 (s, 1H), 8.34 (s, 1H), 8.30 (d, $J = 7.8$ Hz, 1H), 7.91 (d, $J = 7.7$ Hz, 1H), 7.81 (dd, $J = 8.9, 5.3$ Hz, 2H), 7.60 (d, $J = 8.5$ Hz, 1H), 7.52 (dd, $J = 8.5, 2.6$ Hz, 1H).



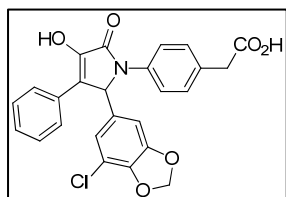
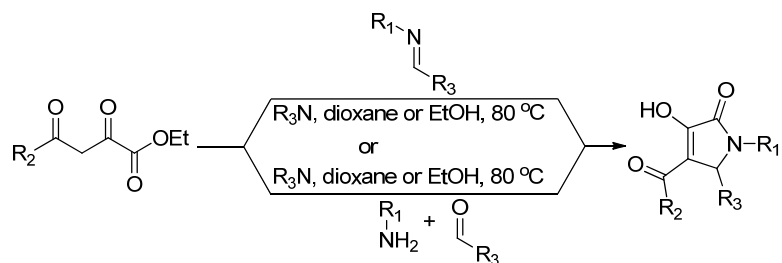
Imine 14: ^1H NMR (500 MHz, CD_3OD) δ 8.71 (s, 1H), 7.79 (s, 1H), 7.65 (s, 1H), 7.58 (s, 1H), 7.37 – 7.28 (m, 2H), 2.59 (s, 3H).



Imine 15: ^1H NMR (500 MHz, CD_3OD) δ 8.71 (s, 1H), 7.67 (d, $J = 8.8$ Hz, 1H), 7.60 (s, 1H), 7.50 (s, 1H), 7.38 (dd, $J = 8.4, 2.6$ Hz, 1H), 6.77 (dd, $J = 8.6, 2.8$ Hz, 1H).

2. Synthesis of pyrrolidinones

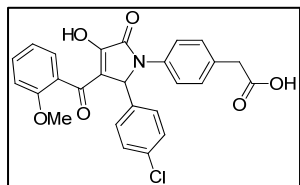
General synthetic scheme for preparation of pyrrolidinones



VPL-001: Sodium phenylpyruvate (200 mg, 0.9797 mmol) was

partitioned between 1M HCl and EtOAc (3x). The combined organic layers were concentrated to an oil (phenylpyruvic acid). This oil was dissolved in EtOH (3.25 mL), and aminophenylacetic acid (148 mg, 0.9797 mmol, 1 eq) and requisite aldehyde(1) (181 mg, 0.9797 mmol, 1 eq) were added to the mixture. The reaction vial was capped and heated to reflux overnight. The crude reaction mixture was concentrated and purified by chromatography on silica gel (0–100% EtOAc/Hexanes + 1% AcOH) then and recrystallization from EtOH/benzene to afford VPL-001 (60 mg, 13%) as a white solid.

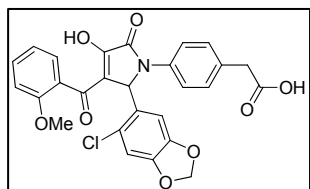
^1H NMR (d_8 -THF, 500 MHz) δ = 10.0 (br s, 1H), 7.79 (d, 2H, J = 7.5 Hz), 7.61 (d, 2H, J = 8.5 Hz), 7.31 (s, 2H), 7.27 (app. t, 2H, J = 7.5 Hz), 7.21 (d, 2H, J = 8.5 Hz), 7.14 (t, 1H, J = 7.0 Hz), 6.74 (s, 1H), 6.51 (d, 2H, J = 6.0 Hz), 5.81 (d, 2H, J = 8.5 Hz), 3.46 (s, 2H).
ESI m/z : 463.8 ($[\text{M}+\text{H}]^+$, $\text{C}_{25}\text{H}_{19}\text{ClNO}_6$ requires 464.1).



VPL-002: Imine 1 (20mg, 0.073mmol), ethyl 4-(2-methoxyphenyl)-2,4-dioxobutanoate (18mg, 0.073mmol), and triethylamine (0.36mmol) were combined in ethanol and heated to

reflux overnight. The crude reaction mixture was concentrated and partitioned between ethyl acetate and 1N HCl. The organic layer was dried over Na_2SO_4 and concentrated under reduced pressure. The product precipitated out of a 10% THF/hexanes mixture to afford the desired product (5mg) as and off white solid.

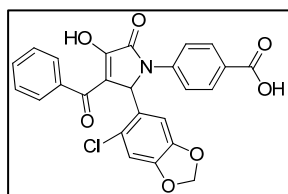
^1H NMR (500 MHz, cd_3cn) δ 7.45 (d, $J = 8.4$ Hz, 2H), 7.42 – 7.38 (m, 1H), 7.19 (d, $J = 8.3$ Hz, 2H), 7.09 (d, $J = 4.2$ Hz, 2H), 7.06 (d, $J = 8.4$ Hz, 2H), 6.96 (d, $J = 8.4$ Hz, 1H), 6.90 (t, $J = 7.4$ Hz, 1H), 5.96 (s, 1H), 3.74 (s, 3H), 3.53 (s, 2H). ESI m/z : 477.8 ($[\text{M}+\text{H}]^+$, $\text{C}_{26}\text{H}_{20}\text{ClNO}_6$ requires 478.0).



VPL-003: Imine 2 (43mg, 0.135mmol), ethyl 4-(2-methoxyphenyl)-2, 4-dioxobutanoate, (34mg, 0.135mmol), and triethylamine (0.677 mmol) were combined in ethanol and

heated to reflux overnight. The crude reaction mixture was concentrated and partitioned between ethyl acetate and 1N HCl. The organic layer was dried over Na_2SO_4 , concentrated under reduced pressure, and purified by chromatography (0–100% Hexanes/Ethyl Acetate followed by 95% EtOAc, 2.5% H_2O , 2.5% formic acid) to afford the desired product (6.6 mg off white solid).

^1H NMR (400 MHz, cd_3cn) δ 7.40 (d, $J = 7.0$ Hz, 2H), 7.22 (d, $J = 7.9$ Hz, 2H), 7.06 (d, $J = 7.6$ Hz, 1H), 6.98 (d, $J = 8.4$ Hz, 1H), 6.90 (t, $J = 7.1$ Hz, 1H), 6.66 (s, 1H), 6.58 (s, 1H), 6.43 (s, 1H), 5.90 (d, $J = 6.9$ Hz, 2H), 3.78 (s, 3H), 3.55 (s, 2H). ESI m/z : 519.8 ($[\text{M}-\text{H}]^-$, $\text{C}_{27}\text{H}_{20}\text{ClNO}_8$ requires 520.0).

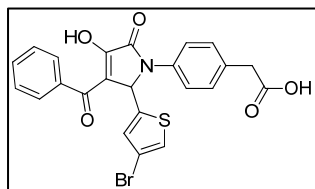


VPL-004: Imine 3 (65mg, 0.213mmol), ethyl 2, 4-dioxo-4-phenylbutanoate (47 mg, 0.213mmol), and triethylamine (1.067 mmol) were combined in ethanol and heated to reflux overnight.

The crude reaction mixture was concentrated and partitioned between ethyl acetate and

1N HCl. The organic layer was dried over Na₂SO₄ and concentrated under reduced pressure and purified by chromatography on silica gel (0–100% Hexanes/Ethyl Acetate followed by 95% EtOAc, 2.5% H₂O, 2.5% formic acid) to afford the desired product (17 mg tan solid).

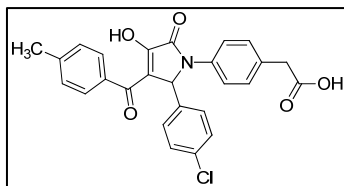
¹H NMR (400 MHz, cd₃od) δ 7.88 (d, *J* = 8.3 Hz, 1H), 7.72 (d, *J* = 7.7 Hz, 1H), 7.58 (d, *J* = 8.3 Hz, 1H), 7.40 – 7.35 (m, 1H), 7.35 – 7.29 (m, 1H), 6.65 (s, 1H), 6.57 (s, 1H), 6.47 (s, 1H), 5.83 (s, 1H). ESI *m/z*: 477.7 ([M+H]⁺, C₂₅H₁₆ClNO₇ requires 478.0).



VPL-005: Imine 4 (15 mg, 0.0454 mmol), ethyl 2, 4-dioxo-4-phenylbutanoate (10 mg, 0.0454 mmol), and diisopropylamine (0.231 mmol) were combined in ethanol and heated to reflux

overnight. The crude reaction mixture was concentrated and partitioned between ethyl acetate and 1N HCl. The organic layer was dried over Na₂SO₄, concentrated under reduced pressure, and purified by chromatography on silica gel (0–100% Hexanes/Ethyl Acetate followed by 95% EtOAc, 2.5% H₂O, 2.5% formic acid) to afford the desired product (4.4 mg tan solid). The compound had very poor solubility in most organic solvents, including DMSO. NMR is very difficult to interpret due to poor solubility.

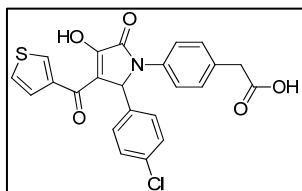
¹H NMR (500 MHz, dmsO) δ 8.42 (s, 2H), 7.79 (d, *J* = 5.8 Hz, 1H), 7.48 (d, *J* = 2.0 Hz, 1H), 7.32 (dd, *J* = 16.5, 6.8 Hz, 2H), 7.23 (s, 2H), 6.95 (s, 1H), 6.27 (s, 1H). ESI *m/z*: 495.6 ([M-H]⁻, C₂₃H₁₆BrNO₅S requires 496.0).



VPL-006: Imine 1, (110mg, 0.402mmol), ethyl 2, 4-dioxo-4-(p-tolyl)butanoate (100mg, 0.402mmol), and triethylamine (2.0mmol) were combined in dioxane and heated to reflux

overnight. The crude reaction mixture was concentrated and partitioned between ethyl acetate and 1N HCl. The organic layer was dried over Na_2SO_4 , concentrated under reduced pressure and purified by chromatography on silica gel (0–100% Hexanes/Ethyl Acetate followed by 95% EtOAc, 2.5% H_2O , 2.5% formic acid) to afford the desired product (63mg tan solid).

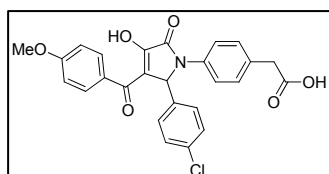
^1H NMR (500 MHz, cd_3cn) δ 7.66 (d, J = 8.1 Hz, 2H), 7.50 (d, J = 8.4 Hz, 2H), 7.33 (d, J = 8.5 Hz, 2H), 7.25 (d, J = 7.8 Hz, 1H), 7.22 (d, J = 8.5 Hz, 1H), 7.18 (d, J = 8.5 Hz, 2H), 6.17 (s, 1H), 3.54 (s, 2H), 2.38 (s, 3H). ESI m/z : 460.8 ($[\text{M}-\text{H}]^-$, $\text{C}_{26}\text{H}_{20}\text{ClNO}_5$ requires 460.0).



VPL-007: Imine 1 (12mg, 0.044 mmol), ethyl 2, 4-dioxo-4-(thiophen-3-yl)butanoate (10mg, 0.044mmol), and triethylamine (0.22 mmol) were combined in ethanol and heated to reflux

overnight. The crude reaction mixture was concentrated and partitioned between dichloromethane and 1N HCl. The organic layer was dried over Na_2SO_4 and concentrated under reduced pressure and purified by chromatography (0–100% Hexanes/Ethyl Acetate followed by 95% EtOAc, 2.5% H_2O , 2.5% formic acid) to afford the desired product (4.5mg tan solid).

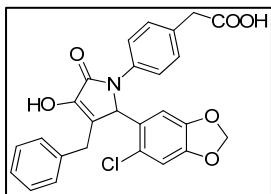
^1H NMR (400 MHz, cd_3cn) δ 8.36 (s, 1H), 7.49 (d, $J = 7.9$ Hz, 2H), 7.45 (d, $J = 4.5$ Hz, 1H), 7.37 (s, 1H), 7.33 (d, $J = 7.7$ Hz, 2H), 7.20 (dd, $J = 14.5, 8.2$ Hz, 4H), 6.15 (s, 1H), 3.55 (s, 2H). ESI m/z : 451.7 ($[\text{M}-\text{H}]^-$, $\text{C}_{23}\text{H}_{16}\text{ClNO}_5\text{S}$ requires 452.0).



VPL-008: Imine 1 (58 mg, 0.212 mmol), ethyl 4-(4-methoxyphenyl)-2,4-dioxobutanoate (53 mg, 0.212 mmol), triethylamine (110mg, 1.09 mmol) were combined in dioxane

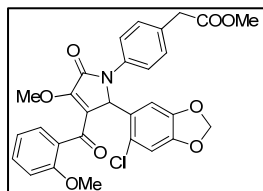
and heated to 80 °C overnight. The crude reaction mixture was concentrated and partitioned between dichloromethane and 1N HCl. The organic layer was dried over Na_2SO_4 and concentrated under reduced pressure and purified by chromatography (0–100% Hexanes/Ethyl Acetate followed by 95% EtOAc, 2.5% H_2O , 2.5% formic acid) to afford the desired product (34mg white solid).

^1H NMR (500 MHz, CD_3CN) δ 7.78 (dd, $J = 8.7, 1.8$ Hz, 2H), 7.56 – 7.45 (m, 2H), 7.33 (d, $J = 6.9$ Hz, 2H), 7.22 (dd, $J = 8.6, 1.4$ Hz, 1H), 7.18 (dd, $J = 7.4, 1.0$ Hz, 1H), 6.95 (dd, $J = 8.6, 1.3$ Hz, 2H), 6.19 (s, 1H), 3.85 (s, 2H), 3.55 (s, 1H). ESI m/z : 476.8 ($[\text{M}-\text{H}]^-$, $\text{C}_{26}\text{H}_{20}\text{ClNO}_6$ requires 476.1).



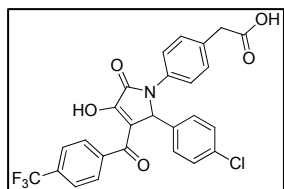
VPL-009: Prepared analogously to VPL-001: Purification (SiO_2 , 0–70% EtOAc/Hex + 1% AcOH) afforded product mixed with other impurities. This mixture was suspended in 1:1 MeCN/ H_2O and a white precipitate formed. The solid was collected as pure product (9 mg, 4%).

^1H NMR (d_8 -THF, 500 MHz) δ =10.80 (br s, 1H), 9.01 (br s, 1H), 7.51 (d, 2H, J = 8.5 Hz), 7.17–7.13 (m, 5H), 7.09 (m, 1H), 6.80 (s, 1H), 6.30 (s, 1H), 5.91 (s, 1H), 5.85 (s, 2H), 3.68 (d, 1H, J = 14.5 Hz), 3.41 (s, 2H), 3.17 (d, 1H, J = 14.5 Hz). ESI m/z : 477.8 ($[\text{M}+\text{H}]^+$, $\text{C}_{26}\text{H}_{21}\text{ClNO}_6$ requires 478.1).



VPL-010: To a dry scintillation vial under nitrogen was added VPL-003 (19mg, 0.0364mmol). This was suspended in 1ml of dichloromethane and 7eq. of methanol. 100ul of trimethylsilyldiazomethane (2.0 M solution in hexanes) was added and the reaction was stirred at room temperature. The solvent was evaporated under reduced pressure. Purification (SiO_2 , 0–10% MeOH/dichloromethane) afforded the desired product.

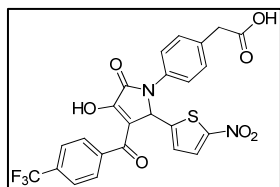
^1H NMR (500 MHz, CDCl_3) δ 7.49 (d, J = 8.5 Hz, 2H), 7.47 – 7.42 (m, 1H), 7.29 (d, J = 7.5 Hz, 1H), 7.23 (d, J = 8.4 Hz, 2H), 6.96 (t, J = 7.5 Hz, 1H), 6.91 (d, J = 8.4 Hz, 2H), 6.59 (s, 1H), 6.47 (s, 1H), 6.40 (s, 1H), 5.89 (d, J = 11.8 Hz, 2H), 4.01 (s, 3H), 3.84 (s, 3H), 3.57 (s, 2H), 3.49 (s, 3H). ESI m/z : 535.8 ($[\text{M}+\text{H}]^+$, $\text{C}_{29}\text{H}_{24}\text{ClNO}_8$ requires 549.8).



VPL-011: Imine 1 (11.6 mg, 0.0423 mmol), ethyl 2, 4-dioxo-4-(4-(trifluoromethyl) phenyl)butanoate (12.2 mg, 0.0423 mmol), diisopropylethylamine (0.211 mmol), were dissolved in dioxane and heated to 80 °C for 2 days. The crude reaction mixture was concentrated and partitioned between dichloromethane and 1N HCl. The organic layer was dried over Na_2SO_4 and concentrated under reduced pressure and purified by chromatography (0–

100% Hexanes/Ethyl Acetate followed by 95% EtOAc, 2.5% H₂O, 2.5% formic acid) to afford the desired product (4.8mg white solid).

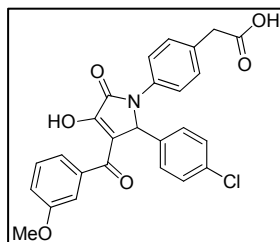
¹H NMR (400 MHz, CD₃CN) δ 7.84 (d, *J* = 8.3 Hz, 2H), 7.71 (d, *J* = 8.3 Hz, 2H), 7.50 (d, *J* = 8.3 Hz, 2H), 7.35 (d, *J* = 8.3 Hz, 12H), 7.20 (t, *J* = 8.4 Hz, 4H), 6.11 (s, 1H), 3.54 (s, 2H). ESI *m/z*: 513.8 ([M-H]⁺, C₂₆H₁₇ClF₃N₂O₅ requires 514.0).



VPL-012: Imine 5 (10 mg, 0.0346 mmol), ethyl 2, 4-dioxo-4-(4-(trifluoromethyl) phenyl)butanoate (10 mg, 0.0346 mmol), and diisopropylethylamine (0.17 mmol) were dissolved in dioxane and

heated to 80 °C overnight. The crude reaction mixture was concentrated and partitioned between dichloromethane and 1N HCl. The organic layer was concentrated and dried over Na₂SO₄ and concentrated under reduced pressure and purified by chromatography (0–100% Hexanes/Ethyl Acetate followed by 95% EtOAc, 2.5% H₂O, 2.5% formic acid) to afford the desired product (3.2 mg white solid).

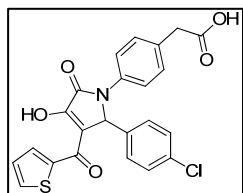
¹H NMR (400 MHz, CD₃CN) δ 7.90 (d, *J* = 7.9 Hz, 1H), 7.74 (d, *J* = 8.0 Hz, 1H), 7.63 (d, *J* = 3.9 Hz, 1H), 7.51 (d, *J* = 8.3 Hz, 1H), 7.28 (d, *J* = 8.4 Hz, 1H), 7.15 (d, *J* = 3.5 Hz, 1H), 6.44 (s, 1H), 3.58 (s, 1H). ESI *m/z*: 530.7 ([M-H]⁺, C₂₄H₁₅F₃N₂O₇S requires 531.0).



VPL-013: Imine 1 (47 mg, 0.17 mmol), ethyl 4-(3-methoxyphenyl)-2,4-dioxobutanoate (43 mg, 0.17 mmol), and triethylamine (0.86

mmol) were dissolved in dioxane and heated to 80 °C overnight. The crude reaction mixture was concentrated and partitioned between dichloromethane and 1N HCl. The organic layer was concentrated and dried over Na₂SO₄ and concentrated under reduced pressure and purified by chromatography (0–100% Hexanes/Ethyl Acetate followed by 95% EtOAc, 2.5% H₂O, 2.5% formic acid) to afford the desired product (2.3 mg white solid).

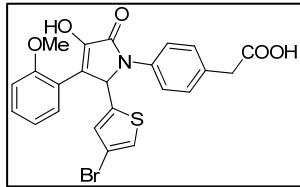
¹H NMR (500 MHz, CD₃CN) δ 7.49 (d, *J* = 8.2 Hz, 2H), 7.36 – 7.27 (m, 4H), 7.21 (d, *J* = 8.6 Hz, 3H), 7.17 (d, *J* = 8.2 Hz, 2H), 7.10 (d, *J* = 7.3 Hz, 1H), 6.15 (s, 1H), 3.79 (s, 3H), 3.54 (s, 2H). ESI *m/z*: 475.8 ([M-H]⁺, C₂₆H₂₀ClNO₆ requires 476.1).



VPL-014; Imine 1 (32.5 mg, 0.118 mmol), ethyl 2, 4-dioxo-4-(thiophen-2-yl) butanoate (26.85 mg, 0.118 mmol), and triethylamine (0.59 mmol) were dissolved in ethanol and heated to 80 °C overnight.

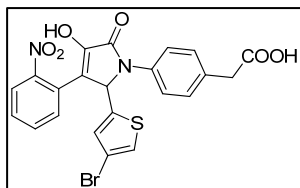
The crude reaction mixture was concentrated and partitioned between dichloromethane and 1N HCl. The organic layer was concentrated and dried over Na₂SO₄ and concentrated under reduced pressure and purified by chromatography (0–100% Hexanes/Ethyl Acetate followed by 95% EtOAc, 2.5% H₂O, 2.5% formic acid) to afford the desired product (15.3mg white solid).

¹H NMR (500 MHz, CD₃CN) δ 8.14 (d, *J* = 2.0 Hz, 1H), 7.73 (d, *J* = 4.6 Hz, 1H), 7.48 (d, *J* = 8.2 Hz, 2H), 7.33 (d, *J* = 8.2 Hz, 2H), 7.19 (dd, *J* = 15.9, 8.2 Hz, 4H), 7.13 (s, 1H), 6.14 (s, 1H), 3.54 (s, 3H). ESI *m/z*: 451.8 ([M-H]⁺, C₂₃H₁₆ClNO₅S requires 452.0)

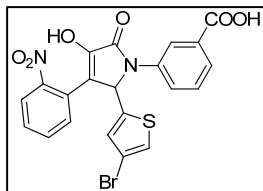


VPL-015: Prepared analogously to VPL-001.

$^1\text{H NMR}$ (d_6 -acetone, 500 MHz) δ = 7.69 (d, 1H, J = 7.5 Hz), 7.66 (d, 2H, J = 7.5 Hz), 7.30 (d, 2H, J = 8.0 Hz), 7.26 (d, 1H, J = 8.0 Hz), 7.25 (s, 1H), 7.11 (s, 1H), 7.03 (d, 1H, J = 8.5 Hz), 6.96 (t, 1H, J = 7.5 Hz), 6.90 (s, 1H), 3.96 (s, 3H), 3.58 (s, 2H). ESI m/z : 497.6 ($[\text{M}-\text{H}]^-$, $\text{C}_{23}\text{H}_{17}\text{BrNO}_5\text{S}$ requires 498.0).

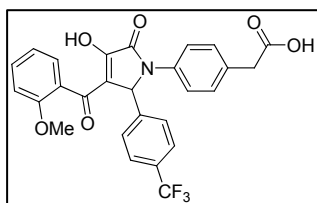


VPL-016: Prepared analogously to VPL-001: $^1\text{H NMR}$ (d_4 -MeOH, 500 MHz) δ = 7.95 (d, 1H, J = 8.0 Hz), 7.65 (dd, 1H, J = 7.0, 7.5 Hz), 7.55 (d, 1H, J = 8.0 Hz), 7.52 (m, 3H), 7.31 (d, 2H, J = 8.5 Hz), 7.20 (s, 1H), 7.00 (s, 1H), 6.58 (s, 1H), 3.59 (s, 2H). ESI m/z : 512.7 ($[\text{M}-\text{H}]^-$, $\text{C}_{22}\text{H}_{14}\text{BrN}_2\text{O}_6\text{S}$ requires 513.0).



VPL-017: Prepared analogously to VPL-001. Upon standing, the product precipitated out of solution as a brown solid (115 mg, 24%).

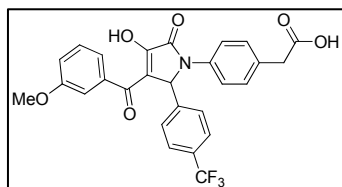
$^1\text{H NMR}$ (d_8 -THF, 500 MHz) δ = 11.48 (br s, 1H), 9.95 (br s, 1H), 8.26 (s, 1H), 7.92 (d, 2H, J = 8.0 Hz), 7.77 (d, 1H, J = 7.5 Hz), 7.63–7.57 (m, 2H), 7.47 (app. t, 1H, J = 8.0 Hz), 7.41 (app. t, 1H, J = 8.0 Hz), 7.22 (s, 1H), 7.11 (s, 1H), 6.62 (s, 1H). ESI m/z : 498.6 ($[\text{M}-\text{H}]^-$, $\text{C}_{21}\text{H}_{12}\text{BrN}_2\text{O}_6\text{S}$ requires 499.0).



VPL-018: Imine 6 (10.4 mg, 0.0338 mmol), ethyl 4-(2-methoxyphenyl)-2, 4-dioxobutanoate (8.5 mg, 0.0338 mmol),

and diisopropylethylamine (0.169 mmol) were dissolved in ethanol and heated to 80 °C overnight. The crude reaction mixture was concentrated and partitioned between dichloromethane and 1N HCl. The organic layer was concentrated and dried over Na₂SO₄ and concentrated under reduced pressure and purified by chromatography (0–100% Hexanes/Ethyl Acetate followed by 95% EtOAc, 2.5% H₂O, 2.5% formic acid) to afford the desired product (2.5mg white solid).

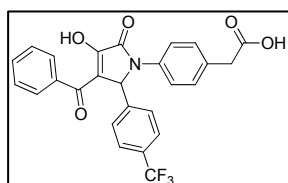
¹H NMR (500 MHz, , CD₃CN) δ 7.47 (d, *J* = 8.3 Hz, 2H), 7.41 (d, *J* = 7.7 Hz, 3H), 7.29 (d, *J* = 8.0 Hz, 2H), 7.20 (d, *J* = 8.2 Hz, 2H), 7.07 (d, *J* = 7.2 Hz, 1H), 6.95 (d, *J* = 8.4 Hz, 1H), 6.89 (t, *J* = 7.4 Hz, 1H), 6.07 (s, 1H), 3.72 (s, 3H), 3.53 (s, 2H). ESI *m/z*: 509.8 ([M–H][–], C₂₇H₂₀F₃NO₆ requires 510.1).



VPL-019: Imine 6 (10.5 mg, 0.0341 mmol), ethyl 4-(3-methoxyphenyl)-2,4-dioxobutanoate (8.5 mg, 0.0341 mmol), and diisopropylethylamine (0.17 mmol) were dissolved in

ethanol and heated to 80 °C overnight. The crude reaction mixture was concentrated and partitioned between dichloromethane and 1N HCl. The organic layer was concentrated and dried over Na₂SO₄ and concentrated under reduced pressure and purified by chromatography (0–100% Hexanes/Ethyl Acetate followed by 95% EtOAc, 2.5% H₂O, 2.5% formic acid) to afford the desired product (2.9mg white solid).

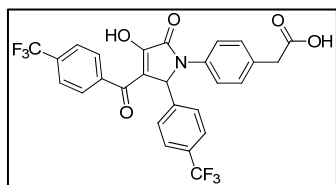
^1H NMR (500 MHz, CD_3CN) δ 7.56 (d, $J = 8.1$ Hz, 2H), 7.51 (t, $J = 8.4$ Hz, 3H), 7.34 (dt, $J = 21.4, 6.7$ Hz, 3H), 7.25 – 7.19 (m, 3H), 7.11 (d, $J = 8.9$ Hz, 1H), 6.24 (s, 1H), 3.80 (s, 3H), 3.54 (s, 2H). ESI m/z : 509.8 ($[\text{M}-\text{H}]^-$, $\text{C}_{27}\text{H}_{20}\text{F}_3\text{NO}_6$ requires 510.1).



VPL-020: Imine 6 (25 mg, 0.0813 mmol), ethyl 2,4-dioxo-4-phenylbutanoate (18mg, 0.0813 mmol), and triethylamine (0.406 mmol) were dissolved in ethanol and heated to 80 °C overnight.

The crude reaction mixture was concentrated and partitioned between dichloromethane and 1N HCl. The organic layer was concentrated and dried over Na_2SO_4 and concentrated under reduced pressure and purified by chromatography (0–100% Hexanes/Ethyl Acetate followed by 95% EtOAc, 2.5% H_2O , 2.5% formic acid) to afford the desired product (19.6mg white solid).

^1H NMR (500 MHz, $\text{thf}-d_8$) δ 7.80 (d, $J = 3.6$ Hz, 2H), 7.65 (d, $J = 8.2$ Hz, 2H), 7.49 (bs, 2H), 7.44 – 7.33 (m, 3H), 7.32 – 7.23 (m, 3H), 7.18 (d, $J = 8.1$ Hz, 2H), 6.25 (s, 1H), 3.43 (s, 2H). ESI m/z : 479.8 ($[\text{M}-\text{H}]^-$, $\text{C}_{26}\text{H}_{18}\text{F}_3\text{NO}_5$ requires 480.1).

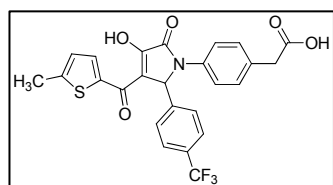


VPL-021: Imine 6 (11mg, 0.0346), ethyl 2,4-dioxo-4-(4-(trifluoromethyl)phenyl)butanoate (10 mg, 0.0346 mmol), and diisopropylethylamine (0.173 mmol) were dissolved in dioxane

and heated to 80 °C overnight. The crude reaction mixture was concentrated and partitioned between dichloromethane and 1N HCl. Heavy precipitate formed in the

organic layer, which was filtered and rinsed with cold hexanes to afford the desired product as white solid. (5.8mg)

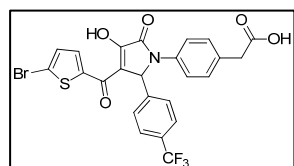
^1H NMR (500 MHz, , CD_3CN) δ 7.85 (d, J = 8.0 Hz, 2H), 7.75 (d, J = 8.2 Hz, 2H), 7.58 (d, J = 8.1 Hz, 2H), 7.52 (d, J = 8.3 Hz, 4H), 7.23 (d, J = 8.4 Hz, 2H), 6.24 (s, 1H), 3.55 (s, 2H). ESI m/z : 547.8 ($[\text{M}-\text{H}]^-$, $\text{C}_{27}\text{H}_{17}\text{F}_6\text{NO}_5$ requires 548.1)



VPL-022: Imine 6 (20 mg, 0.065 mmol), ethyl 4-(5-methylthiophen-2-yl)-2,4-dioxobutanoate (15.6 mg, 0.065 mmol), and diisopropylethylamine (0.325 mmol) were dissolved

in ethanol and heated to 80 °C overnight. The crude reaction mixture was concentrated and partitioned between dichloromethane and 1N HCl. The organic layer was concentrated and dried over Na_2SO_4 and concentrated under reduced pressure and purified by chromatography (0–100% Hexanes/Ethyl Acetate followed by 95% EtOAc, 2.5% H_2O , 2.5% formic acid) to afford the desired product (14.4mg white solid).

^1H NMR (400 MHz, CD_3CN) δ 7.99 (d, J = 3.1 Hz, 1H), 7.52 (dd, J = 19.6, 8.6 Hz, 6H), 7.21 (d, J = 8.5 Hz, 2H), 6.84 (d, J = 2.7 Hz, 1H), 6.20 (s, 1H), 3.54 (s, 2H), 2.47 (s, 3H). ESI m/z : 499.8 ($[\text{M}-\text{H}]^-$, $\text{C}_{25}\text{H}_{18}\text{F}_3\text{NO}_5\text{S}$ requires 520.1)

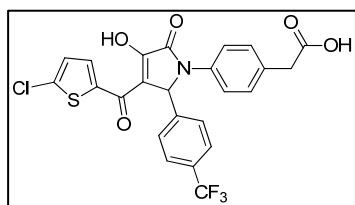


VPL-023: Imine 6 (20 mg, 0.065 mmol), ethyl 4-(5-bromothiophen-2-yl)-2,4-dioxobutanoate (20 mg, 0.065 mmol), and diisopropylethylamine (0.325 mmol) were dissolved in ethanol

and heated to 80 °C overnight. The crude reaction mixture was concentrated and

partitioned between dichloromethane and 1N HCl. The organic layer was concentrated and dried over Na₂SO₄ and concentrated under reduced pressure and purified by chromatography (0–100% Hexanes/Ethyl Acetate followed by 95% EtOAc, 2.5% H₂O, 2.5% formic acid) to afford the desired product (19.5 mg white solid).

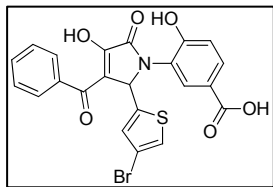
¹H NMR (400 MHz, , CD₃CN) δ 8.10 (s, 1H), 7.55 (d, *J* = 8.6 Hz, 2H), 7.51 (d, *J* = 8.2 Hz, 3H), 7.21 (d, *J* = 8.2 Hz, 3H), 7.17 (d, *J* = 3.6 Hz, 1H), 6.16 (s, 1H), 3.54 (s, 2H). ESI *m/z*: 563.6 ([M–H][–], C₂₄H₁₅BrF₃NO₅S requires 563.9)



VPL-024: Imine 6 (20 mg, 0.065 mmol), ethyl 4-(5-chlorothiophen-2-yl)-2,4-dioxobutanoate (17 mg, 0.065 mmol), and diisopropylethylamine (0.325 mmol) were

dissolved in ethanol and heated to 80 °C overnight. The crude reaction mixture was concentrated and partitioned between dichloromethane and 1N HCl. The organic layer was concentrated and dried over Na₂SO₄ and concentrated under reduced pressure and purified by chromatography (0–100% Hexanes/Ethyl Acetate followed by 95% EtOAc, 2.5% H₂O, 2.5% formic acid) to afford the desired product (24 mg white solid).

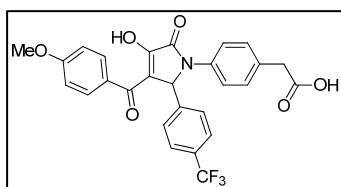
¹H NMR (400 MHz, thf) δ 10.84 (s, 1H), 8.01 (s, 1H), 7.61 (d, *J* = 7.5 Hz, 1H), 7.56 (d, *J* = 7.6 Hz, 1H), 7.48 (d, *J* = 7.6 Hz, 1H), 7.20 (d, *J* = 8.4 Hz, 1H), 7.04 (s, 1H), 6.29 (s, 1H), 3.45 (s, 2H). ESI *m/z*: 519.7 ([M–H][–], C₂₄H₁₅ClF₃NO₅S requires 520.0)



VPL-025: Imine 7 (22 mg, 0.0676 mmol), ethyl 2,4-dioxo-4-phenylbutanoate (14.9 mg, 0.0676 mmol), and diisopropylethylamine (0.325 mmol) were dissolved in ethanol and

heated to 80 °C overnight. The crude reaction mixture was concentrated and partitioned between dichloromethane and 1N HCl. The organic layer was concentrated and dried over Na₂SO₄ and concentrated under reduced pressure and purified by chromatography (0–100% Hexanes/Ethyl Acetate followed by 95% EtOAc, 2.5% H₂O, 2.5% formic acid) to afford the desired product (9.8 mg white solid).

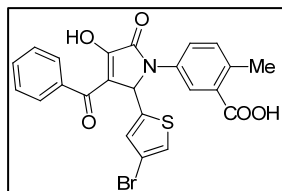
¹H NMR (400 MHz, thf) δ 9.63 (s, 1H), 7.91 (s, 2H), 7.87 (d, *J* = 5.7 Hz, 2H), 7.77 (d, *J* = 8.3 Hz, 1H), 7.50 (dt, *J* = 19.1, 9.9 Hz, 2H), 7.39 (t, *J* = 7.1 Hz, 2H), 7.14 (s, 1H), 6.90 (d, *J* = 8.4 Hz, 2H), 6.62 (s, 1H). ESI *m/z*: 497.7 ([M–H][–], C₂₂H₁₄BrNO₆S requires 497.97)



VPL-026: Imine 6 (12.3mg, 0.04mmol), ethyl 4-(4-methoxyphenyl)-2,4-dioxobutanoate (10 mg, 0.04mmol), and diisopropylethylamine (0.2mmol) were dissolved in ethanol

and heated to 80 °C overnight. The crude reaction mixture was concentrated and partitioned between dichloromethane and 1N HCl. The organic layer was concentrated and dried over Na₂SO₄ and concentrated under reduced pressure and purified by chromatography (0–100% Hexanes/Ethyl Acetate followed by 95% EtOAc, 2.5% H₂O, 2.5% formic acid) to afford the desired product (5.1 mg white solid).

^1H NMR (500 MHz, CD_3CN) δ 7.78 (d, $J = 8.7$ Hz, 2H), 7.56 (d, $J = 8.2$ Hz, 2H), 7.51 (t, $J = 9.3$ Hz, 4H), 7.22 (d, $J = 8.3$ Hz, 2H), 6.94 (d, $J = 8.7$ Hz, 2H), 6.27 (s, 1H), 3.84 (s, 3H), 3.54 (s, 2H). ESI m/z : 509.8 ($[\text{M}-\text{H}]^-$, $\text{C}_{27}\text{H}_{20}\text{F}_3\text{NO}_6$ requires 510.2)

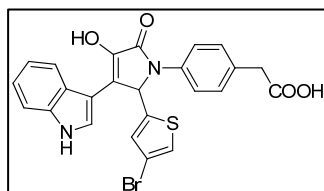


VPL-027: Ethyl 2,4-dioxo-4-phenylbutanoate (61 mg, 0.188 mmol, 2 equiv) and imine 14 (20.7 mg, 0.094 mmol, 1 equiv) were suspended in EtOH (0.73 mL) and Et_3N (0.065 mL, 5 equiv) was

added. The reaction was heated at 80°C overnight. The crude reaction mixture was concentrated and purified by chromatography (SiO_2 , 0–20% MeOH/DCM + 1% AcOH) to afford the desired product.

Poor solubility properties prevent interpretation of the ^1H NMR.

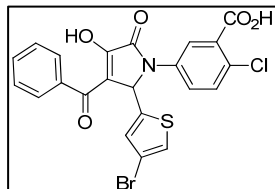
ESI m/z : 495.7 ($[\text{M}-\text{H}]^-$, $\text{C}_{23}\text{H}_{15}\text{BrNO}_5\text{S}$ requires 496.0).



VPL-028: Prepared analogously to VPL-001. The crude product purified by chromatography (SiO_2 , 0–3% MeOH/dichloromethane +1% AcOH) to afford the desired

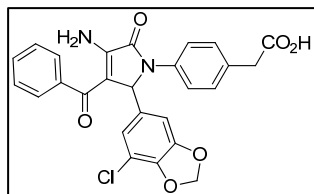
product mixed with 4-aminophenylacetic acid. This mixture was dissolved in EtOAc and extracted with satd. aq. NaHCO_3 . The organic layer was removed, and the aqueous layer was heated. Upon cooling to room temperature, the desired product precipitated out of solution as fine plate-like crystals.

^1H NMR (d_4 -MeOH, 500 MHz) δ = 8.06 (d, 1H, J = 8.0 Hz), 7.52 (s, 1H), 7.45 (m, 2H), 7.33 (m, 3H), 7.11 (t, 1H, J = 7.0 Hz), 7.08 (s, 1H), 7.07 (s, 1H), 7.04 (t, 1H, J = 8.0 Hz), 6.55 (s, 1H), 3.46 (s, 2H). ESI m/z : 506.7 ($[\text{M}-\text{H}]^-$, $\text{C}_{24}\text{H}_{16}\text{BrN}_2\text{O}_4\text{S}$ requires 507.0).



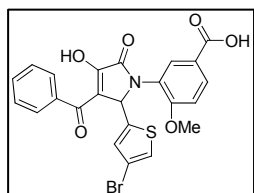
VPL-029: Ethyl 2,4-dioxo-4-phenylbutanoate (21.8 mg, 0.0990 mmol) was combined with imine 14 (136 mg, 0.3960 mmol) and *N,N*-diisopropylethylamine (0.086 mL, 0.4950 mmol) in EtOH (0.5 mL) and the mixture was heated at reflux overnight. The resulting mixture was concentrated and purified by chromatography (SiO_2 , 0–20% MeOH/DCM +1% AcOH). The resulting fractions containing product were combined and concentrated. The product was precipitated out of a 10% THF/MeOH mixture to afford the desired product (6.0 mg) as a very insoluble white solid.

^1H NMR (d_6 -DMSO, 600 MHz) δ = 7.90 (br s, 1H), 7.76 (d, 2H, J = 6.6 Hz), 7.47 (dd, 1H, J = 2.4, 9.0 Hz), 7.35 (t, 1H, J = 7.2 Hz), 7.31–7.27 (m, 5H), 6.98 (s, 1H), 6.28 (s, 1H). ESI m/z : 515.6 ($[\text{M}-\text{H}]^-$, $\text{C}_{22}\text{H}_{12}\text{BrClNO}_5\text{S}$ requires 515.9).



VPL-030: GA-228 (9.0 mg, 0.0407 mmol) and ammonium formate (2.2 mg, 0.0732 mmol) were dissolved in 2-methoxyethanol (0.15 mL) and heated at reflux overnight. The resulting mixture was concentrated and purified by chromatography (0–20% MeOH/DCM) to afford the desired product (4.0 mg, 44%).

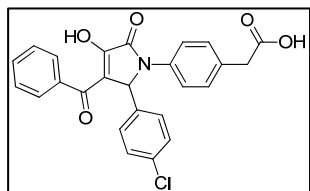
^1H NMR (d_4 -MeOH, 500 MHz) δ = 7.49 (t, 1H, J = 8.5 Hz), 7.42–7.39 (m, 4H), 7.33 (d, 2H, J = 7.5 Hz), 7.25 (d, 2H, J = 8.5 Hz), 6.15 (s, 1H), 6.03 (s, 1H), 5.99 (s, 1H), 5.86 (s, 1H), 5.83 (s, 1H), 3.49 (s, 2H). ESI m/z : 488.8 ($[\text{M}-\text{H}]^-$, $\text{C}_{26}\text{H}_{18}\text{ClN}_2\text{O}_6$ requires 489.1).



VPL-031: Imine 8 (21mg, 0.061mmol), ethyl 2,4-dioxo-4-phenylbutanoate (3.5mg, 0.061 mmol), and diisopropylethylamine (0.305 mmol) were combined in ethanol and heated to reflux

overnight. The crude reaction mixture was concentrated and partitioned between dichloromethane and 1N HCl. The organic layer was dried over Na_2SO_4 and concentrated under reduced pressure and purified by chromatography (0–100% Hexanes/Ethyl Acetate followed by 95% EtOAc, 2.5% H_2O , 2.5% formic acid) to afford the desired product (4.5mg tan solid).

^1H NMR (400 MHz, $\text{thf}-d_8$) δ 7.94 – 7.86 (m, 3H), 7.52 – 7.43 (m, 2H), 7.43 – 7.34 (m, 2H), 7.15 – 7.06 (m, 2H), 6.88 (s, 1H), 6.47 (s, 1H), 3.93 (s, 3H). ESI m/z : 511.6 ($[\text{M}-\text{H}]^-$, $\text{C}_{23}\text{H}_{16}\text{BrNO}_6\text{S}$ requires 511.99).

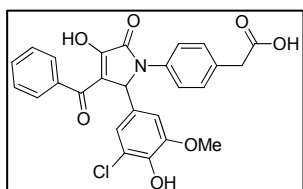


VPL-032: Imine 1 (18.4mg, 0.0672mmol), ethyl 2,4-dioxo-4-phenylbutanoate (14.8 mg, 0.0672 mmol), and diisopropylethylamine (0.336 mmol) were combined in ethanol

and heated to reflux overnight. The crude reaction mixture was concentrated and

partitioned between dichloromethane and 1N HCl. The organic layer was dried over Na_2SO_4 and concentrated under reduced pressure and purified by chromatography (0–100% Hexanes/Ethyl Acetate followed by 95% EtOAc, 2.5% H_2O , 2.5% formic acid) to afford the desired product (6.2 mg tan solid).

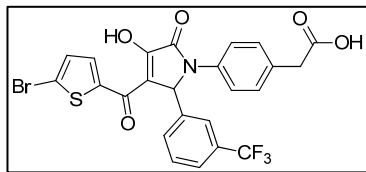
^1H NMR (400 MHz, CD_3CN) δ 7.73 (d, J = 7.3 Hz, 2H), 7.60 – 7.54 (m, 1H), 7.50 (d, J = 8.4 Hz, 2H), 7.47 – 7.39 (m, 2H), 7.32 (d, J = 8.0 Hz, 2H), 7.20 (dd, J = 16.2, 8.2 Hz, 4H), 6.18 (s, 1H), 3.55 (s, 2H). ESI m/z : 445.8 ($[\text{M}-\text{H}]^-$, $\text{C}_{25}\text{H}_{18}\text{ClNO}_5$ requires 446.08).



VPL-033: Imine 9 (58 mg, 0.18 mmol), ethyl 2,4-dioxo-4-phenylbutanoate (40 mg, 0.18 mmol), and triethylamine (0.9 mmol) were combined in dioxane and heated to reflux

overnight. The crude reaction mixture was concentrated and partitioned between dichloromethane and 1N HCl. The organic layer was dried over Na_2SO_4 and concentrated under reduced pressure and purified by chromatography (0–100% Hexanes/Ethyl Acetate followed by 95% EtOAc, 2.5% H_2O , 2.5% formic acid) to afford the desired product (33 mg tan solid).

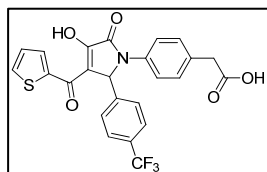
^1H NMR (400 MHz, CD_3CN) δ 7.76 (d, J = 7.8 Hz, 2H), 7.58 (t, J = 8.3 Hz, 1H), 7.53 – 7.42 (m, 4H), 7.24 (d, J = 8.2 Hz, 2H), 6.89 (s, 1H), 6.76 (s, 1H), 6.09 (s, 1H), 3.73 (s, 3H), 3.56 (s, 2H). ESI m/z : 491.8 ($[\text{M}-\text{H}]^-$, $\text{C}_{26}\text{H}_{20}\text{ClNO}_7$ requires 492.09).



VPL-034: Imine 10 (24 mg, 0.078 mmol), ethyl 4-(5-bromothiophen-2-yl)-2,4-dioxobutanoate (11.9 mg, 0.078 mmol), and triethylamine (0.195 mmol) were combined in

dioxane and heated to reflux overnight. The crude reaction mixture was concentrated and partitioned between dichloromethane and 1N HCl. The organic layer was dried over Na_2SO_4 and concentrated under reduced pressure and purified by chromatography (0–100% Hexanes/Ethyl Acetate followed by 95% EtOAc, 2.5% H_2O , 2.5% formic acid) to afford the desired product (12.4 mg white solid).

^1H NMR (400 MHz, CD_3CN) δ 7.94 (d, J = 2.7 Hz, 1H), 7.71 (s, 1H), 7.62 (d, J = 7.7 Hz, 1H), 7.49 (d, J = 8.0 Hz, 2H), 7.42 – 7.34 (m, 1H), 7.27 – 7.11 (m, 4H), 6.18 (s, 1H), 3.54 (s, 2H). ESI m/z : 563.6 ($[\text{M}-\text{H}]^-$, $\text{C}_{24}\text{H}_{15}\text{BrF}_3\text{NO}_6\text{S}$ requires 563.98).

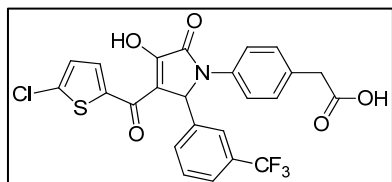


VPL-035: Imine 6 (30mg, 0.1mmol), ethyl 2,4-dioxo-4-(thiophen-2-yl)butanoate (11.2 mg, 0.05mmol), and triethylamine (0.25 mmol) were combined in dioxane and heated to reflux overnight. The

crude reaction mixture was concentrated and partitioned between dichloromethane and 1N HCl. The organic layer was dried over Na_2SO_4 and concentrated under reduced pressure and purified by chromatography (0–100% Hexanes/Ethyl Acetate followed by 95% EtOAc, 2.5% H_2O , 2.5% formic acid) followed by a trituration with DCM to afford the desired product (8.9 mg white solid).

^1H NMR (500 MHz, acetone) δ 9.36 (s, 1H), 7.71 (d, J = 7.6 Hz, 2H), 7.57 (d, J = 7.7 Hz, 2H), 7.53 (d, J = 3.2 Hz, 2H), 7.44 (bs, 2H), 7.24 (d, J = 7.1 Hz, 2H), 7.03 (s, 1H), 6.15 (s, 1H), 3.54 (s, 2H).

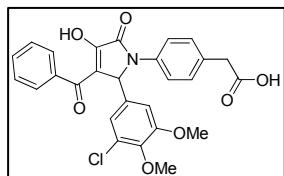
ESI m/z : 485.8 ($[\text{M}-\text{H}]^-$, $\text{C}_{24}\text{H}_{16}\text{F}_3\text{NO}_5\text{S}$ requires 486.07).



VPL-036: Imine 10 (26mg, 0.084mmol), ethyl 4-(5-chlorothiophen-2-yl)-2,4-dioxobutanoate (11 mg, 0.042 mmol), and triethylamine (0.21 mmol) were combined in

dioxane and heated to reflux overnight. The crude reaction mixture was concentrated and partitioned between dichloromethane and 1N HCl. The organic layer was dried over Na_2SO_4 and concentrated under reduced pressure and purified by chromatography (0–100% Hexanes/Ethyl Acetate followed by 95% EtOAc, 2.5% H_2O , 2.5% formic acid) followed by a trituration with DCM to afford the desired product (4.4 mg white solid).

^1H NMR (500 MHz, acetone) δ 8.14 (d, J = 4.0 Hz, 1H), 7.85 (s, 1H), 7.74 (d, J = 7.5 Hz, 1H), 7.66 (d, J = 8.3 Hz, 2H), 7.50 (d, J = 8.0 Hz, 1H), 7.49 – 7.43 (m, 1H), 7.28 (d, J = 8.3 Hz, 2H), 7.17 (d, J = 4.1 Hz, 1H), 6.41 (s, 1H), 3.56 (s, 2H). ESI m/z : 519.7 ($[\text{M}-\text{H}]^-$, $\text{C}_{24}\text{H}_{15}\text{ClF}_3\text{NO}_5\text{S}$ requires 520.0).

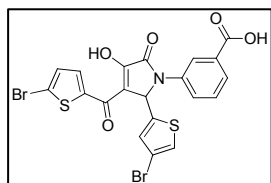


VPL-037: 4-aminophenyl acetic acid (27mg, 0.18mmol), 3-chloro-4, 5-dimethoxybenzaldehyde (36 mg, 0.18 mmol), ethyl 2,4-dioxo-

4-phenylbutanoate (20mg, 0.09mmol), and triethylamine (0.9 mmol) were combined in 2 ml of ethanol and heated at reflux overnight. The crude reaction mixture was concentrated and partitioned between dichloromethane and 1N HCl. The organic layer was dried over Na₂SO₄ and concentrated under reduced pressure and purified by chromatography (0–100% Hexanes/Ethyl Acetate followed by 95% EtOAc, 2.5% H₂O, 2.5% formic acid) to afford the desired product (16.2mg white solid).

¹H NMR (500 MHz, acetone) δ 7.89 (d, *J* = 7.3 Hz, 2H), 7.68 (d, *J* = 8.4 Hz, 2H), 7.62 – 7.53 (m, 1H), 7.48 (t, *J* = 7.3 Hz, 2H), 7.30 (d, *J* = 8.3 Hz, 2H), 7.14 (d, *J* = 9.2 Hz, 2H), 6.30 (s, 1H), 3.79 (s, 3H), 3.64 (s, 3H), 3.58 (s, 2H).

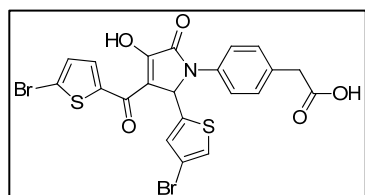
ESI *m/z*: 505.8 ([M–H][–], C₂₇H₂₂ClNO₇ requires 506.1).



VPL-038: Imine 11 (18.1 mg, 0.058 mmol), ethyl 4-(5-bromothiophen-2-yl)-2,4-dioxobutanoate (8.9 mg, 0.029 mmol), and triethylamine (0.145 mmol) were combined in ethanol and heated to

reflux overnight. The crude reaction mixture was concentrated and partitioned between dichloromethane and 1N HCl. The organic layer was dried over Na₂SO₄ and concentrated under reduced pressure and purified by chromatography (0–100% Hexanes/Ethyl Acetate followed by 95% EtOAc, 2.5% H₂O, 2.5% formic acid) to afford the desired product (3.8 mg white solid). Compound had very poor solubility in most organic solvents.

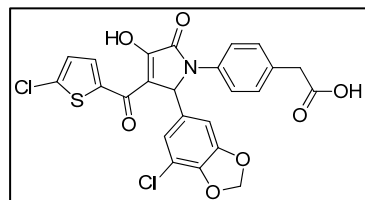
^1H NMR (500 MHz, acetone- d_6) δ 8.96 (s, 1H), 8.44 (d, $J = 1.2$ Hz, 1H), 7.93 (d, $J = 5.1$ Hz, 1H), 7.84 (d, $J = 6.7$ Hz, 1H), 7.60 – 7.41 (m, 1H), 7.12 (d, $J = 10.9$ Hz, 3H), 6.53 (s, 1H). ESI m/z : 565.5 ($[\text{M}-\text{H}]^-$, $\text{C}_{20}\text{H}_{11}\text{Br}_2\text{NO}_5\text{S}_2$ requires 565.8).



VPL-039: Imine 4 (40 mg, 0.12 mmol), ethyl 4-(5-bromothiophen-2-yl)-2,4-dioxobutanoate (37.6 mg, 0.12 mmol), and triethylamine (0.617 mmol) were combined in

dioxane and heated at reflux overnight. The crude reaction mixture was concentrated and partitioned between dichloromethane and 1N HCl. The organic layer was dried over Na_2SO_4 and concentrated under reduced pressure and purified by chromatography (0–100% Hexanes/Ethyl Acetate followed by 95% EtOAc, 2.5% H_2O , 2.5% formic acid) followed precipitation from ethyl acetate and hexanes to afford the desired product (21.2 mg white solid).

^1H NMR (500 MHz, acetone- d_6) δ 8.31 (s, 1H), 7.66 (dd, $J = 11.5, 8.3$ Hz, 2H), 7.33 (d, $J = 7.2$ Hz, 2H), 7.22 (d, $J = 23.7$ Hz, 3H), 6.56 (s, 1H), 3.61 (s, 2H). ESI m/z : 579.5 ($[\text{M}-\text{H}]^-$, $\text{C}_{21}\text{H}_{13}\text{Br}_2\text{NO}_5\text{S}_2$ requires 579.8).

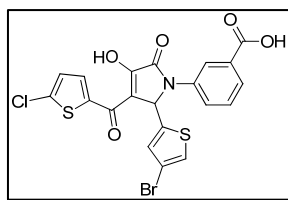


VPL-040: Imine 12 (73 mg, 0.23 mmol), ethyl 4-(5-chlorothiophen-2-yl)-2,4-dioxobutanoate (30 mg, 0.115 mmol), and triethylamine (0.575 mmol) were combined in

dioxane and heated to reflux overnight. The crude reaction mixture was concentrated and partitioned between dichloromethane and 1N HCl. The organic layer was dried

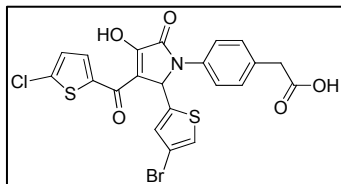
over Na₂SO₄ and concentrated under reduced pressure and purified by chromatography (0–100% Hexanes/Ethyl Acetate followed by 95% EtOAc, 2.5% H₂O, 2.5% formic acid) followed precipitation from tetrahydrofuran and toluene to afford the desired product (12.1 mg white solid).

¹H NMR (500 MHz, acetone-*d*₆) δ 9.22 (s, 1H), 7.71 (d, *J* = 7.9 Hz, 2H), 7.27 (d, *J* = 6.8 Hz, 2H), 7.20 – 7.06 (m, 1H), 6.93 (d, *J* = 19.3 Hz, 2H), 6.74 (s, 1H), 5.96 (s, 2H), 3.57 (s, 2H). ESI *m/z*: 529.7 ([M–H][–], C₂₄H₁₅Cl₂NO₇S requires 529.99).



VPL-041: Imine 11 (71mg, 0.23mmol), ethyl 4-(5-chlorothiophen-2-yl)-2,4-dioxobutanoate -diketoester (30 mg, 0.115 mmol), and triethylamine (0.575 mmol) were combined in ethanol and heated to reflux overnight. The crude reaction mixture was concentrated and partitioned between dichloromethane and 1N HCl. The organic layer was dried over Na₂SO₄ and concentrated under reduced pressure and purified by chromatography (0–100% Hexanes/Ethyl Acetate followed by 95% EtOAc, 2.5% H₂O, 2.5% formic acid) followed precipitation from ethyl acetate:hexanes to afford the desired product (9.8 mg off-white solid).

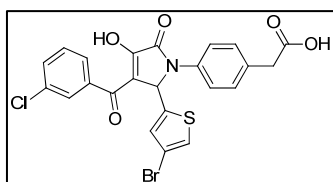
¹H NMR (500 MHz, acetone-*d*₆) δ 8.38 (s, 1H), 8.19 (d, *J* = 0.8 Hz, 1H), 7.92 (d, *J* = 7.8 Hz, 1H), 7.87 (d, *J* = 7.4 Hz, 1H), 7.54 (t, *J* = 7.8 Hz, 1H), 7.31 (s, 1H), 7.26 (s, 1H), 7.20 (s, 1H), 6.73 (s, 1H). ESI *m/z*: 521.6 ([M–H][–], C₂₀H₁₁BrClNO₅S₂ requires 521.9).



VPL-042: 4-aminophenyl acetic acid (59 mg, 0.38 mmol), 4-bromo-2-thiophenecarboxaldehyde (73 mg, 0.38 mmol), ethyl 4-(5-chlorothiophen-2-yl)-2,4-dioxobutanoate (50 mg, 0.19

mmol), and triethylamine (97 mg, 0.96 mmol) were combined in 2 ml of dioxane and heated at reflux overnight. The crude reaction mixture was concentrated and partitioned between dichloromethane and 1N HCl. The organic layer was dried over Na₂SO₄ and concentrated under reduced pressure and purified by chromatography (0–100% Hexanes/Ethyl Acetate followed by 95% EtOAc, 2.5% H₂O, 2.5% formic acid) followed precipitation from ethyl acetate:hexanes to afford the desired product (22.6 mg white solid).

¹H NMR (500 MHz, acetone-*d*₆) δ 8.18 (s, 1H), 7.65 (d, *J* = 8.5 Hz, 2H), 7.35 (d, *J* = 8.4 Hz, 2H), 7.31 (s, 1H), 7.25 (s, 1H), 7.20 (d, *J* = 3.0 Hz, 1H), 6.62 (s, 1H), 3.62 (s, 2H). ESI *m/z*: 535.6 ([*M*–H][–], C₂₁H₁₃BrClNO₅S₂ requires 535.9).

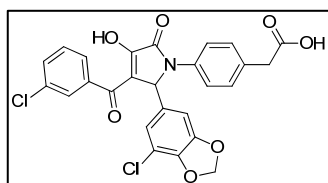


VPL-043: 4-aminophenyl acetic acid (59 mg, 0.38 mmol), 4-bromo-2-thiophenecarboxaldehyde (73 mg, 0.38 mmol), ethyl 4-(3-chlorophenyl)-2,4-dioxobutanoate (50 mg, 0.19 mmol),

and triethylamine (97 mg, 0.96 mmol) were combined in 2 ml of dioxane and heated at reflux overnight. The crude reaction mixture was concentrated and partitioned between dichloromethane and 1N HCl. The organic layer was dried over Na₂SO₄ and concentrated under reduced pressure and purified by chromatography (0–100%

Hexanes/Ethyl Acetate followed by 95% EtOAc, 2.5% H₂O, 2.5% formic acid) followed precipitation from acetone to afford the desired product (13.4 mg yellow solid).

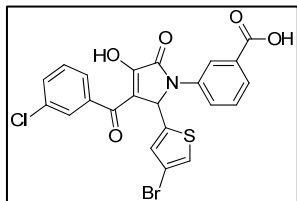
¹H NMR (500 MHz, thf) δ 7.85 (s, 1H), 7.78 (d, *J* = 7.6 Hz, 1H), 7.62 (d, *J* = 8.3 Hz, 2H), 7.55 (d, *J* = 7.9 Hz, 1H), 7.43 (t, *J* = 7.8 Hz, 1H), 7.28 (d, *J* = 8.3 Hz, 2H), 7.19 (s, 1H), 7.15 (s, 1H), 6.56 (s, 1H), 3.58 (s, 2H). ESI *m/z*: 529.6 ([*M*-H]⁻, C₂₃H₁₅BrClNO₅S requires 529.9).



VPL-044: 4-aminophenyl acetic acid (59mg, 0.393mmol), 7-chlorobenzo[d][1,3]dioxole-5-carbaldehyde (72mg, 0.393mmol), ethyl 4-(3-chlorophenyl)-2,4-dioxobutanoate

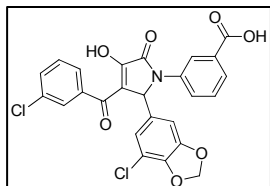
(50mg, 0.19mmol), and triethylamine (97mg, 0.96mmol) were combined in 2ml of dioxane and heated at reflux overnight. The crude reaction mixture was concentrated and partitioned between dichloromethane and 1N HCl. The organic layer was dried over Na₂SO₄ and concentrated under reduced pressure and purified by chromatography (0–100% Hexanes/Ethyl Acetate followed by 95% EtOAc, 2.5% H₂O, 2.5% formic acid) to afford the desired product (17.1 mg white solid).

¹H NMR (500 MHz, acetone-*d*₆) δ 7.87 (d, *J* = 1.6 Hz, 1H), 7.84 (d, *J* = 7.7 Hz, 1H), 7.67 (d, *J* = 8.5 Hz, 2H), 7.62 (d, *J* = 7.9 Hz, 1H), 7.54 – 7.48 (m, 1H), 7.32 (d, *J* = 8.5 Hz, 2H), 7.13 (s, 1H), 6.99 (s, 1H), 6.25 (s, 1H), 6.00 (d, *J* = 4.0 Hz, 2H), 3.60 (s, 2H). ESI *m/z*: 523.7 ([*M*-H]⁻, C₂₆H₁₇Cl₂NO₇ requires 524.0).



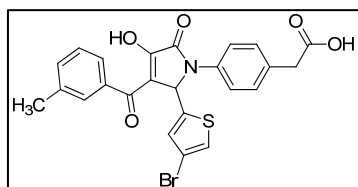
VPL-045: 3-aminobenzoic acid (54 mg, 0.393 mmol), 4-bromo-2-thiophenecarboxaldehyde (75 mg, 0.393 mmol), ethyl 4-(3-chlorophenyl)-2,4-dioxobutanoate (50 mg, 0.19 mmol), and triethylamine (97 mg, 0.96 mmol) were combined in 2ml of dioxane and heated at reflux overnight. The crude reaction mixture was concentrated and partitioned between dichloromethane and 1N HCl. The organic layer was dried over Na₂SO₄ and concentrated under reduced pressure and purified by chromatography (0–100% Hexanes/Ethyl Acetate followed by 95% EtOAc, 2.5% H₂O, 2.5% formic acid) to afford the desired product (15.8 mg white solid).

¹H NMR (500 MHz, thf-*d*₈) δ 8.35 (s, 1H), 7.87 (d, *J* = 7.9 Hz, 2H), 7.80 (t, *J* = 8.6 Hz, 2H), 7.55 (d, *J* = 7.9 Hz, 1H), 7.43 (t, *J* = 7.8 Hz, 2H), 7.20 (s, 1H), 7.16 (s, 1H), 6.64 (s, 1H). ESI *m/z*: 515.6 ([M–H][–], C₂₂H₁₃ BrClNO₅S requires 515.9).



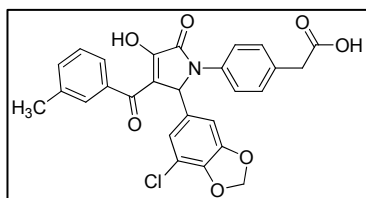
VPL-046: 3-aminobenzoic acid (54 mg, 0.39 mmol), 7-chlorobenzo[d][1,3]dioxole-5-carbaldehyde (72 mg, 0.39 mmol), α -diketoester (50 mg, 0.19 mmol), and triethylamine (97 mg, 0.96 mmol) were combined in 2 ml of dioxane and heated at reflux overnight. The crude reaction mixture was concentrated and partitioned between dichloromethane and 1N HCl. The organic layer was dried over Na₂SO₄ and concentrated under reduced pressure and purified by chromatography (0–100% Hexanes/Ethyl Acetate followed by 95% EtOAc, 2.5% H₂O, 2.5% formic acid) to afford the desired product.

^1H NMR (500 MHz, acetone- d_6) δ 8.42 (s, 1H), 7.97 – 7.87 (m, 2H), 7.83 (dd, J = 14.3, 7.6 Hz, 2H), 7.62 (d, J = 7.4 Hz, 1H), 7.51 (dd, J = 15.4, 7.6 Hz, 2H), 7.15 (s, 1H), 7.03 (s, 1H), 6.34 (s, 1H), 5.99 (d, J = 4.7 Hz, 2H). ESI m/z : 509.7 ($[\text{M}-\text{H}]^-$, $\text{C}_{25}\text{H}_{15}\text{Cl}_2\text{NO}_7$ requires 510.0).



VPL-047: 4-aminophenyl acetic acid (65 mg, 0.43 mmol), 4-bromo-2-thiophenecarboxaldehyde (82 mg, 0.43 mmol), ethyl 2, 4-dioxo-4-(*m*-tolyl)butanoate (50 mg, 0.213 mmol), and triethylamine (1.07 mmol) were combined in 2ml of dioxane and heated at reflux overnight. The crude reaction mixture was concentrated and partitioned between dichloromethane and 1N HCl. The organic layer was dried over Na_2SO_4 and concentrated under reduced pressure and purified by chromatography (0–100% Hexanes/Ethyl Acetate followed by 95% EtOAc, 2.5% H_2O , 2.5% formic acid) and rinsed with ether to afford the desired product.

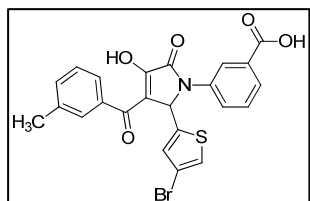
^1H NMR (500 MHz, acetone- d_6) δ 7.69 (dd, J = 12.8, 7.3 Hz, 4H), 7.46 – 7.37 (m, 2H), 7.35 (d, J = 8.4 Hz, 2H), 7.23 (s, 1H), 6.68 (s, 1H), 3.62 (s, 3H), 2.39 (s, 3H). ESI m/z : 509.7 ($[\text{M}-\text{H}]^-$, $\text{C}_{24}\text{H}_{18}\text{BrNO}_5\text{S}$ requires 510.0).



VPL-048: 4-aminophenyl acetic acid (65 mg, 0.43 mmol), 7-chlorobenzo[*d*][1,3]dioxole-5-carbaldehyde (79 mg, 0.427 mmol), ethyl 2,4-dioxo-4-(*m*-tolyl)butanoate (50 mg, 0.213

mmol), and triethylamine (1.07 mmol) were combined in 2ml of dioxane and heated at reflux overnight. The crude reaction mixture was concentrated and partitioned between dichloromethane and 1N HCl. The organic layer was dried over Na₂SO₄ and concentrated under reduced pressure and purified by chromatography (0–100% Hexanes/Ethyl Acetate followed by 95% EtOAc, 2.5% H₂O, 2.5% formic acid) to afford the desired product.

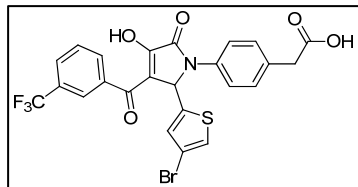
¹H NMR (500 MHz, acetone-*d*₆) δ 7.74 – 7.65 (m, 4H), 7.41 (d, J = 7.1 Hz, 1H), 7.37 (d, J = 7.7 Hz, 1H), 7.32 (d, J = 8.1 Hz, 2H), 7.09 (s, 1H), 6.94 (s, 1H), 6.27 (s, 1H), 6.01 (d, J = 4.4 Hz, 2H), 3.61 (s, 2H), 2.39 (s, 3H). ESI *m/z*: 503.8 ([M–H][–], C₂₇H₂₀ClNO₇ requires 504.0).



VPL-049: 3-aminobenzoic acid (59 mg, 0.427 mmol), 4-bromo-2-thiophenecarboxaldehyde (82 mg, 0.43 mmol), ethyl 2,4-dioxo-4-(*m*-tolyl)butanoate (50 mg, 0.213 mmol), and triethylamine (1.07 mmol) were combined in 2 ml of dioxane and heated at reflux

overnight. The crude reaction mixture was concentrated and partitioned between dichloromethane and 1N HCl. The organic layer was dried over Na₂SO₄ and concentrated under reduced pressure and purified by chromatography (0–100% Hexanes/Ethyl Acetate followed by 95% EtOAc, 2.5% H₂O, 2.5% formic acid) to afford the desired product.

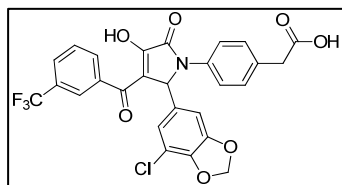
^1H NMR (500 MHz, acetone- d_6) δ 8.41 (d, J = 2.8 Hz, 1H), 7.97 – 7.90 (m, 1H), 7.90 – 7.83 (m, 1H), 7.71 (d, J = 4.6 Hz, 2H), 7.55 (dd, J = 13.3, 7.7 Hz, 1H), 7.46 – 7.35 (m, 2H), 7.32 (d, J = 4.3 Hz, 1H), 7.26 (d, J = 4.3 Hz, 1H), 6.79 (d, J = 5.2 Hz, 1H), 2.39 (d, J = 4.9 Hz, 3H). ESI m/z : 495.7 ($[\text{M}-\text{H}]^-$, $\text{C}_{23}\text{H}_{16}\text{BrNO}_5\text{S}$ requires 495.99).



VPL-050: 4-aminophenyl acetic acid (52.4 mg, 0.347 mmol), 4-bromo-2-thiophenecarboxaldehyde (66.3 mg, 0.347 mmol), ethyl 2,4-dioxo-4-(3-(trifluoromethyl)phenyl)butanoate (50

mg, 0.173 mmol), and triethylamine (1.07 mmol) were combined in 2 ml of dioxane and heated at reflux overnight. The crude reaction mixture was concentrated and partitioned between dichloromethane and 1N HCl. The organic layer was dried over Na_2SO_4 and concentrated under reduced pressure and purified by chromatography (0–100% Hexanes/Ethyl Acetate followed by 95% EtOAc, 2.5% H_2O , 2.5% formic acid) to afford the desired product.

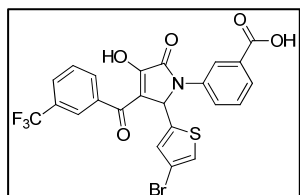
^1H NMR (400 MHz, acetone- d_6) δ 8.17 (d, J = 7.7 Hz, 2H), 7.95 (d, J = 7.7 Hz, 1H), 7.77 (t, J = 7.7 Hz, 1H), 7.67 (d, J = 8.3 Hz, 2H), 7.36 (d, J = 8.3 Hz, 2H), 7.32 (s, 1H), 7.29 (s, 1H), 6.68 (s, 1H), 3.62 (s, 2H). ESI m/z : 563.6 ($[\text{M}-\text{H}]^-$, $\text{C}_{24}\text{H}_{15}\text{BrF}_3\text{NO}_5\text{S}$ requires 563.98).



VPL-051: 4-aminophenylacetic acid (52 mg, 0.35mmol), 7-chlorobenzo[d][1,3]dioxole-5-carbaldehyde (64mg, 0.35mmol), ethyl 2,4-dioxo-4-(3-(trifluoromethyl)phenyl)butanoate (50 mg,

0.17 mmol), and triethylamine (97 mg, 0.96 mmol) were combined in 2ml of dioxane and heated at reflux overnight. The crude reaction mixture was concentrated and partitioned between dichloromethane and 1N HCl. The organic layer was dried over Na₂SO₄ and concentrated under reduced pressure and purified by chromatography (0–100% Hexanes/Ethyl Acetate followed by 95% EtOAc, 2.5% H₂O, 2.5% formic acid) to afford the desired product.

¹H NMR (500 MHz, acetone-*d*₆) δ 8.17 (d, *J* = 7.2 Hz, 2H), 7.93 (d, *J* = 7.7 Hz, 1H), 7.73 (t, *J* = 7.6 Hz, 1H), 7.68 (d, *J* = 8.5 Hz, 2H), 7.32 (d, *J* = 8.4 Hz, 2H), 7.14 (s, 1H), 7.01 (s, 1H), 6.28 (s, 1H), 5.99 (d, *J* = 3.1 Hz, 2H), 3.59 (s, 2H). ESI *m/z*: 557.7 ([M–H][–], C₂₇H₁₇ClF₃NO₇ requires 558.0).

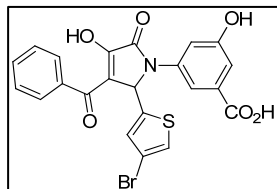


VPL-052: Imine 11 (54mg, 0.17mmol), ethyl 2,4-dioxo-4-(3-(trifluoromethyl)phenyl)butanoate (50 mg, 0.17 mmol), and triethylamine (0.87 mmol) were combined in dioxane and heated

to reflux overnight. The crude reaction mixture was concentrated and partitioned between dichloromethane and 1N HCl. The organic layer was dried over Na₂SO₄ and concentrated under reduced pressure and purified by chromatography (0–100% Hexanes/Ethyl Acetate followed by 95% EtOAc, 2.5% H₂O, 2.5% formic acid) followed precipitation from ethyl acetate:hexanes to afford the desired product.

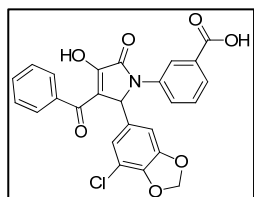
¹H NMR (500 MHz, acetone-*d*₆) δ 8.41 (s, 1H), 8.18 (d, *J* = 8.4 Hz, 2H), 7.95 (t, *J* = 8.7 Hz, 2H), 7.87 (d, *J* = 7.7 Hz, 1H), 7.77 (t, *J* = 7.6 Hz, 1H), 7.55 (t, *J* = 7.9 Hz, 1H), 7.32

(d, $J = 9.8$ Hz, 1H), 6.77 (s, 1H). ESI m/z : 549.6 ($[M-H]^-$, $C_{23}H_{13}BrF_3NO_5S$ requires 549.96).



VPL-053: Prepared analogously to VPL-001. The crude reaction mixture was concentrated, and partitioned between DCM and 1M HCl (3x). Upon standing, a light colored precipitate fell out of the organic extract. The tan solid was collected via filtration. LC/MS and ¹H NMR revealed this precipitate to be the desired product (18.8 mg, 17%).

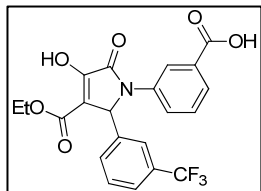
¹H NMR (d_4 -MeOH, 500 MHz) $\delta = 7.82$ (d, 2H, $J = 8.0$ Hz), 7.71 (s, 1H), 7.58 (t, 1H, $J = 7.0$ Hz), 7.47 (app. t, 2H, $J = 7.5$ Hz), 7.29 (s, 1H), 7.28 (d, 1H, $J = 1.5$ Hz), 7.203 (s, 1H), 7.08 (s, 1H), 6.55 (s, 1H). ESI m/z : 497.6 ($[M-H]^-$, $C_{22}H_{13}BrNO_6S$ requires 498.0).



VPL-055: 3-aminobenzoic acid (31 mg, 0.227mmol), 7-chlorobenzo[d][1,3]dioxole-5-carbaldehyde (42mg, 0.227mmol), ethyl 2,4-dioxo-4-phenylbutanoate (50mg, 0.227 mmol), and

triethylamine (1.13 mmol) were combined in 2 ml of dioxane and heated at reflux overnight. The crude reaction mixture was concentrated and partitioned between dichloromethane and 1N HCl. The organic layer was dried over Na_2SO_4 and concentrated under reduced pressure and purified by chromatography (0–100% Hexanes/Ethyl Acetate followed by 95% EtOAc, 2.5% H_2O , 2.5% formic acid) to afford the desired product.

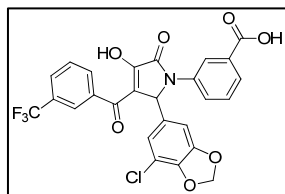
^1H NMR (500 MHz, acetone- d_6) δ 8.43 (s, 1H), 7.91 (d, J = 6.8 Hz, 3H), 7.81 (d, J = 7.6 Hz, 1H), 7.60 (t, J = 7.2 Hz, 1H), 7.50 (q, J = 7.6 Hz, 3H), 7.12 (s, 1H), 6.99 (s, 1H), 6.36 (s, 1H), 5.99 (d, J = 4.0 Hz, 2H). ESI m/z : 475.7 ($[\text{M}-\text{H}]^-$, $\text{C}_{25}\text{H}_{16}\text{ClNO}_7$ requires 476.0).



VPL-056: 3-(trifluoromethyl)benzaldehyde (348 mg, 2.0 mmol), 3-aminobenzoic acid (274 mg, 2.0 mmol), diethyl oxalacetate (188 mg, 1.0 mmol), and triethylamine (5.0 mmol) were dissolved in 5ml

of dioxane and heated to reflux overnight. The crude reaction mixture was concentrated and partitioned between dichloromethane and 1N HCl. The organic layer was dried over Na_2SO_4 and concentrated under reduced pressure and purified by chromatography (0–100% Hexanes/Ethyl Acetate followed by 95% EtOAc, 2.5% H_2O , 2.5% formic acid) to afford the desired product.

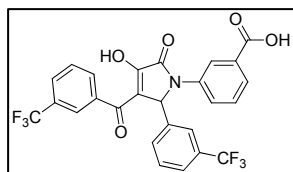
^1H NMR (500 MHz, acetone- d_6) δ 8.35 (s, 1H), 7.96 – 7.85 (m, 2H), 7.77 (d, J = 7.7 Hz, 1H), 7.68 (d, J = 7.3 Hz, 1H), 7.57 (d, J = 7.3 Hz, 1H), 7.52 (t, J = 7.6 Hz, 1H), 7.45 (t, J = 7.9 Hz, 1H), 6.30 (s, 1H), 4.15 (dd, J = 9.8, 7.4 Hz, 2H), 1.16 (t, J = 7.1 Hz, 3H). ESI m/z : 433.8 ($[\text{M}-\text{H}]^-$, $\text{C}_{21}\text{H}_{16}\text{F}_3\text{NO}_6$ requires 434.1).



VPL-057: 3-aminobenzoic acid (48 mg, 0.35 mmol), 7-chlorobenzo[d][1,3]dioxole-5-carbaldehyde (64 mg, 0.35 mmol),

ethyl 2,4-dioxo-4-(3-(trifluoromethyl)phenyl)butanoate (50 mg, 0.17 mmol), and triethylamine (0.87 mmol) were combined in 3ml of dioxane and heated at reflux overnight. The crude reaction mixture was concentrated and partitioned between dichloromethane and 1N HCl. The organic layer was dried over Na₂SO₄ and concentrated under reduced pressure and purified by chromatography (0–100% Hexanes/Ethyl Acetate followed by 95% EtOAc, 2.5% H₂O, 2.5% formic acid) to afford the desired product.

¹H NMR (500 MHz, acetone-*d*₆) δ 8.43 (d, *J* = 0.5 Hz, 1H), 8.19 (s, 2H), 7.92 (d, *J* = 7.7 Hz, 2H), 7.81 (d, *J* = 7.6 Hz, 1H), 7.77 – 7.66 (m, 1H), 7.50 (t, *J* = 7.6 Hz, 1H), 7.16 (s, 1H), 7.03 (s, 1H), 6.34 (s, 1H), 5.99 (s, 2H). ESI *m/z*: 543.7 ([M–H][–], C₂₆H₁₅F₃NO₇ requires 544.0).

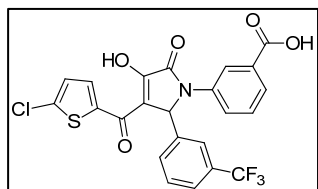


VPL-058: 3-aminobenzoic acid (47 mg, 0.35 mmol), 3-(trifluoromethyl)benzaldehyde (60 mg, 0.35 mmol), ethyl 2,4-dioxo-4-(3-(trifluoromethyl)phenyl)butanoate (50 mg, 0.17 mmol),

and triethylamine (0.87 mmol) were combined in 2 ml of dioxane and heated at reflux overnight. The crude reaction mixture was concentrated and partitioned between dichloromethane and 1N HCl. A precipitant was formed during the work-up, which was filtered and dried to afford the desired product. (59 mg white solid).

¹H NMR (500 MHz, acetone-*d*₆) δ 8.41 (s, 1H), 8.15 (d, *J* = 6.6 Hz, 2H), 7.98 (s, 1H), 7.93 (dd, *J* = 6.4, 4.2 Hz, 2H), 7.87 (d, *J* = 7.0 Hz, 1H), 7.79 (d, *J* = 7.7 Hz, 1H), 7.74 (t,

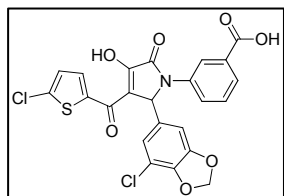
$J = 8.0$ Hz, 1H), 7.53 – 7.45 (m, 3H), 6.57 (s, 1H). ESI m/z : 533.8 ($[M-H]^-$, $C_{26}H_{15}F_6NO_5$ requires 534.09).



VPL-059: 3-aminobenzoic acid (53 mg, 0.38 mmol), 3-(trifluoromethyl)benzaldehyde (67 mg, 0.38 mmol), ethyl 2,4-dioxo-4-(3-(trifluoromethyl)phenyl)butanoate (50 mg, 0.19 mmol), and triethylamine (0.96 mmol) were combined in 2 ml of

dioxane and heated at reflux overnight. The crude reaction mixture was concentrated and partitioned between dichloromethane and 1N HCl. The organic layer was dried over Na_2SO_4 and concentrated under reduced pressure and purified by chromatography (0–100% Hexanes/Ethyl Acetate followed by 95% EtOAc, 2.5% H_2O , 2.5% formic acid) to afford the desired product.

1H NMR (500 MHz, acetone- d_6) δ 8.39 (s, 1H), 8.16 (d, $J = 4.2$ Hz, 1H), 7.92 (dd, $J = 8.1, 1.2$ Hz, 1H), 7.89 (s, 1H), 7.78 (d, $J = 7.7$ Hz, 2H), 7.51 (d, $J = 7.8$ Hz, 1H), 7.47 (t, $J = 8.0$ Hz, 2H), 7.18 (d, $J = 4.2$ Hz, 1H), 6.51 (s, 1H). ESI m/z : 506.7 ($[M-H]^-$, $C_{23}H_{13}ClF_3NO_5S$ requires 506.0).

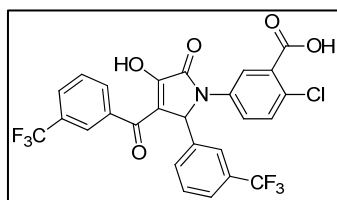


VPL-060: 3-aminobenzoic acid (53 mg, 0.38 mmol), 7-chlorobenzo[d][1,3]dioxole-5-carbaldehyde (71 mg, 0.38 mmol), ethyl 4-(5-chlorothiophen-2-yl)-2,4-dioxobutanoate (50 mg, 0.19

mmol), and triethylamine (97 mg, 0.96 mmol) were combined in 2 ml of dioxane and heated at reflux overnight. The crude reaction mixture was concentrated and partitioned

between dichloromethane and 1N HCl. A white precipitate formed in the DCM layer which was filtered and rinsed with cold DCM to afford the desired product (30.1 mg).

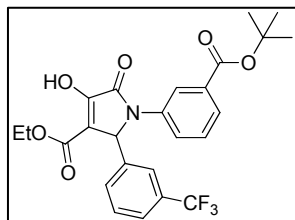
^1H NMR (500 MHz, acetone- d_6) δ 8.40 (d, J = 1.5 Hz, 1H), 8.18 (d, J = 4.1 Hz, 1H), 7.90 (dd, J = 8.1, 2.0 Hz, 1H), 7.81 (d, J = 7.7 Hz, 1H), 7.50 (t, J = 7.9 Hz, 1H), 7.19 (d, J = 4.1 Hz, 1H), 7.10 (d, J = 1.4 Hz, 1H), 6.94 (d, J = 1.5 Hz, 1H), 6.30 (s, 1H), 6.00 (d, J = 1.1 Hz, 2H). ESI m/z : 515.6 ($[\text{M}-\text{H}]^-$, $\text{C}_{23}\text{H}_{13}\text{Cl}_2\text{NO}_7\text{S}$ requires 515.0).



VPL-061: 3-(trifluoromethyl)benzaldehyde (47 mg, 0.27 mmol), 5-amino-2-chloro-benzoic acid (46 mg, 0.27 mmol), and ethyl 2,4-dioxo-4-(3-(trifluoromethyl)phenyl)butanoate (39 mg,

0.135 mmol), and triethylamine (68 mg, 0.67 mmol) were combined in dioxane and heated at reflux overnight. The crude reaction mixture was concentrated and partitioned between dichloromethane and 1N HCl. A white precipitate formed in the DCM layer which was filtered and rinsed with cold DCM to afford the desired product (32 mg).

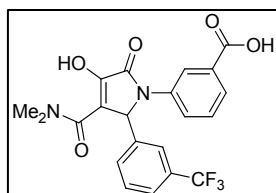
^1H NMR (500 MHz, acetone- d_6) δ 8.30 (d, J = 2.7 Hz, 1H), 8.13 (s, 2H), 8.00 (s, 1H), 7.93 (d, J = 7.8 Hz, 1H), 7.90 – 7.84 (m, 2H), 7.73 (t, J = 8.0 Hz, 1H), 7.53 (t, J = 6.7 Hz, 1H), 7.49 (d, J = 8.7 Hz, 2H), 6.55 (s, 1H). ESI m/z : 567.7 ($[\text{M}-\text{H}]^-$, $\text{C}_{26}\text{H}_{14}\text{ClF}_6\text{NO}_5$ requires 568.0)



VPL-062: Diethyl oxalacetate (75 mg, 0.399 mmol), tert-butyl-3-aminobenzoate (154 mg, 0.8 mmol), 3-trifluoromethylbenzaldehyde (139 mg, 0.8 mmol), and triethylamine (202 mg, 1.99 mmol) were combined in 3ml dioxane

and heated at reflux overnight. The crude reaction mixture was concentrated and partitioned between dichloromethane and 1N HCl. The organic layer was concentrated and dried over Na₂SO₄ and concentrated under reduced pressure and purified by chromatography (0–100% Hexanes/Ethyl Acetate followed by 95% EtOAc, 2.5% H₂O, 2.5% formic acid) to afford the desired product (27 mg tan solid).

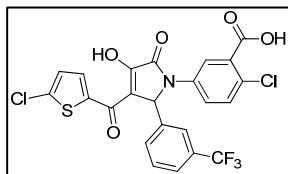
¹H NMR (500 MHz, acetone-*d*₆) δ 8.21 (s, 1H), 7.93 (d, *J* = 7.4 Hz, 1H), 7.70 – 7.63 (m, 2H), 7.57 (d, *J* = 6.1 Hz, 1H), 7.52 (d, *J* = 8.3 Hz, 1H), 7.41 (t, *J* = 7.9 Hz, 1H), 6.25 (s, 1H), 4.14 (dd, *J* = 14.6, 7.0 Hz, 2H), 1.56 (s, 9H), 1.14 (t, *J* = 6.3 Hz, 3H). ESI *m/z*: 489.8 ([M-H]⁻, C₂₅H₂₄F₃NO₆ requires 490.0).



VPL-063: 3-aminobenzoic acid (73 mg, 0.534 mmol), 3-(trifluoromethyl)benzaldehyde (93 mg, 0.534 mmol), ethyl 4-(dimethylamino)-2,4-dioxobutanoate (50 mg, 0.267 mmol), and

triethylamine (1.33 mmol) were combined in 2 ml of dioxane and heated at reflux overnight. The crude reaction mixture was concentrated and partitioned between dichloromethane and 1N HCl.

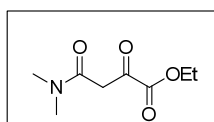
¹H NMR (500 MHz, acetone-*d*₆) δ 8.41 (s, 1H), 7.88 (d, *J* = 7.5, 1H), 7.79 (s, 1H), 7.75 (d, *J* = 7.3, 1H), 7.70 (d, *J* = 7.0, 1H), 7.57 (d, *J* = 7.0, 1H), 7.51 (t, *J* = 7.3, 1H), 7.44 (t, *J* = 7.7, 1H), 6.40 (s, 1H), 2.91 (s, 6H). ESI *m/z*: 432.8 ([M-H]⁻, C₂₁H₁₇F₃N₂O₅ requires 490.0).



VPL-064: Imine 13 (126mg, 0.38mmol), ethyl 4-(5-chlorothiophen-2-yl)-2,4-dioxobutanoate (50 mg, 0.19 mmol), and triethylamine (0.96 mmol) were combined in dioxane and heated to reflux

overnight. The crude reaction mixture was concentrated and partitioned between dichloromethane and 1N HCl. The organic layer was dried over Na₂SO₄ and concentrated under reduced pressure and purified by chromatography (0–100% Hexanes/Ethyl Acetate followed by 95% EtOAc, 2.5% H₂O, 2.5% formic acid) followed precipitation from ethyl acetate:hexanes to afford the desired product.

¹H NMR (500 MHz, acetone-*d*₆) δ 8.29 (d, *J* = 2.6, 1H), 8.15 (d, *J* = 4.1, 1H), 7.92 (s, 1H), 7.87 (dd, *J* = 2.6, 8.8, 1H), 7.79 (d, *J* = 7.6, 1H), 7.54 (d, *J* = 7.7, 1H), 7.49 (t, *J* = 7.3, 2H), 7.18 (d, *J* = 4.1, 1H), 6.50 (s, 1H). ESI *m/z*: 539.7 ([M-H]⁻, C₂₃H₁₂Cl₂F₃NO₅S requires 539.98).



Ethyl 4-(dimethylamino)-2,4-dioxobutanoate(2)

To a dry round bottom flask was added dimethylacetamide (11.48mmol) and 60ml of dry THF. The mixture was cooled to -78C in a dry ice/acetone bath. Lithium diisopropylamide (12.62mmol) was added drop wise, so that the temperature of the flask did not exceed -70C. The mixture was stirred for 10 minutes before the addition of diethyl oxalate (11.48mmol) in 5ml of THF (drop wise). The mixture was warmed to room temperature and stirred for 12 hours, re-cooled to -78C

and a solution of acetic acid in THF was added. After warming to room temperature the reaction was partitioned between water and diethyl ether. The aqueous layer was extracted 3X. The combined organic extracts were dried Na_2SO_4 , concentrated and purified by chromatography (0–100% Hexanes/Ethyl Acetate) to afford the desired product.

^1H NMR (500 MHz, CDCl_3) δ 6.25 (s, 1H), 4.34 (q, $J = 7.0$ Hz, 2H), 3.06 (d, $J = 27.8$ Hz, 7H), 1.36 (t, $J = 7.1$ Hz, 4H).

References

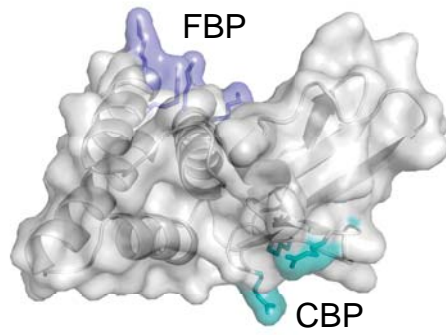
1. Weisse K, H. (1911) Action of Sulfur Monochloride and of Sulfuryl Chloride on Piperonaldehyde. *Chem. Berichte*, 43:2605-2606.
2. Goldup SM, Pilkington CJ, White AJ, Burton A, & Barrett AG (2006) A simple, short, and flexible synthesis of viridifungin derivatives. (Translated from eng) *J Org Chem* 71(16):6185-6191 (in eng).

Supplementary Tables

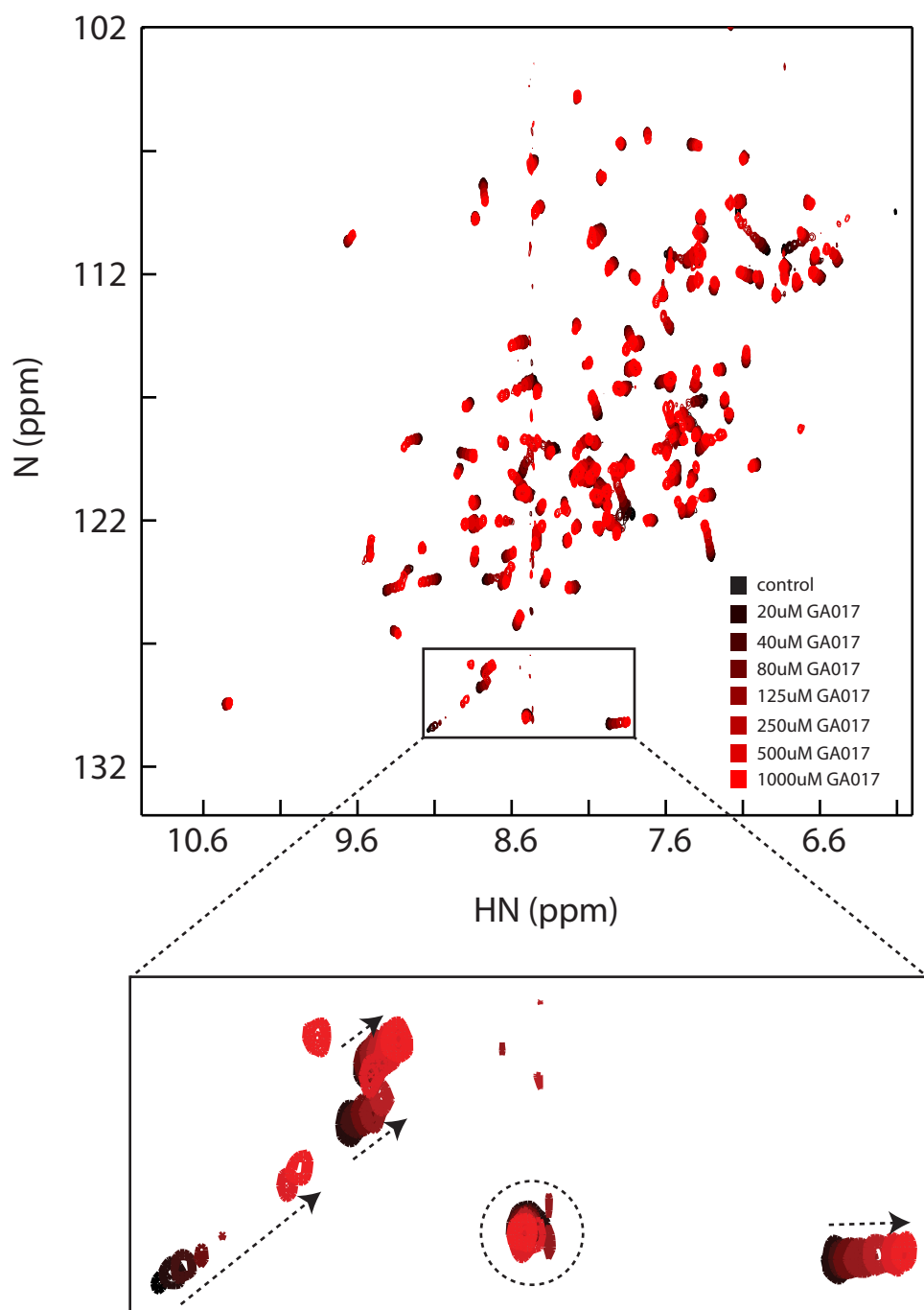
Supplementary Table 1. Effect of functional groups of the pyrrolidinone scaffold on the potency of small molecule binding. Dissociation constants (K_D) are measured by NMR.

Supplementary Table 2. Small molecules arranged by functional groups. Same compounds as Supplementary Table 1 arranged according to the different functional groups at ring B, C, and D.

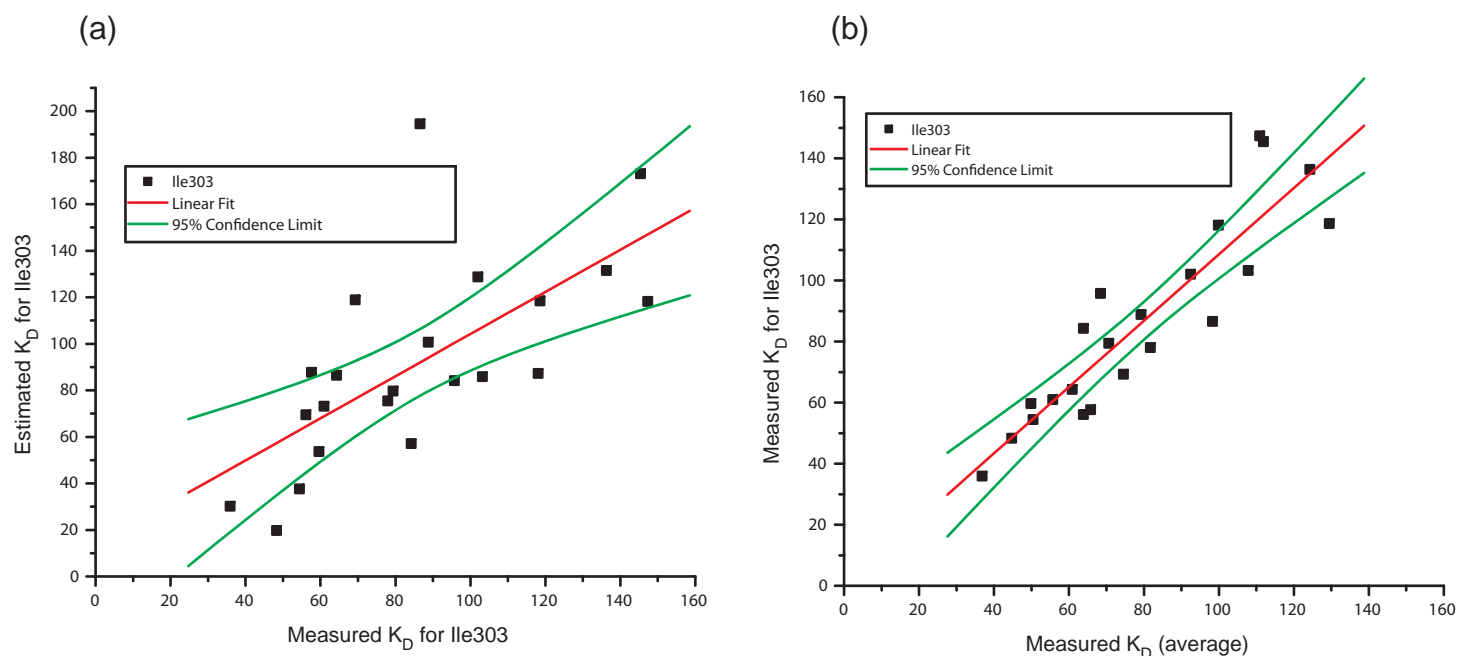
SI Figures



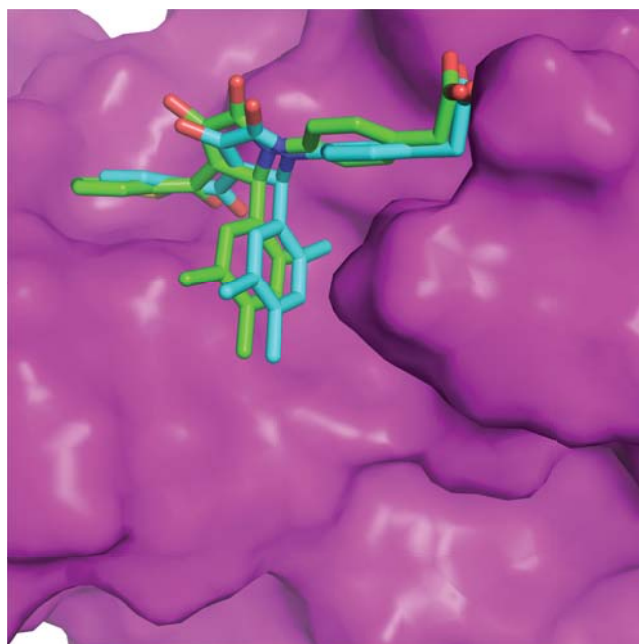
Supplementary Fig. 1. Filoviral VP35 IIDs contain two highly conserved basic patches termed Central Basic Patch (CBP) and First Basic Patch (FBP). Surface representation of VP35 IID with CBP and FBP labeled.



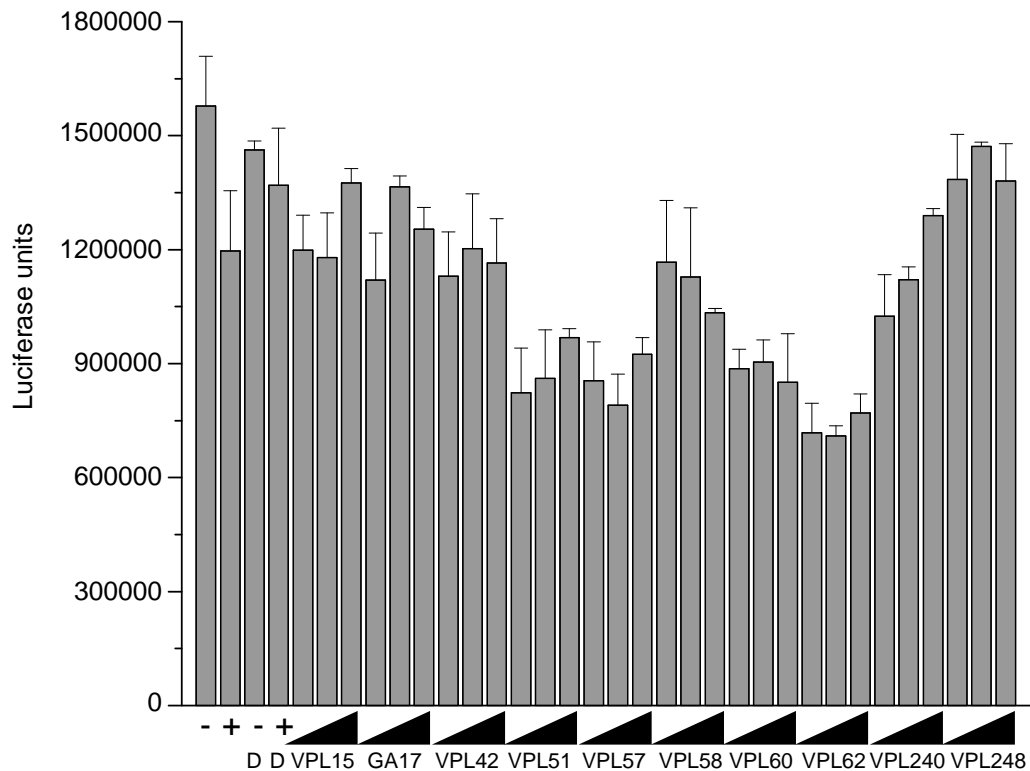
Supplementary Fig. 2. GA017-VP35 eIID interactions are in the fast exchange regime. 1H-15N HSQC spectrum of 15N-enriched eIID in the absence (black) or presence of increasing concentrations (dark red to light red) of GA017.



Supplementary Fig. 3. Chemical shift of I303 residue serves as a reliable reporter for estimating binding affinity from HSQC data. Correlation coefficients for:(a) estimated binding affinity from single point Ile303 chemical shift changes vs. measured binding affinity from Ile303 titration data ($r^2 = 0.91 \pm 0.22$), and (b) measured binding affinity from Ile303 titration data vs. measured binding affinity from averaged titration data for several residues in the binding pocket ($r^2 = 1.09 \pm 0.11$).

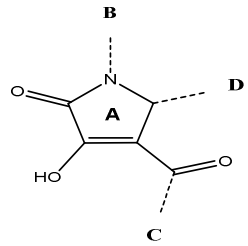
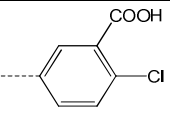
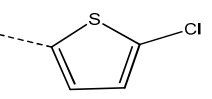
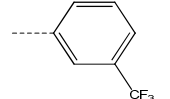
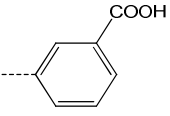
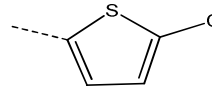
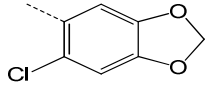
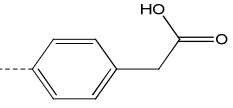
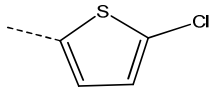
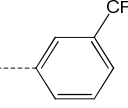
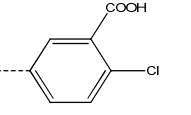
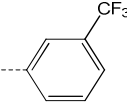
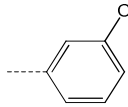
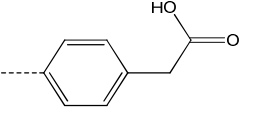
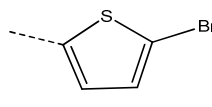
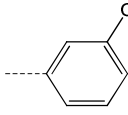
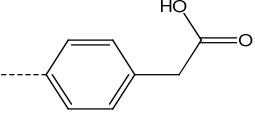
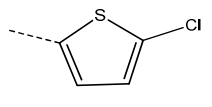
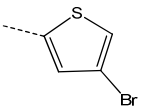
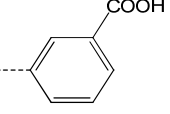
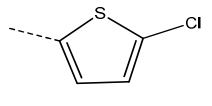
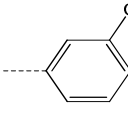
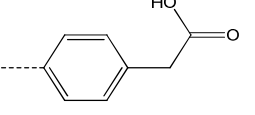
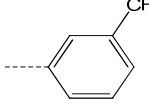
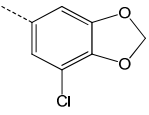


Supplementary Fig. 4. Docked structures closely resemble experimentally derived ligand bound complexes. Docked (green) and experimentally derived structures (blue) of GA017.

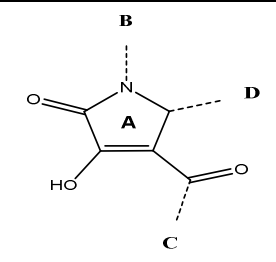
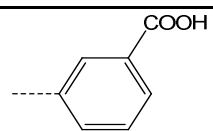
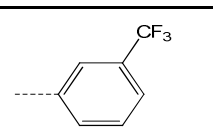
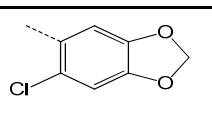
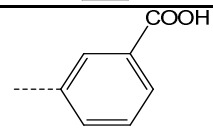
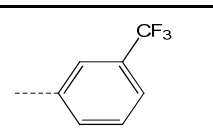
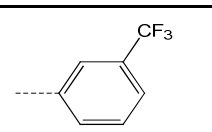
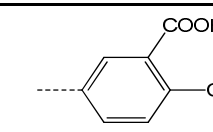
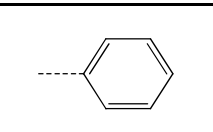
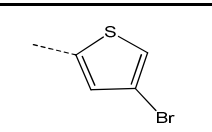
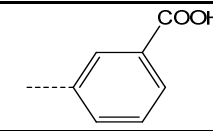
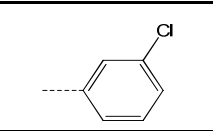
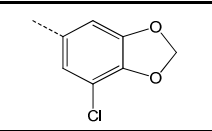
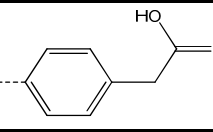
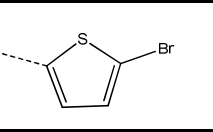
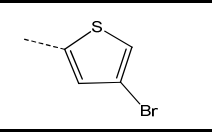
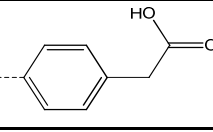
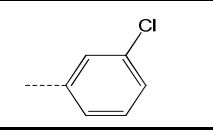
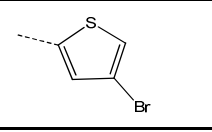
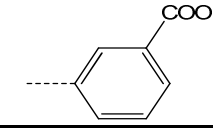
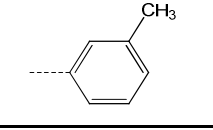
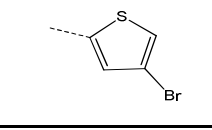
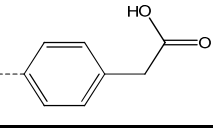
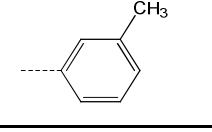
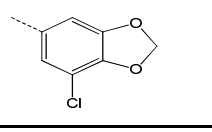


Supplementary Fig. 5. Firefly luciferase activity does not show a dose dependence with increasing compound concentrations. Experimentally measured Firefly luciferase levels for control and experimental conditions. Plus/minus indicate experiments with and without VP35. DMSO (D) lanes are with the addition of 0.5% DMSO, which was the highest concentration used in these assays as a co-solvent. Error bars represent standard errors in triplicate experiments. For each compound the Firefly luciferase activity between different doses is not statistically significant.

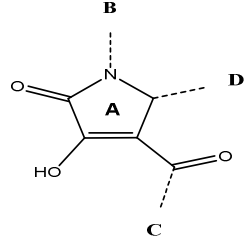
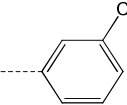
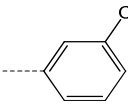
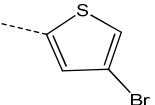
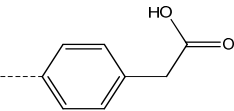
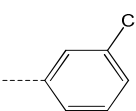
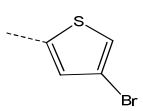
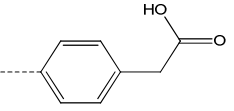
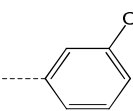
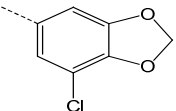
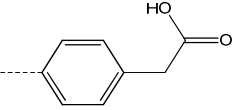
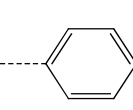
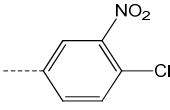
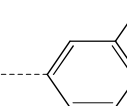
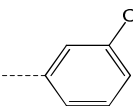
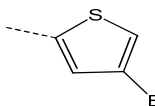
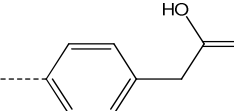
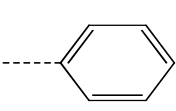
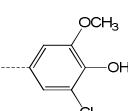
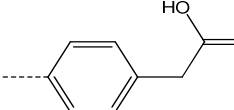
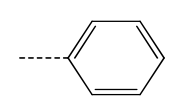
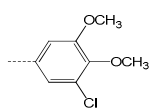
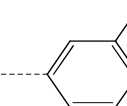
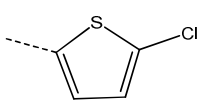
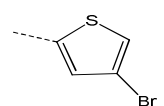
Supplementary Table 1: Substructures by potency

Scaffold					
	smx	K_D (μM , estimate)	K_D (μM , NMR)	N1 (B)	4-keto (C)
VPL-64	30 ± 7	58.90 ± 21.1			
VPL-60	33 ± 7	50.4 ± 4.7			
VPL-36	36 ± 13	49.9 ± 9.8			
VPL-61	36 ± 10	38.7 ± 16.0			
VPL-34	39 ± 16	63.9 ± 17.7			
VPL-42	46 ± 19	36.8 ± 8.1			
VPL-59	47 ± 38	55.7 ± 4.9			
VPL-51	49 ± 35	44.8 ± 3.2			

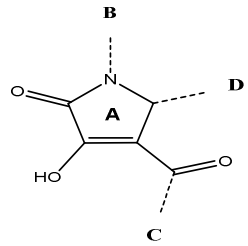
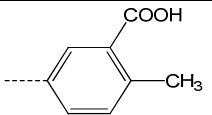
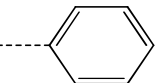
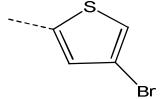
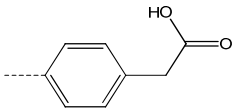
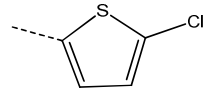
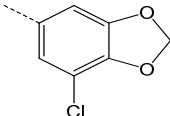
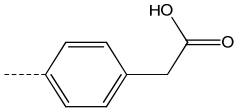
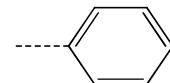
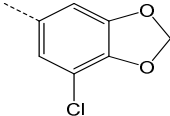
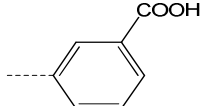
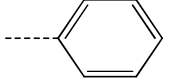
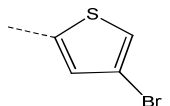
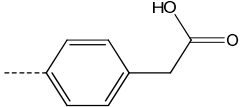
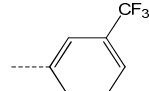
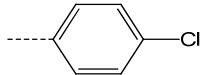
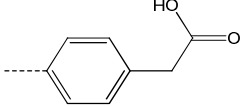
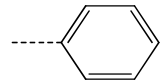
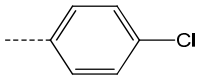
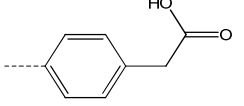
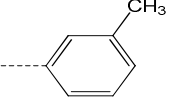
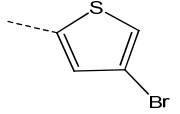
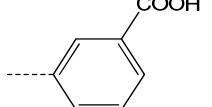
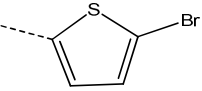
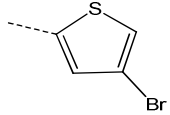
Supplementary Table 1: Substructures by potency

Scaffold					
	smx	K_D (μM , estimate)	K_D (μM , NMR)	N1 (B)	4-keto (C)
VPL-57	52 ± 10	73.0 ± 31.0			
VPL-58	52 ± 45	47.0 ± 4.0			
VPL-29	60 ± 16	70.6 ± 7.9			
VPL-46	63 ± 18	68.5 ± 33.0			
VPL-39	70 ± 14	65.8 ± 10.2			
VPL-43	77 ± 15	81.7 ± 6.1			
VPL-49	79 ± 17	79.2 ± 8.5			
VPL-48	79 ± 3	108.0 ± 7.0			

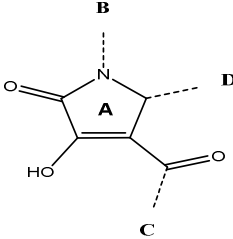
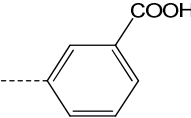
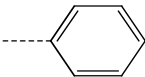
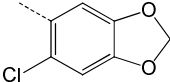
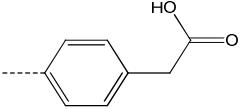
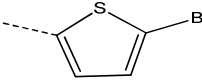
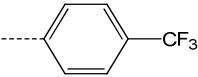
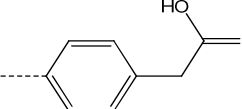
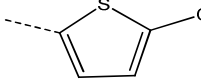
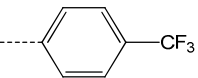
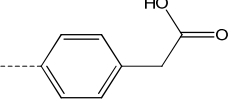
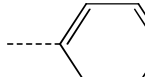
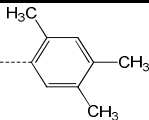
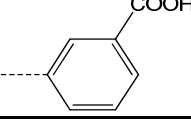
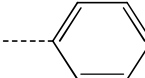
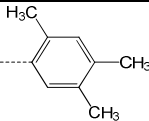
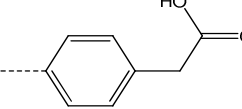
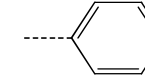
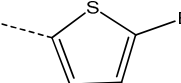
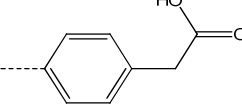
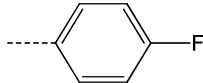
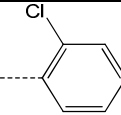
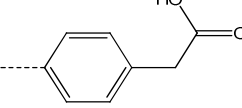
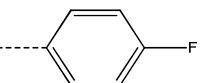
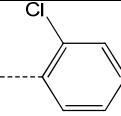
Supplementary Table 1: Substructures by potency

Scaffold					
	smx	K_D (μM , estimate)	K_D (μM , NMR)	N1 (B)	4-keto (C)
VPL-52	80 ± 3	60.9 ± 3.0			
VPL-50	80 ± 26	63.9 ± 7.4			
VPL-44	89 ± 14	99.9 ± 25.9			
GA312=GA259	101 ± 40	103.8 ± 41.7			
VPL-45	101 ± 25	92.5 ± 8.4			
VPL-33	109 ± 2	110.9 ± 41.2			
VPL-37	117 ± 12	74.6 ± 14.5			
VPL-41	120 ± 11	129.5 ± 35.1			

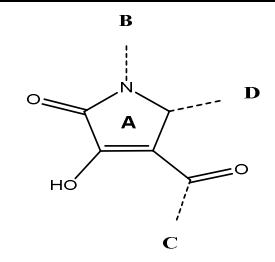
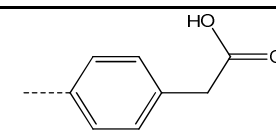
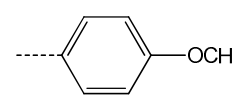
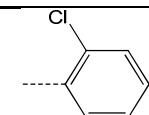
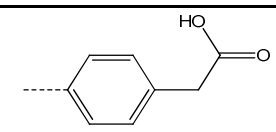
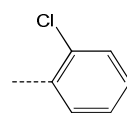
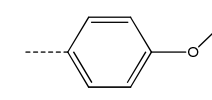
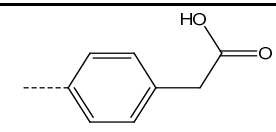
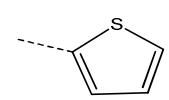
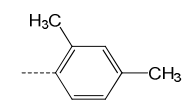
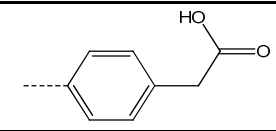
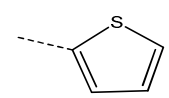
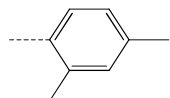
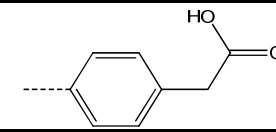
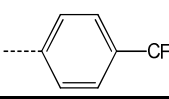
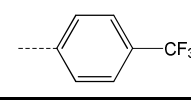
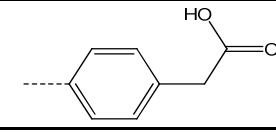
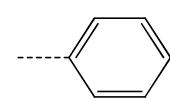
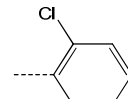
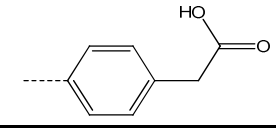
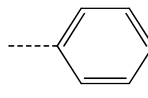
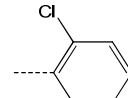
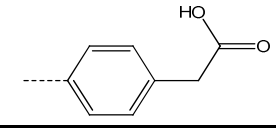
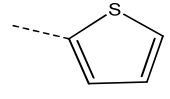
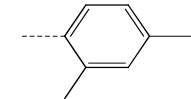
Supplementary Table 1: Substructures by potency

Scaffold					
	smx	K_D (μM , estimate)	K_D (μM , NMR)	N1 (B)	4-keto (C)
VPL-27	124 ± 36	214.6 ± 24.9			
VPL-40	126 ± 32	369.8 ± 173.3			
GA228=GA292	127 ± 5	291.9 ± 17.5			
GA272	128 ± 34	111.9 ± 30.7			
VPL-11	134 ± 11	124.3 ± 16.2			
VPL-32	135 ± 44	280.2 ± 51.2			
VPL-47	138 ± 40				
VPL-38	149 ± 45	98.0 ± 36.0			

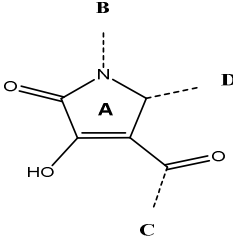
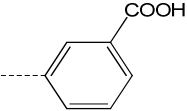
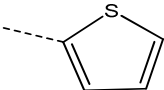
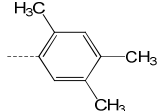
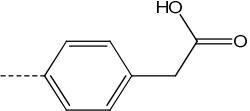
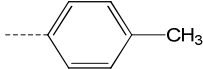
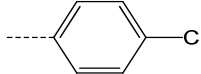
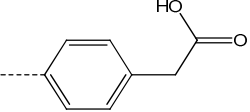
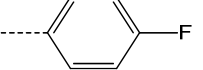
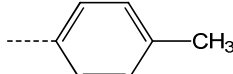
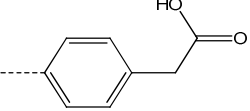
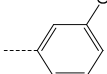
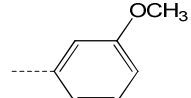
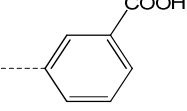
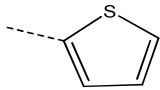
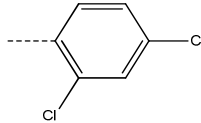
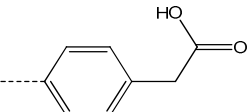
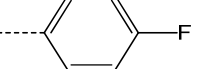
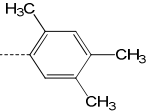
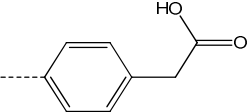
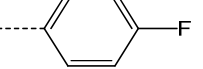
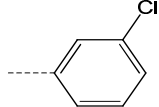
Supplementary Table 1: Substructures by potency

Scaffold					
smx	K_D (μM , estimate)	K_D (μM , NMR)	N1 (B)	4-keto (C)	5-aryl (D)
VPL-55	152 ± 40				
VPL-23	161 ± 86				
VPL-24	161 ± 82				
GA307	179 ± 72				
GA307	179 ± 72				
GA272-B	204 ± 28	114.1 ± 20.6			
GA286	238 ± 48				
GA286	238 ± 48				

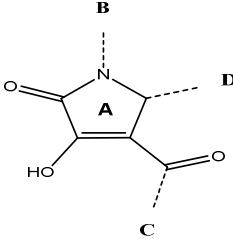
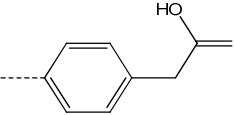
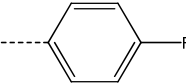
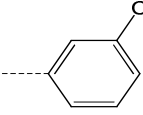
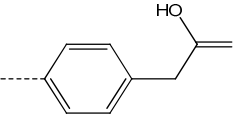
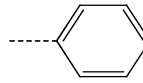
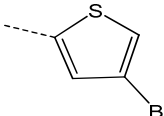
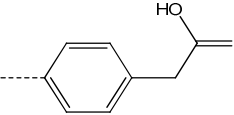
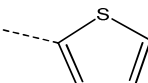
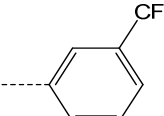
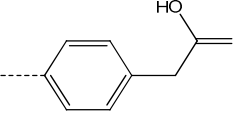
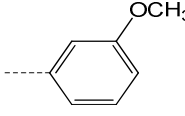
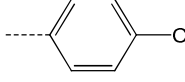
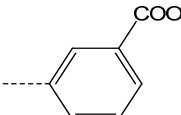
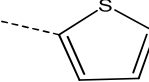
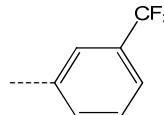
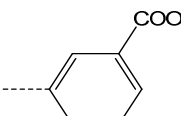
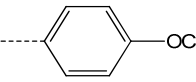
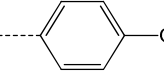
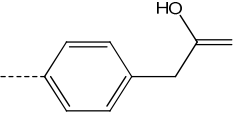
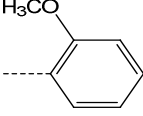
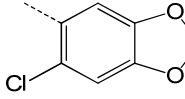
Supplementary Table 1: Substructures by potency

Scaffold						
	smx	K_D (μM , estimate)	K_D (μM , NMR)	N1 (B)	4-keto (C)	5-aryl (D)
GA315	260 ± 49					
GA315	260 ± 49					
GA274=GA322	264 ± 63					
GA274	264 ± 63					
VPL-21	266 ± 47					
GA294	275 ± 39					
GA294	275 ± 39					
GA322	281 ± 78					

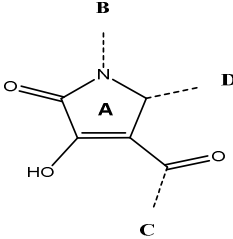
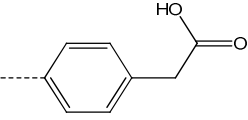
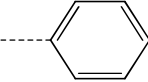
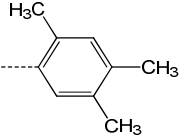
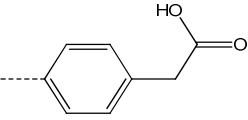
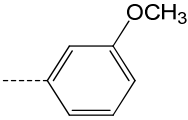
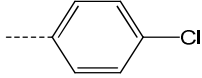
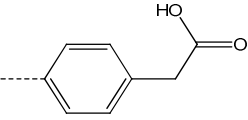
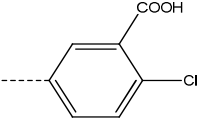
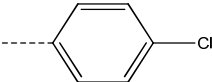
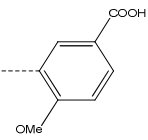
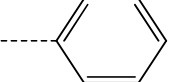
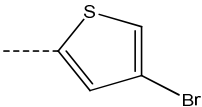
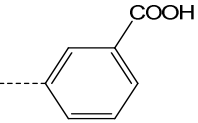
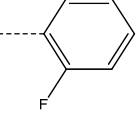
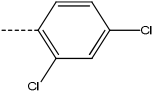
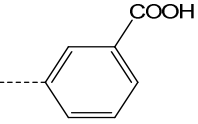

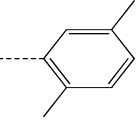
Supplementary Table 1: Substructures by potency

Scaffold					
smx	K_D (μM , estimate)	K_D (μM , NMR)	N1 (B)	4-keto (C)	5-aryl (D)
GA017-D	296 ± 111				
VPL-6	307 ± 51				
GA314	313 ± 88				
GA239	323 ± 109				
GA239	323 ± 109				
GA256	330 ± 158				
GA212	331 ± 62				

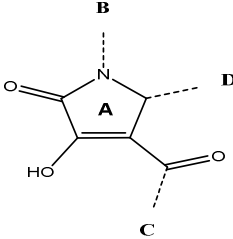
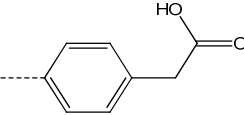
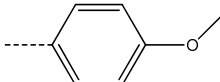
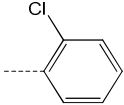
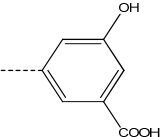
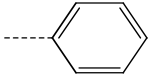
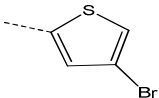
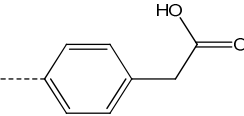
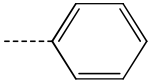
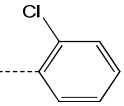
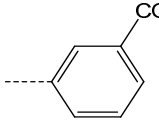
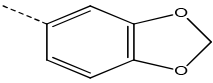
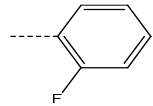
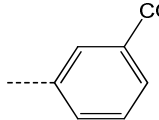
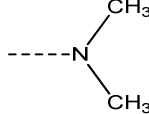
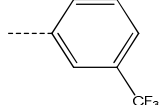
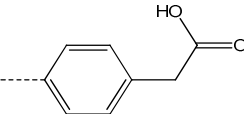
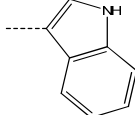
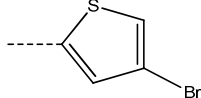
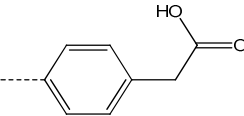
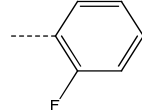
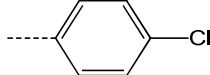
Supplementary Table 1: Substructures by potency

Scaffold					
smx	K_D (μM , estimate)	K_D (μM , NMR)	N1 (B)	4-keto (C)	5-aryl (D)
GA212	331 ± 62				
VPL-5	335 ± 38				
GA222	346 ± 136				
VPL-19	346 ± 168				
GA229	353 ± 159				
VPL-8	357 ± 68				
VPL-3	361 ± 24				

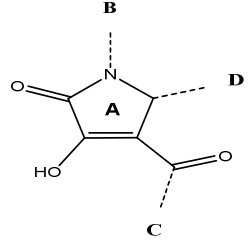
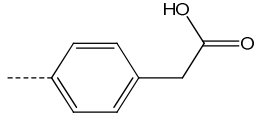
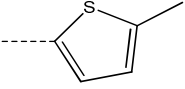
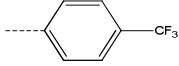
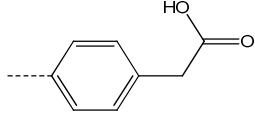
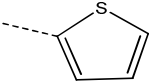

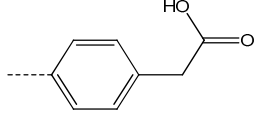
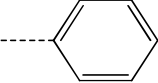

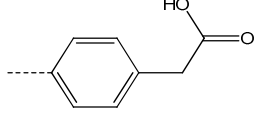
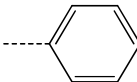
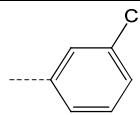
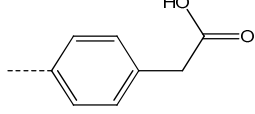
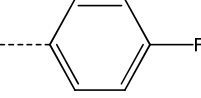
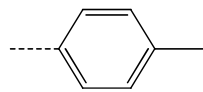
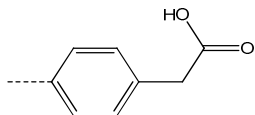
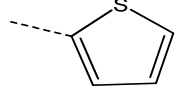
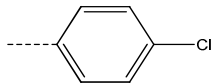
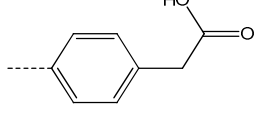
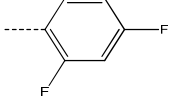
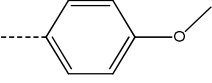
Supplementary Table 1: Substructures by potency

Scaffold					
smx	K_D (μM , estimate)	K_D (μM , NMR)	N1 (B)	4-keto (C)	5-aryl (D)
GA251	369 ± 134				
VPL-13	372 ± 87				
VPL-7	378 ± 72				
VPL-31	384 ± 76				
GA234	385 ± 145				
GA243=GA301	386 ± 83				

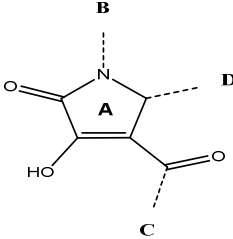
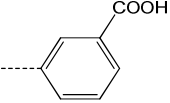
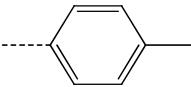
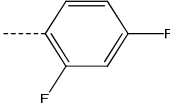
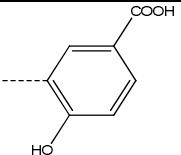
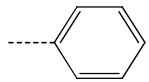
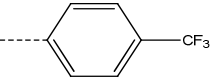
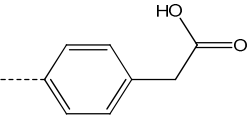
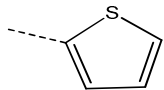
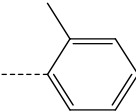
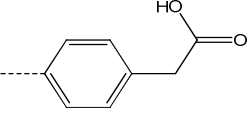
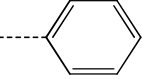
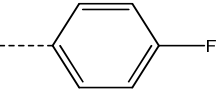
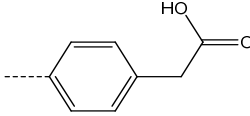
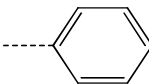
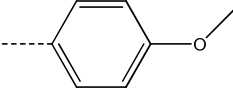
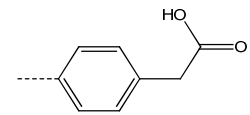
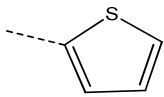
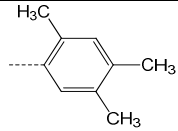
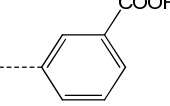
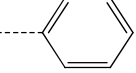
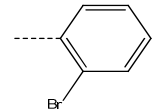
Supplementary Table 1: Substructures by potency

Scaffold					
smx	K_D (μM , estimate)	K_D (μM , NMR)	N1 (B)	4-keto (C)	5-aryl (D)
GA263	417 ± 107				
VPL-53	418 ± 70				
GA231	447 ± 100				
GA218	453 ± 91				
VPL-63	453 ± 252	518.1 ± 310.2			
VPL-28	458 ± 108				
GA310	475 ± 60				

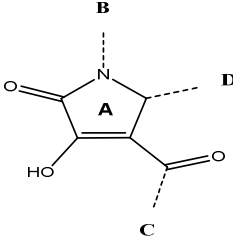
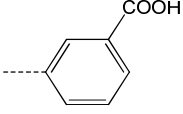
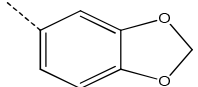
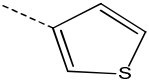
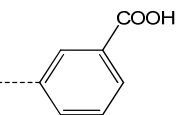
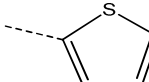
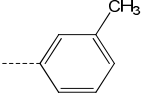
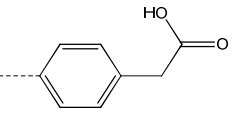
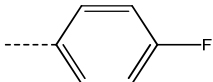
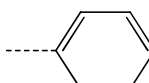
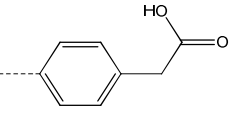
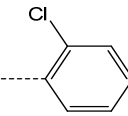
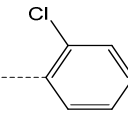
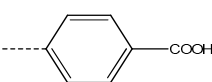
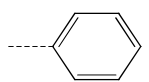
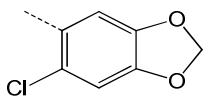
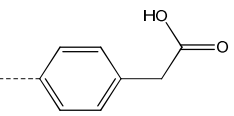
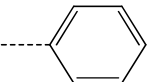
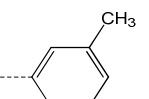
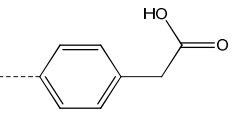

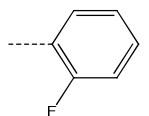
Supplementary Table 1: Substructures by potency

Scaffold					
	smx	K_D (μM , estimate)	K_D (μM , NMR)	N1 (B)	4-keto (C)
VPL-22	478 ± 187				
VPL-35	483 ± 134				
VPL-20	485 ± 172				
GA293	502 ± 52				
GA262	504 ± 204				
VPL-14	512 ± 94				
GA313	516 ± 92				

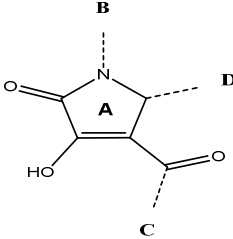
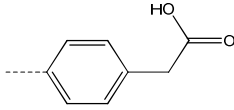
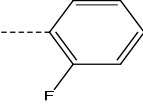
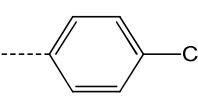
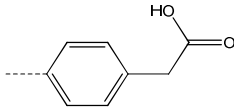
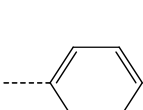
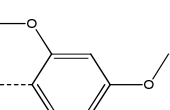
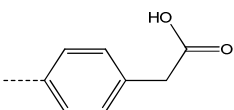
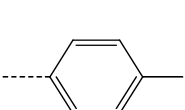
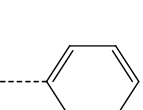
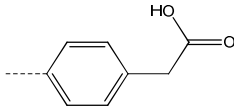
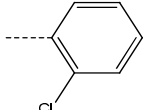
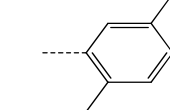
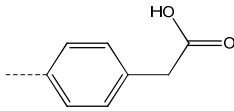
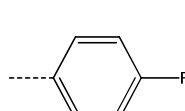
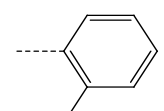
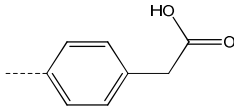
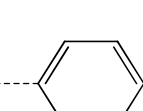
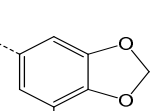
Supplementary Table 1: Substructures by potency

Scaffold					
smx	K_D (μM , estimate)	K_D (μM , NMR)	N1 (B)	4-keto (C)	5-aryl (D)
GA249	517 ± 127				
VPL-25	533 ± 60				
GA235=GA297	537 ± 62				
GA287	547 ± 48				
GA299	552 ± 149				
GA017	555 ± 112	270.7 ± 80.0			
GA250=GA306	565 ± 237				

Supplementary Table 1: Substructures by potency

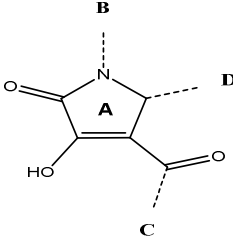
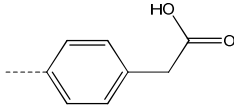
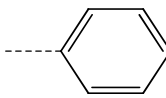
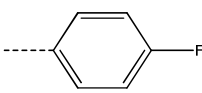
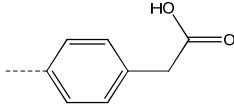
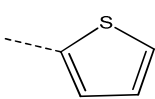
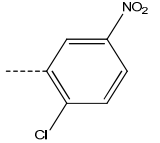
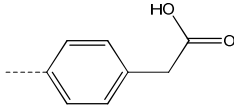
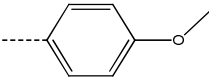
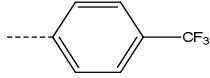
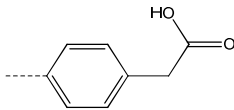
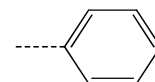
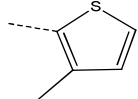
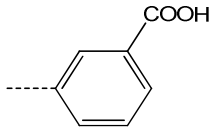
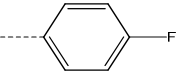
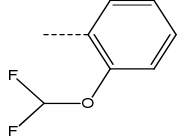
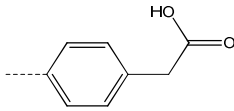
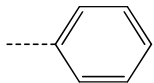
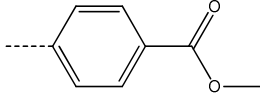
Scaffold					
smx	K_D (μM , estimate)	K_D (μM , NMR)	N1 (B)	4-keto (C)	5-aryl (D)
GA324	585 ± 34				
GA241	609 ± 101				
GA285	626 ± 109				
GA304	629 ± 98				
VPL-4	655 ± 183				
GA230	659 ± 231				
GA311	690 ± 104				

Supplementary Table 1: Substructures by potency

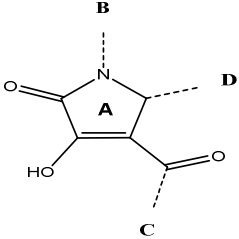
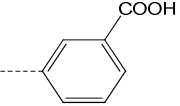
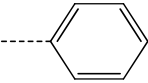
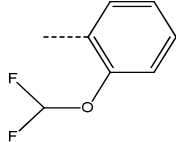
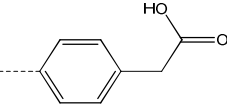
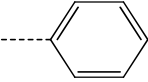
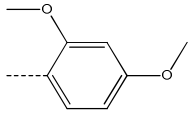
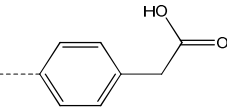
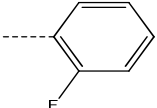
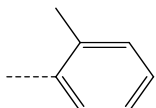
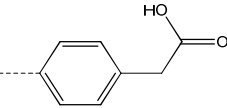
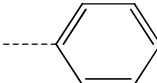
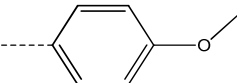
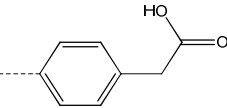
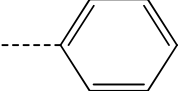
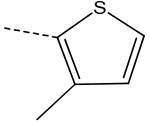
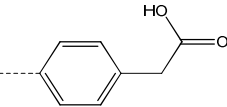
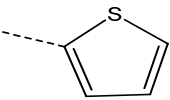
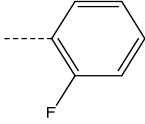
Scaffold					
smx	K_D (μM , estimate)	K_D (μM , NMR)	N1 (B)	4-keto (C)	5-aryl (D)
GA254=GA318	475 ± 60				
GA320	726 ± 151				
GA210	752 ± 175				
GA022	753 ± 74				
GA258	760 ± 166				
VPL-30	764 ± 383				

NH2 on ring

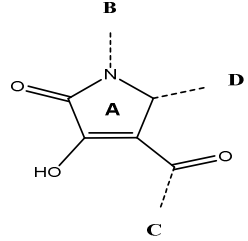
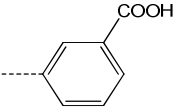
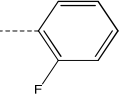
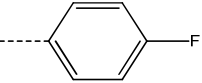
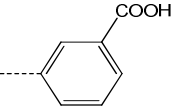
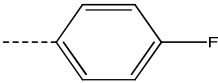
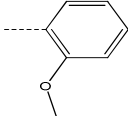
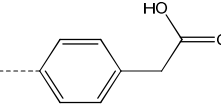
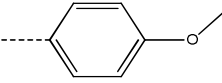
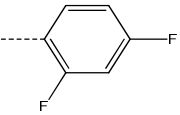
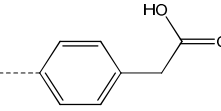
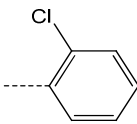
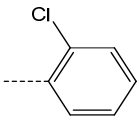
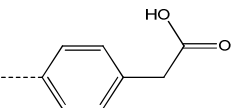
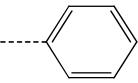
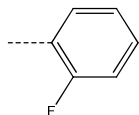
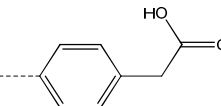
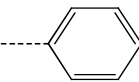
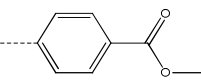
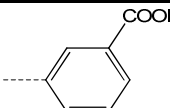
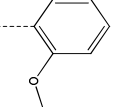
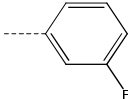
Supplementary Table 1: Substructures by potency

Scaffold					
smx	K_D (μM , estimate)	K_D (μM , NMR)	N1 (B)	4-keto (C)	5-aryl (D)
GA213	773 ± 142				
GA217=GA288	420 ± 70				
VPL-26	834 ± 324				
GA271	836 ± 279				
GA224	837 ± 521				
GA300	840 ± 155				

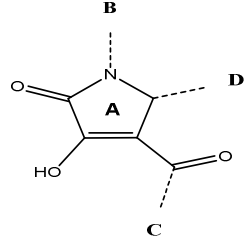
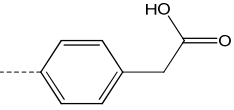
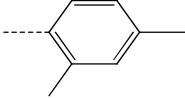
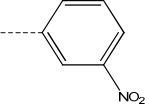
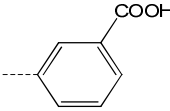
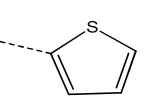
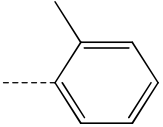
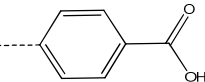
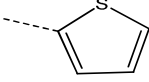
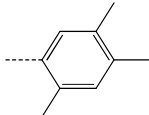
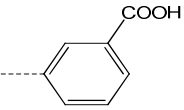
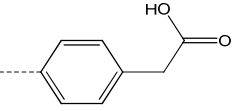
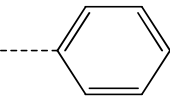
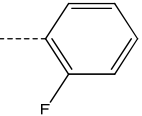
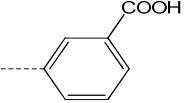
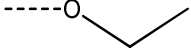
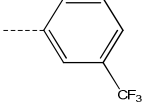
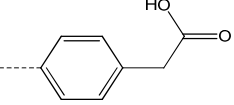
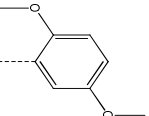
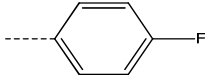
Supplementary Table 1: Substructures by potency

Scaffold					
smx	K_D (μM , estimate)	K_D (μM , NMR)	N1 (B)	4-keto (C)	5-aryl (D)
GA226	851 ± 150				
GA269	876 ± 266				
GA267	888 ± 122				
GA237	889 ± 218				
GA321	924 ± 233				
GA223=GA290	927 ± 112				

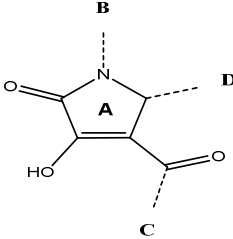
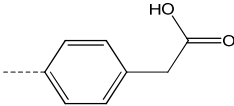
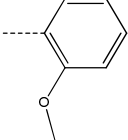
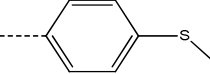
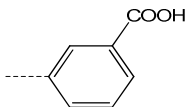
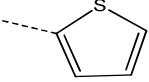
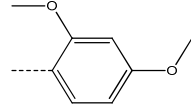
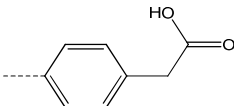
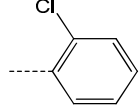
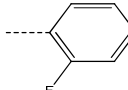
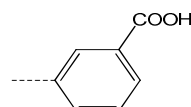
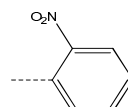
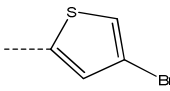
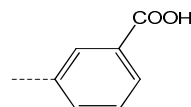
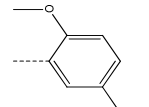
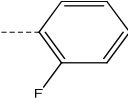
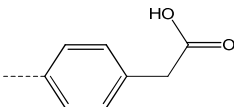
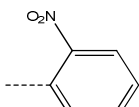
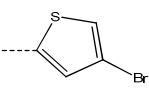
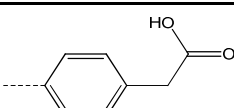
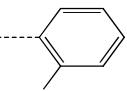
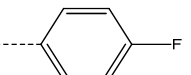
Supplementary Table 1: Substructures by potency

Scaffold					
	smx	K_D (μM , estimate)	K_D (μM , NMR)	N1 (B)	4-keto (C)
GA308	936 ± 30				
GA242	983 ± 167				
GA260	988 ± 260				
GA246	1049 ± 328				
GA232	1069 ± 193				
GA238	1120 ± 374				
GA221	1137 ± 268				

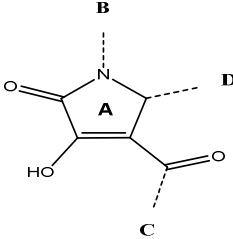
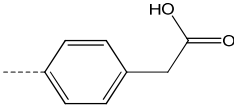
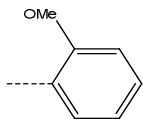
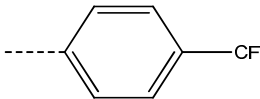
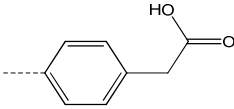
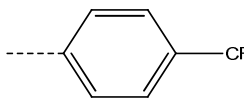
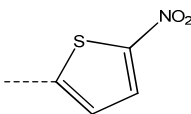
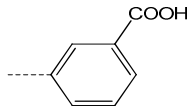
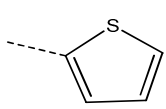
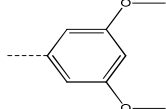
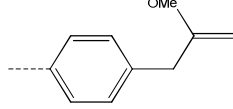
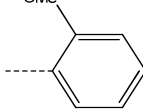
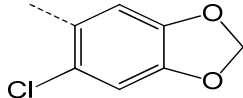
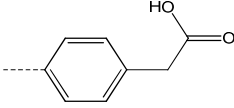
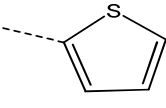
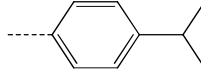
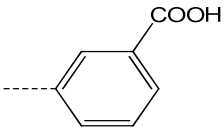
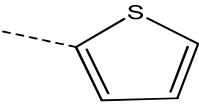
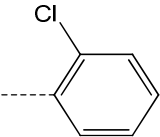
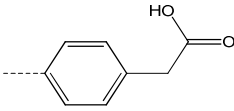
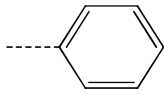
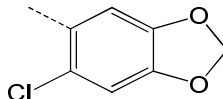
Supplementary Table 1: Substructures by potency

Scaffold						
	smx	K_D (μM , estimate)	K_D (μM , NMR)	N1 (B)	4-keto (C)	5-aryl (D)
GA019	1177 ± 54					
GA255	1210 ± 278					
GA017-E	1211 ± 1356					
GA023	1215 ± 459					
GA295	1222 ± 144					
VPL-56	1232 ± 115					
GA264=GA316	1256 ± 335					

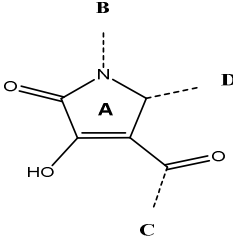
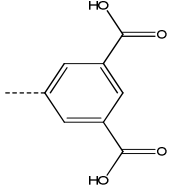
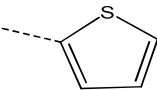
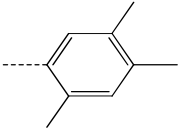
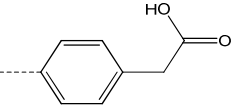
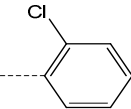
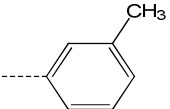
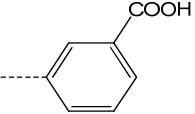
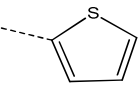
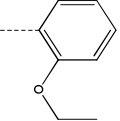
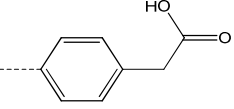
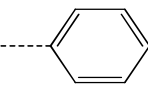
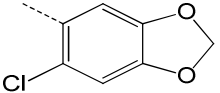
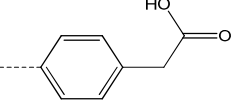
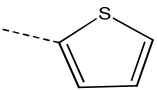
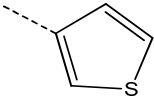
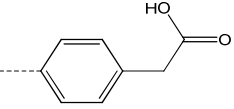
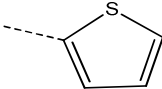
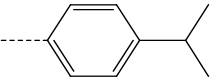
Supplementary Table 1: Substructures by potency

Scaffold					
smx	K_D (μM , estimate)	K_D (μM , NMR)	N1 (B)	4-keto (C)	5-aryl (D)
GA021	1283 ± 138				
GA244=GA302	1309 ± 406				
GA298	1324 ± 402				
VPL-17	1385 ± 983				
GA227	1423 ± 268				
VPL-16	1436 ± 717				
GA252	1472 ± 332				

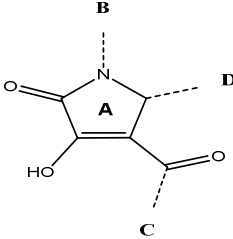
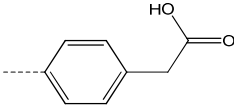
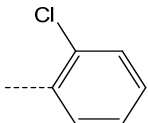
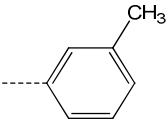
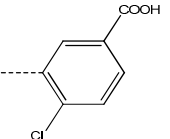
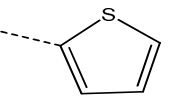
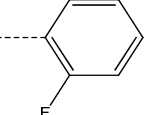
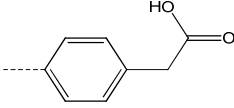
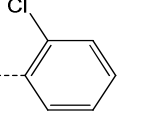
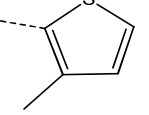
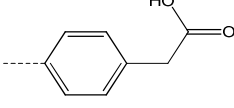
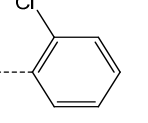
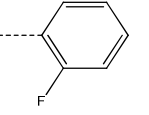
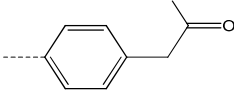
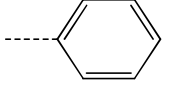
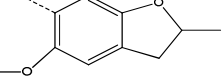
Supplementary Table 1: Substructures by potency

Scaffold					
smx	K_D (μM , estimate)	K_D (μM , NMR)	N1 (B)	4-keto (C)	5-aryl (D)
VPL-18	1537 ± 514				
VPL-12	1588 ± 620				
GA219	1618 ± 1034				
VPL-10	1631 ± 1125				
GA225	1860 ± 876				
GA216	1890 ± 1834				
VPL-9	2005 ± 671				

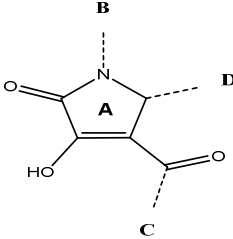
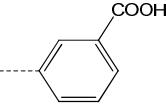
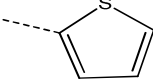
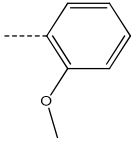
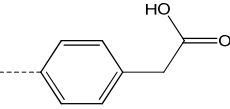
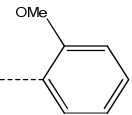
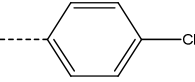
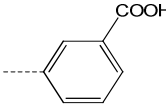
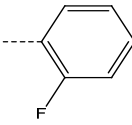
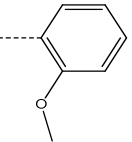
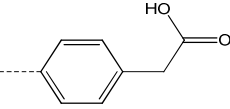
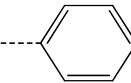
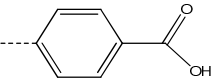
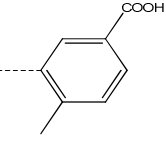
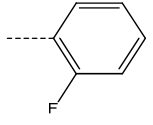
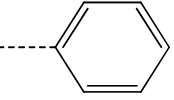
Supplementary Table 1: Substructures by potency

Scaffold					
smx	K_D (μM , estimate)	K_D (μM , NMR)	N1 (B)	4-keto (C)	5-aryl (D)
GA017-F2	2023 \pm 2434				
GA303	2152 \pm 201				
GA214	2348 \pm 1423				
VPL-1	2354 \pm 2418				
GA266	2474 \pm 1011				
GA291	2508 \pm 2240				

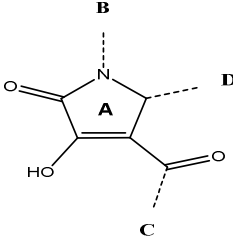
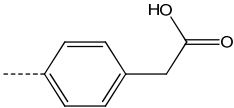
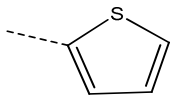
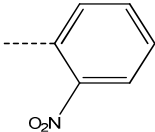
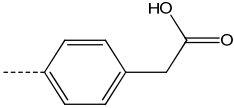
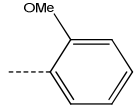
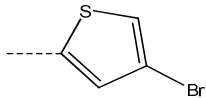
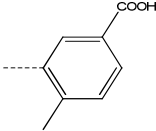
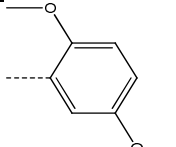
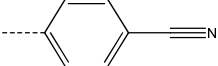
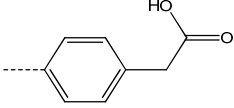
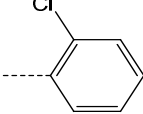
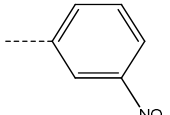
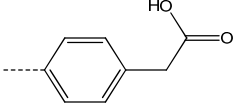
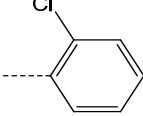
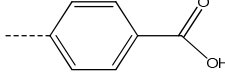
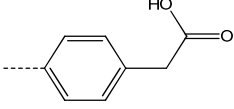
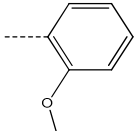
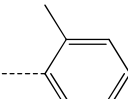
Supplementary Table 1: Substructures by potency

Scaffold					
smx	K_D (μM , estimate)	K_D (μM , NMR)	N1 (B)	4-keto (C)	5-aryl (D)
GA245	2540 ± 1214				
GA270	2675 ± 1621				
GA257	2749 ± 1535				
GA236	3060 ± 2222				
GA233	3160 ± 1317				

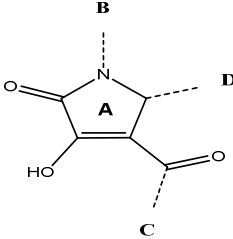
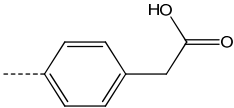
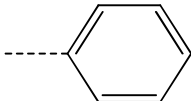
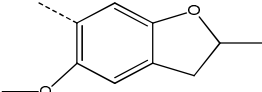
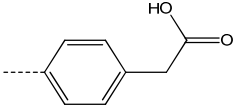
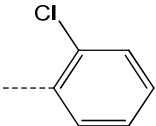
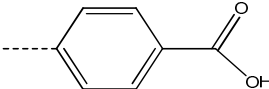
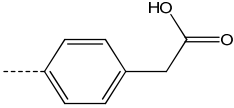
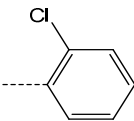
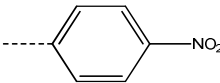
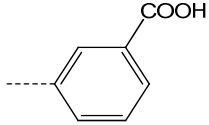
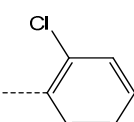
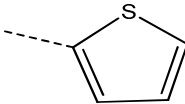
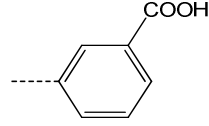
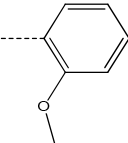
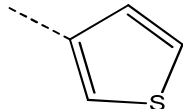
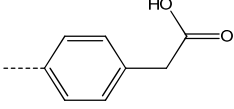
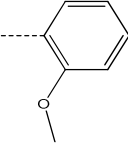
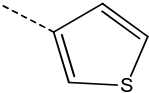
Supplementary Table 1: Substructures by potency

Scaffold					
smx	K_D (μM , estimate)	K_D (μM , NMR)	N1 (B)	4-keto (C)	5-aryl (D)
GA247	3247 ± 2066				
VPL-2	3279 ± 2052				
GA215	3385 ± 1232				
GA248	3646 ± 1077				
GA276	3692 ± 432				

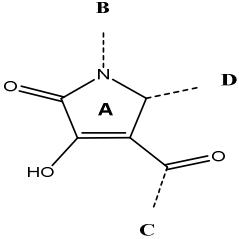
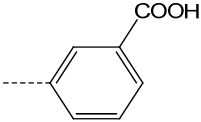
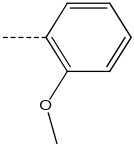
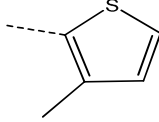
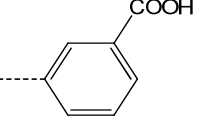
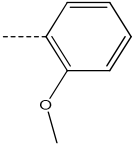
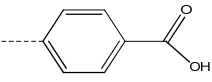
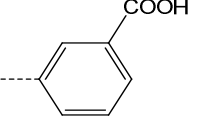
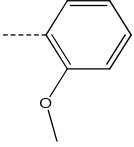
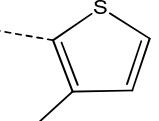
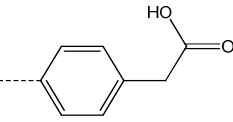
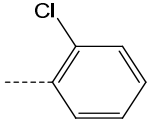
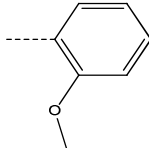
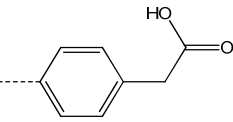
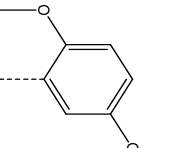
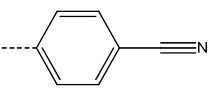
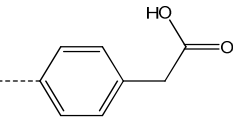
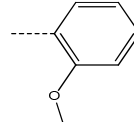
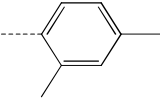
Supplementary Table 1: Substructures by potency

Scaffold					
smx	K_D (μM , estimate)	K_D (μM , NMR)	N1 (B)	4-keto (C)	5-aryl (D)
GA280	3962 ± 2054				
VPL-15	4044 ± 1631				
GA268=GA319	4094 ± 1324				
GA278	4192 ± 1465				
GA220	4501 ± 1785				
GA281	4580 ± 1266				

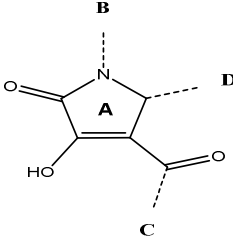
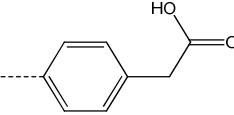
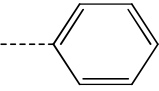
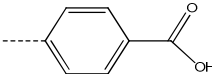
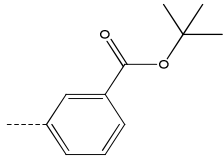
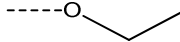
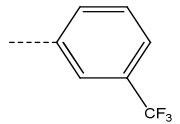
Supplementary Table 1: Substructures by potency

Scaffold					
smx	K_D (μM , estimate)	K_D (μM , NMR)	N1 (B)	4-keto (C)	5-aryl (D)
GA296	4595 \pm 3288				
GA289	4851 \pm 3780				
GA277	4860 \pm 2405				
GA240	4930 \pm 2335				
GA282	5034 \pm 2330				
GA273	5264 \pm 2274				

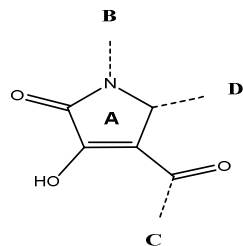
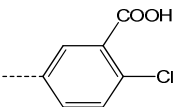
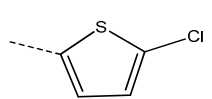
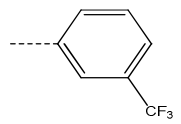
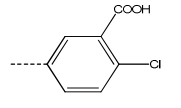
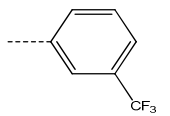
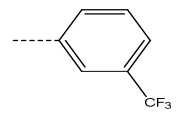
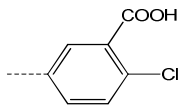
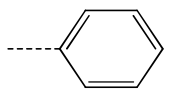
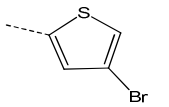
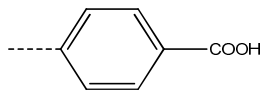
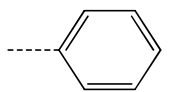
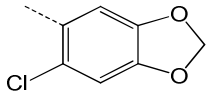
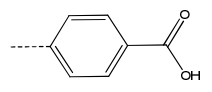
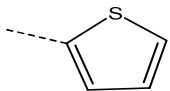
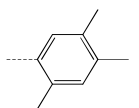
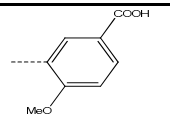
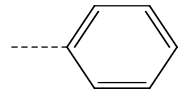
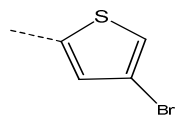
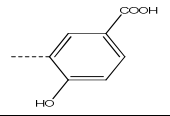
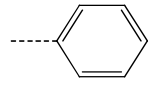
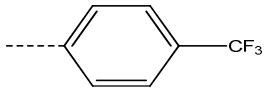
Supplementary Table 1: Substructures by potency

Scaffold					
smx	K_D (μM , estimate)	K_D (μM , NMR)	N1 (B)	4-keto (C)	5-aryl (D)
GA265	5267 ± 3437				
GA261	5282 ± 2286				
GA317	5414 ± 2964				
GA323	5477 ± 4894				
GA283	5623 ± 5341				
GA279	6340 ± 4469				

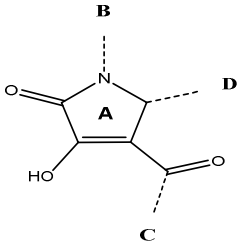
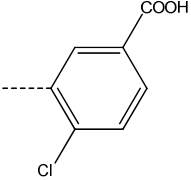
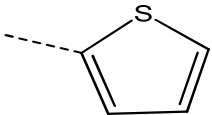
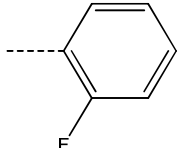
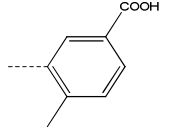
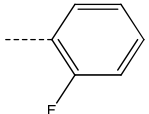
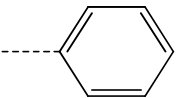
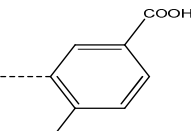
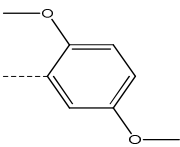
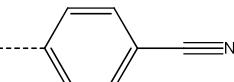
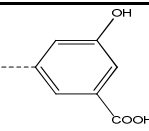
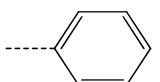
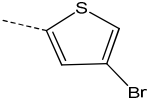
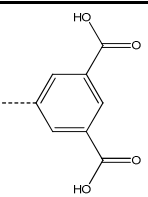
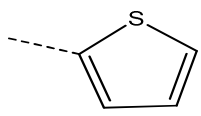
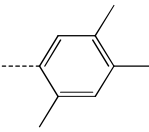
Supplementary Table 1: Substructures by potency

Scaffold					
smx	K_D (μM , estimate)	K_D (μM , NMR)	N1 (B)	4-keto (C)	5-aryl (D)
GA305	8240 ± 8960				
VPL-62	-	ND			

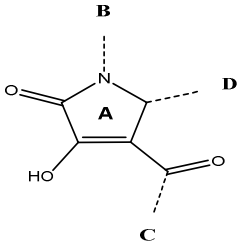
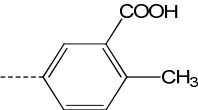
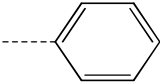
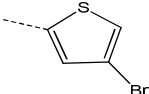
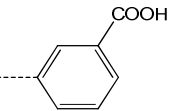
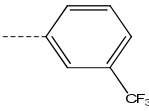
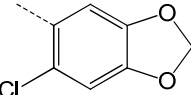
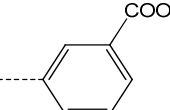
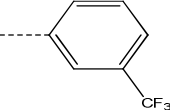
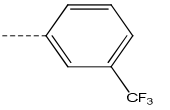
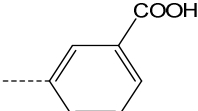
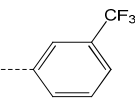
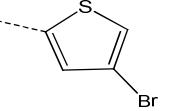
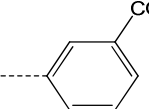
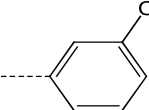
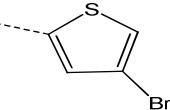
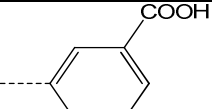
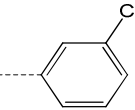
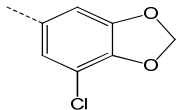
Supplementary Table 2: Substructures by functional groups

Scaffold						
smx	K_D (μM , estimate)	K_D (μM , NMR)	N1 (B)	4-keto (C)	5-aryl (D)	scaffold changes
VPL-64	30 ± 7	58.90 ± 21.1				
VPL-61	36 ± 10	38.7 ± 16.0				
VPL-29	60 ± 16	70.6 ± 7.9				
VPL-4	655 ± 183					
GA017-E	1211 ± 1356					
VPL-31	384 ± 76					
VPL-25	533 ± 60					

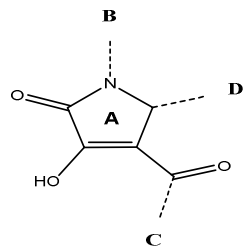
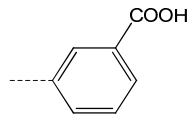
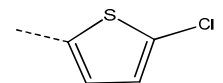
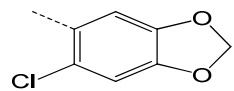
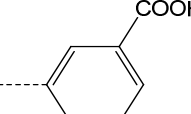
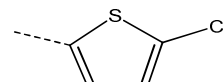
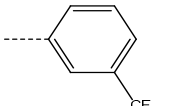
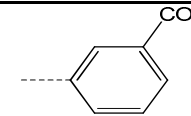
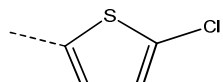
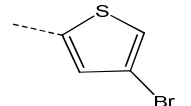
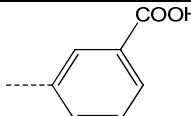
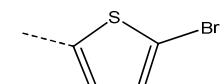
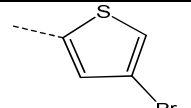
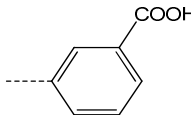
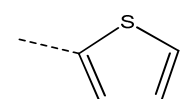
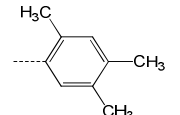
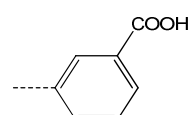
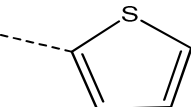
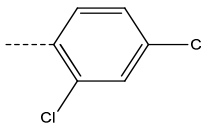
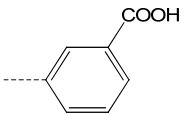
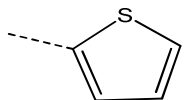
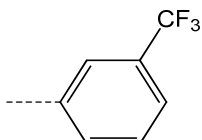
Supplementary Table 2: Substructures by functional groups

Scaffold						
smx	K_D (μM , estimate)	K_D (μM , NMR)	N1 (B)	4-keto (C)	5-aryl (D)	scaffold changes
GA270	2675 ± 1621					
GA276	3692 ± 432					
GA268=GA319	4094 ± 1324					
VPL-53	418 ± 70					
GA017-F2	2023 ± 2434					

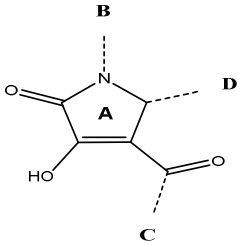
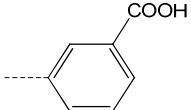
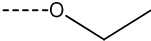
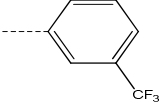
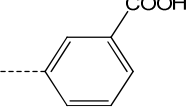
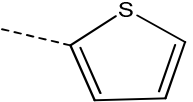
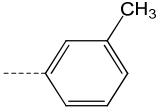
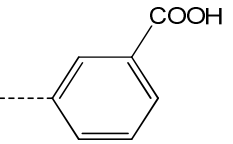
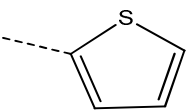
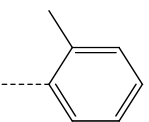
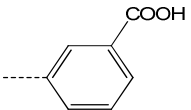
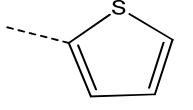
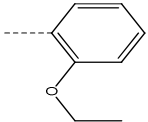
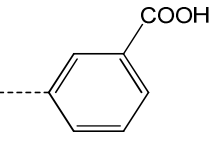
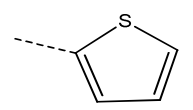
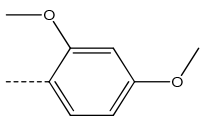
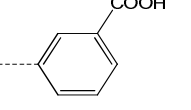
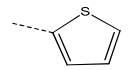
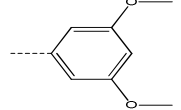
Supplementary Table 2: Substructures by functional groups

Scaffold						
smx	K_D (μM , estimate)	K_D (μM , NMR)	N1 (B)	4-keto (C)	5-aryl (D)	scaffold changes
VPL-27	124 ± 36	214.6 ± 24.9				
VPL-57	52 ± 10	73.0 ± 31.0				
VPL-58	52 ± 10	73.0 ± 31.0				
VPL-52	80 ± 3	60.9 ± 3.0				
VPL-45	101 ± 25	92.5 ± 8.4				
VPL-46	63 ± 18	70.6 ± 7.9				

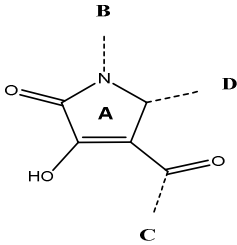
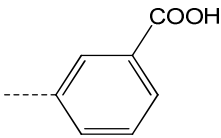
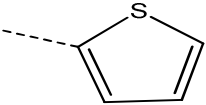
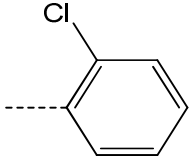
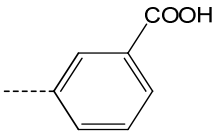
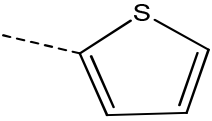
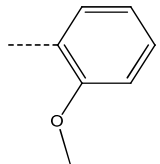
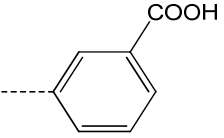
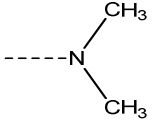
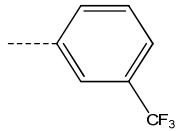
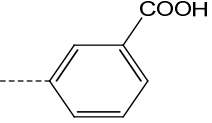
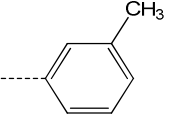
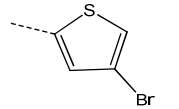
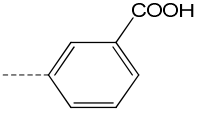
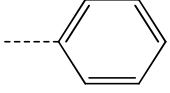
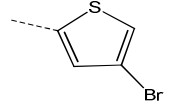
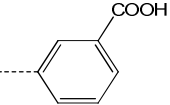
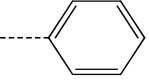
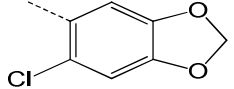
Supplementary Table 2: Substructures by functional groups

Scaffold						
smx	K_D (μM , estimate)	K_D (μM , NMR)	N1 (B)	4-keto (C)	5-aryl (D)	scaffold changes
VPL-60	33 ± 7	50.4 ± 4.7				
VPL-59	47 ± 38	55.7 ± 4.9				
VPL-41	120 ± 11	129.5 ± 35.1				
VPL-38	149 ± 45	98.0 ± 36.0				
GA017-D	296 ± 111					
GA239	323 ± 109					
GA229	353 ± 159					

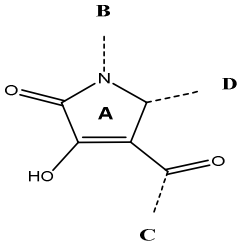
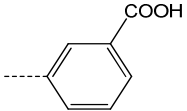
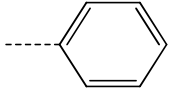
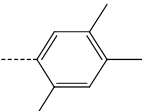
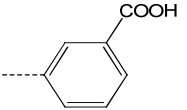
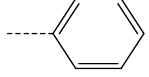
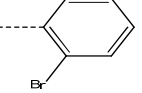
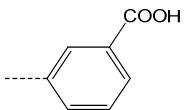
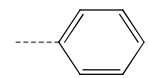
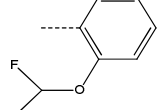
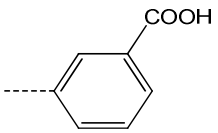
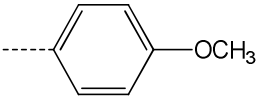
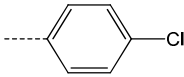
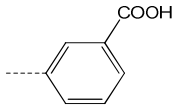
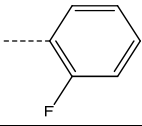
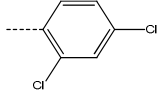
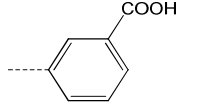
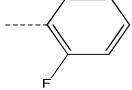
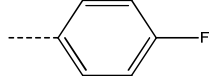
Supplementary Table 2: Substructures by functional groups

Scaffold						
smx	K_D (μM , estimate)	K_D (μM , NMR)	N1 (B)	4-keto (C)	5-aryl (D)	scaffold changes
VPL-56	1232 ± 115					
GA241	609 ± 101					
GA255	1210 ± 278					
GA214	2348 ± 1423					
GA244=GA302	1309 ± 406					
GA219	1618 ± 1034					

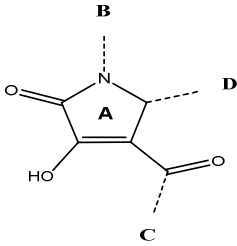
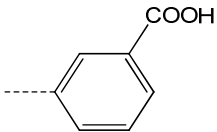
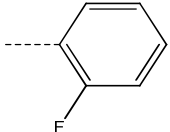
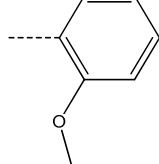
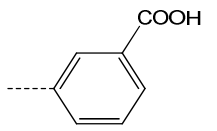
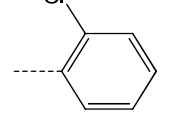
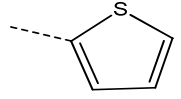
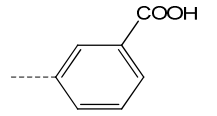
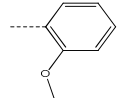
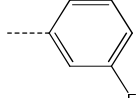
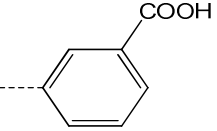
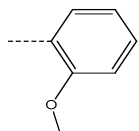
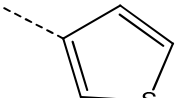
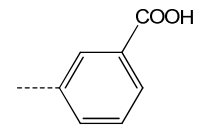
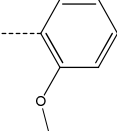
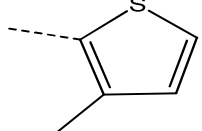
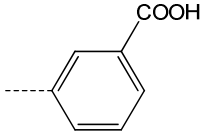
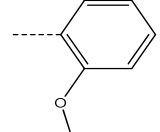
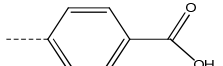
Supplementary Table 2: Substructures by functional groups

Scaffold						
smx	K_D (μM , estimate)	K_D (μM , NMR)	N1 (B)	4-keto (C)	5-aryl (D)	scaffold changes
GA216	1890 ± 1834					
GA247	3247 ± 2066					
VPL-63	453 ± 252	518.1 ± 310.2				
VPL-49	79 ± 17	79.2 ± 8.5				
GA272	128 ± 34	111.90				
VPL-55	152 ± 40	111.9 ± 30.7				

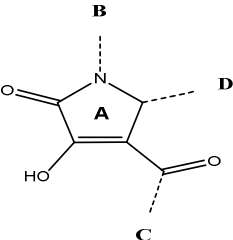
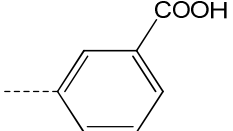
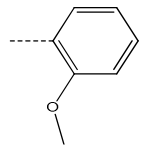
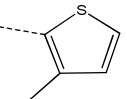
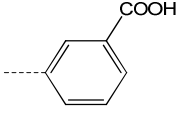
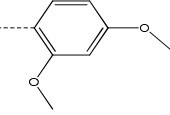
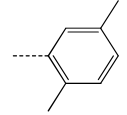
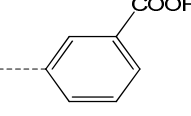
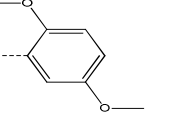
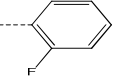
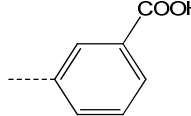
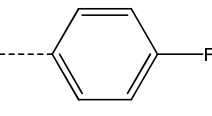
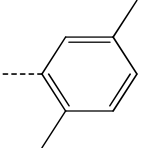
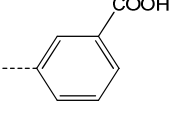
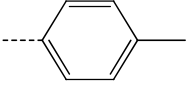
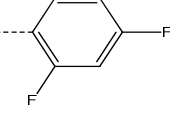
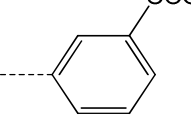
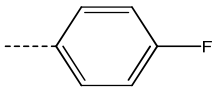
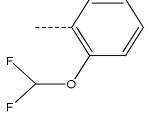
Supplementary Table 2: Substructures by functional groups

Scaffold						
smx	K_D (μM , estimate)	K_D (μM , NMR)	N1 (B)	4-keto (C)	5-aryl (D)	scaffold changes
GA307	179 ± 72					
GA250=GA306	565 ± 237					
GA226	851 ± 150					
VPL-8	357 ± 68					
GA234	385 ± 145					
GA308	936 ± 30					

Supplementary Table 2: Substructures by functional groups

Scaffold						
smx	K_D (μM , estimate)	K_D (μM , NMR)	N1 (B)	4-keto (C)	5-aryl (D)	scaffold changes
GA215	3385 ± 1232					
GA240	4930 ± 2335					
GA221	1137 ± 268					
GA282	5034 ± 2330					
GA265	5267 ± 3437					
GA261	5282 ± 2286					

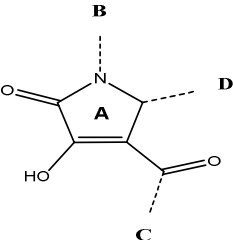
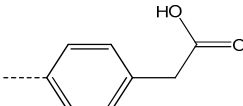
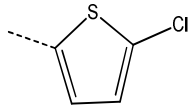
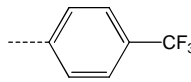
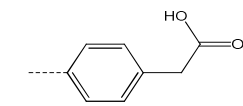
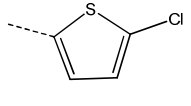
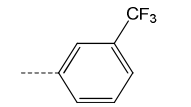
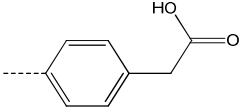
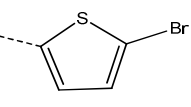
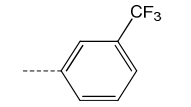
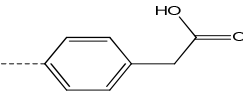
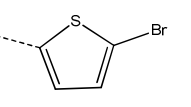
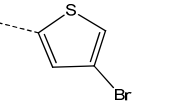
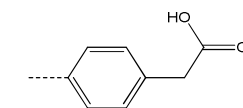
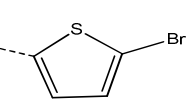
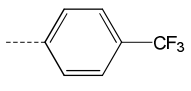
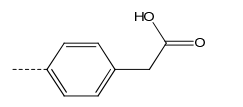
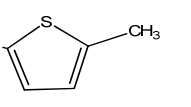
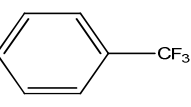
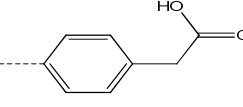
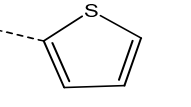
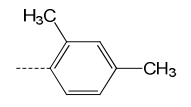
Supplementary Table 2: Substructures by functional groups

Scaffold						
smx	K_D (μM , estimate)	K_D (μM , NMR)	N1 (B)	4-keto (C)	5-aryl (D)	scaffold changes
GA317	5414 ± 2964					
GA023	1215 ± 459					
GA227	1423 ± 268					
GA243=GA301	386 ± 83					
GA249	517 ± 127					
GA224	837 ± 521					

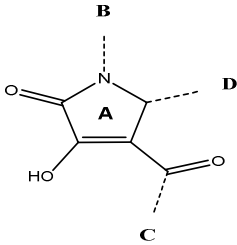
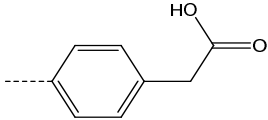
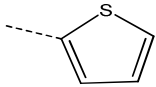
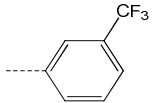
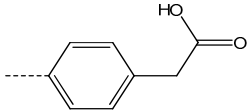
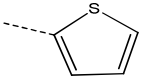
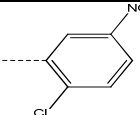
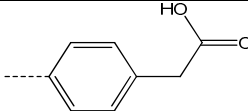
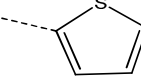
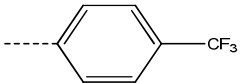
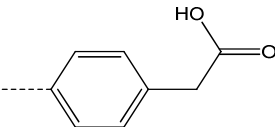
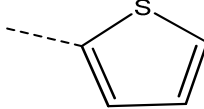
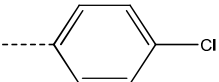
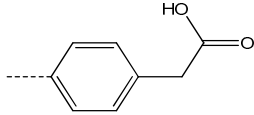
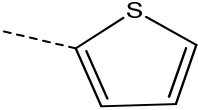
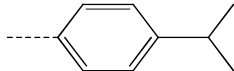
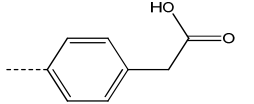
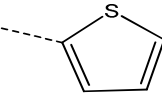
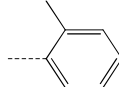
Supplementary Table 2: Substructures by functional groups

Scaffold						
smx	K_D (μM , estimate)	K_D (μM , NMR)	N1 (B)	4-keto (C)	5-aryl (D)	scaffold changes
GA242	983 ± 167					
GA218	453 ± 91					
GA324	585 ± 34					
VPL-17	1385 ± 983					
VPL-42	46 ± 19	36.8 ± 8.1				
VPL-40	126 ± 32	369.8 ± 173.3				

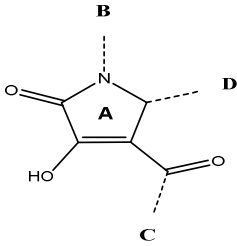
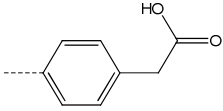
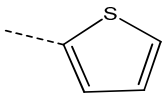
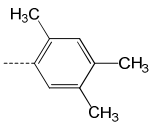
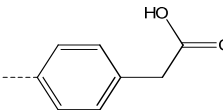
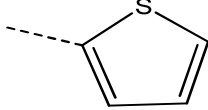
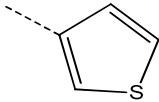
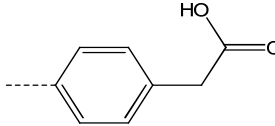
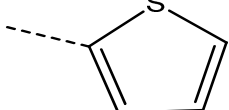
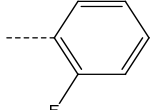
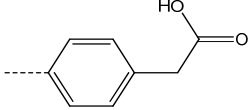
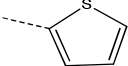
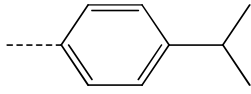
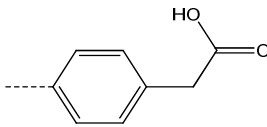
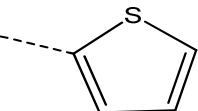
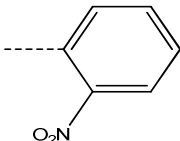
Supplementary Table 2: Substructures by functional groups

Scaffold						
smx	K_D (μM , estimate)	K_D (μM , NMR)	N1 (B)	4-keto (C)	5-aryl (D)	scaffold changes
VPL-24	161 ± 82					
VPL-36	36 ± 13	49.9 ± 9.8				
VPL-34	39 ± 16	63.9 ± 17.7				
VPL-39	70 ± 14	65.8 ± 10.2				
VPL-23	161 ± 86					
VPL-22	478 ± 187					
GA274=GA322	264 ± 63					

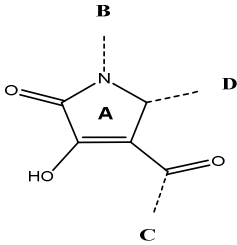
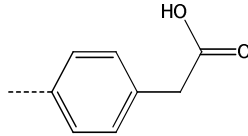
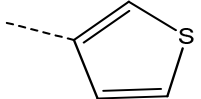
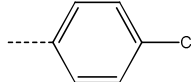
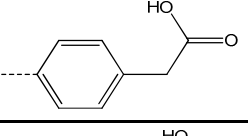
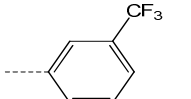
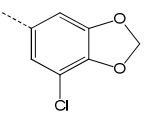
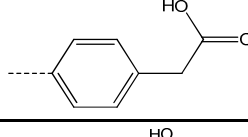
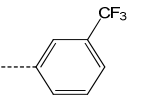
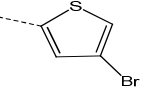
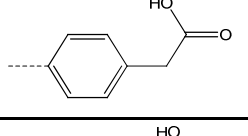
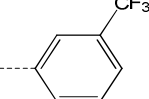
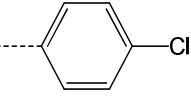
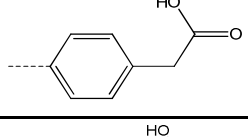
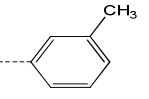
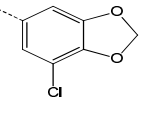
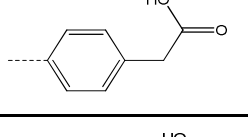
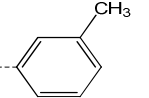
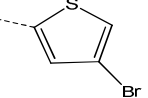
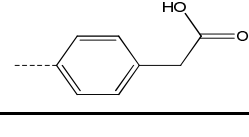
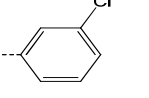
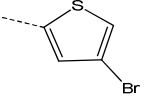
Supplementary Table 2: Substructures by functional groups

Scaffold						
smx	K_D (μM , estimate)	K_D (μM , NMR)	N1 (B)	4-keto (C)	5-aryl (D)	scaffold changes
GA222	346 ± 136					
GA217=GA288	420 ± 70					
VPL-35	483 ± 134					
VPL-14	512 ± 94					
GA291	2508 ± 2240					
GA235=GA297	537 ± 62					

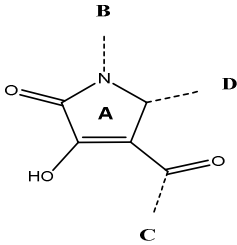
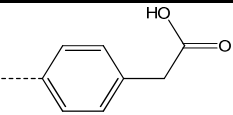
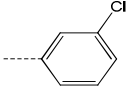
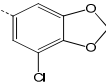
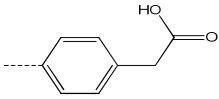
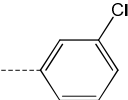
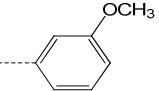
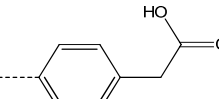
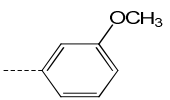
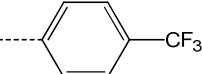
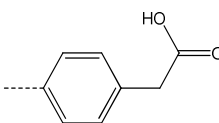
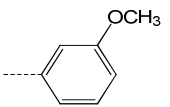
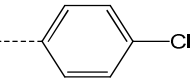
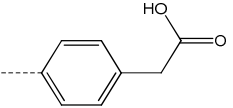
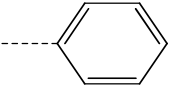
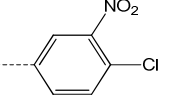
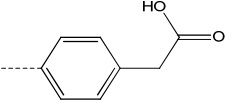
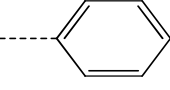
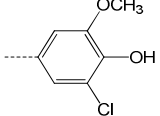
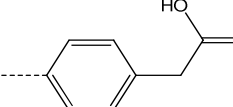
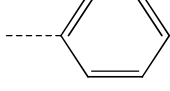
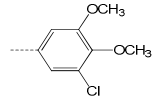
Supplementary Table 2: Substructures by functional groups

Scaffold						
smx	K_D (μM , estimate)	K_D (μM , NMR)	N1 (B)	4-keto (C)	5-aryl (D)	scaffold changes
GA017	555 ± 112	270.7 ± 80.0				
GA266	2474 ± 1011					
GA223=GA290	927 ± 112					
GA225	1860 ± 876					
GA280	3962 ± 2054					

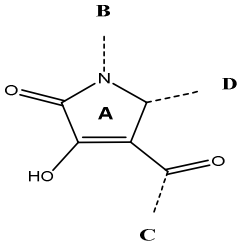
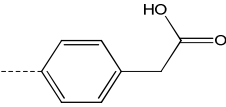
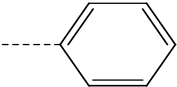
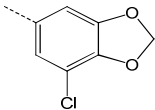
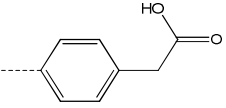
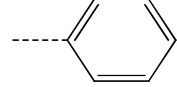
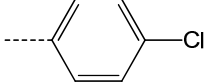
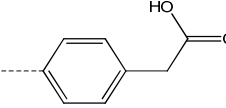
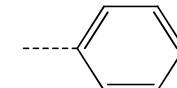
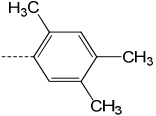
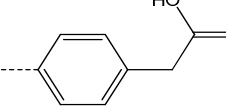
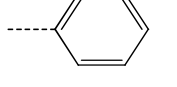
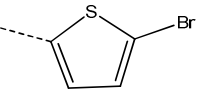
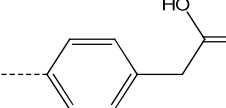
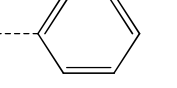
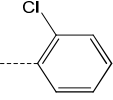
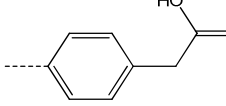
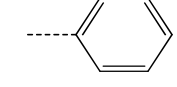
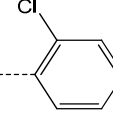
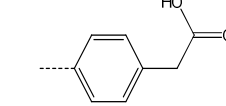
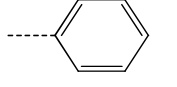
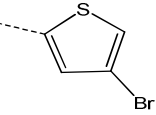
Supplementary Table 2: Substructures by functional groups

Scaffold						
smx	K_D (μM , estimate)	K_D (μM , NMR)	N1 (B)	4-keto (C)	5-aryl (D)	scaffold changes
VPL-7	378 ± 72					
VPL-51	49 ± 35	44.8 ± 3.2				
VPL-50	80 ± 26	63.9 ± 7.4				
VPL-11	134 ± 11	124.3 ± 16.2				
VPL-48	79 ± 3	108.0 ± 7.0				
VPL-47	138 ± 40					
VPL-43	77 ± 15	81.7 ± 6.1				

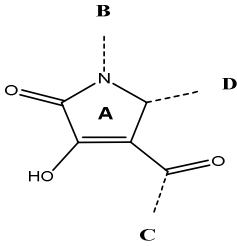
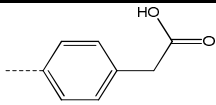
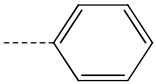
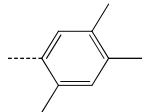
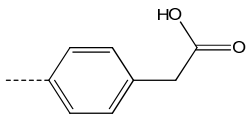
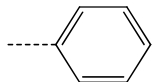
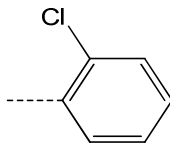
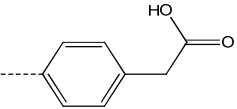
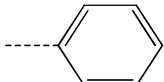
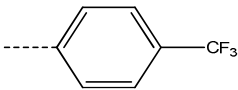
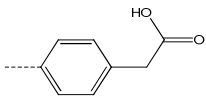
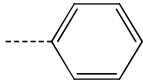
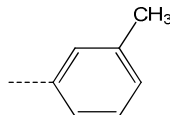
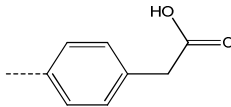
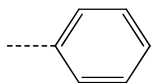
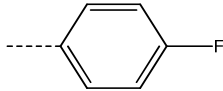
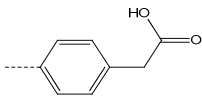
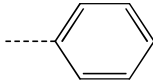
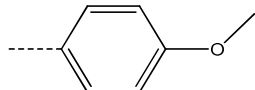
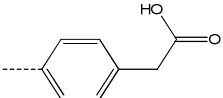
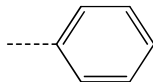
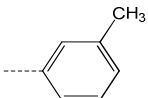
Supplementary Table 2: Substructures by functional groups

Scaffold						
smx	K_D (μM , estimate)	K_D (μM , NMR)	N1 (B)	4-keto (C)	5-aryl (D)	scaffold changes
VPL-44	89 ± 14	99.9 ± 25.9				
GA239	323 ± 109					
VPL-19	346 ± 168					
VPL-13	372 ± 87					
GA312=GA259	101 ± 40	103.8 ± 41.7				
VPL-33	109 ± 2	110.9 ± 41.2				
VPL-37	117 ± 12	74.6 ± 14.5				

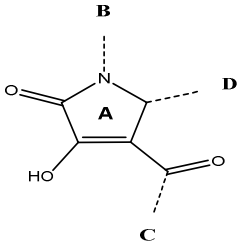
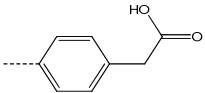
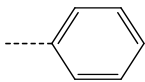
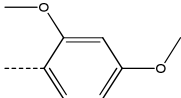
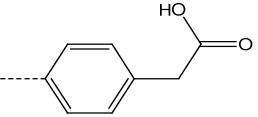
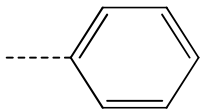
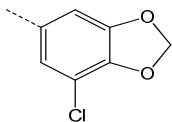
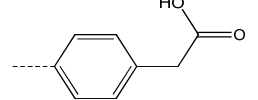
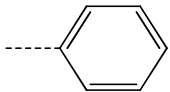
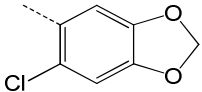
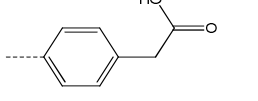
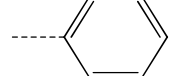
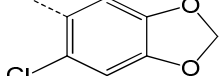
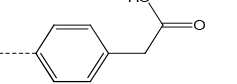
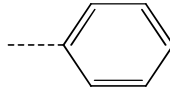
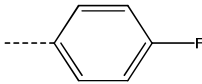
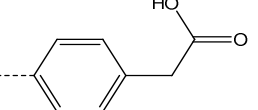
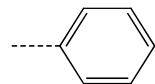
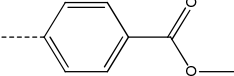
Supplementary Table 2: Substructures by functional groups

Scaffold						
smx	K_D (μM , estimate)	K_D (μM , NMR)	N1 (B)	4-keto (C)	5-aryl (D)	scaffold changes
GA228=GA292	127 ± 5	291.9 ± 17.5				
VPL-32	135 ± 44	280.2 ± 51.2				
GA307	179 ± 72					
GA272-B	204 ± 28	114.1 ± 20.6				
GA294	275					
GA294	275 ± 39					
VPL-5	335 ± 38					

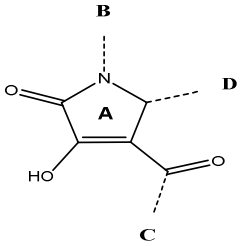
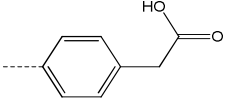
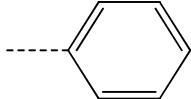
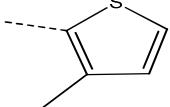
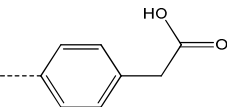
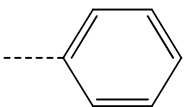
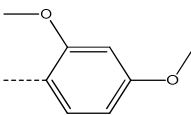
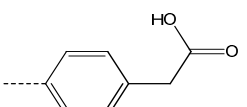
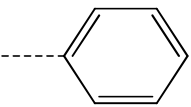
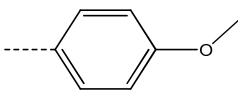
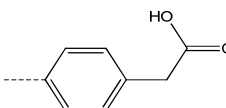
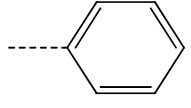
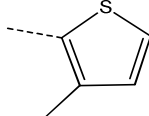
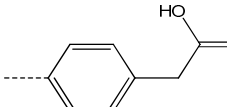
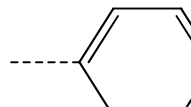
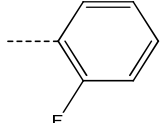
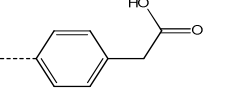
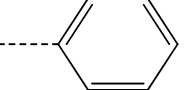
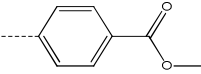
Supplementary Table 2: Substructures by functional groups

Scaffold						
smx	K_D (μM , estimate)	K_D (μM , NMR)	N1 (B)	4-keto (C)	5-aryl (D)	scaffold changes
GA251	369 ± 134					
GA231	447 ± 100					
VPL-20	485 ± 172					
GA293	502 ± 52					
GA287	547 ± 48					
GA299	552 ± 149					
GA230	659 ± 231					

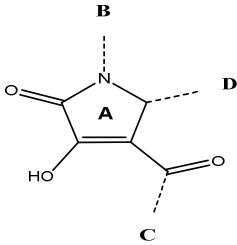
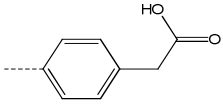
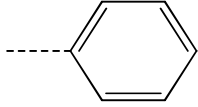
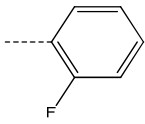
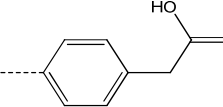
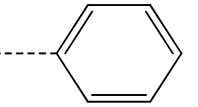
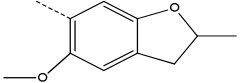
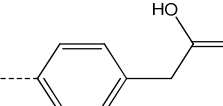
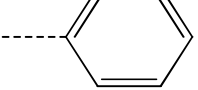
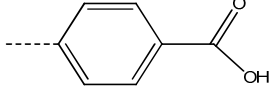
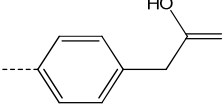
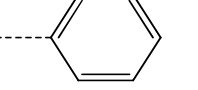
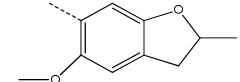
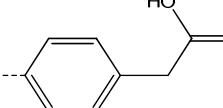
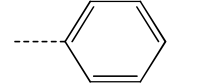
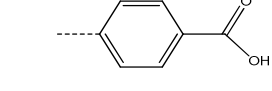
Supplementary Table 2: Substructures by functional groups

Scaffold						
smx	K_D (μM , estimate)	K_D (μM , NMR)	N1 (B)	4-keto (C)	5-aryl (D)	scaffold changes
GA320	726 ± 151					
VPL-30	764 ± 383					
VPL-9	2005 ± 671					no carbonyl
VPL-1	2354 ± 2418					
GA213	773 ± 142					
GA300	840 ± 155					

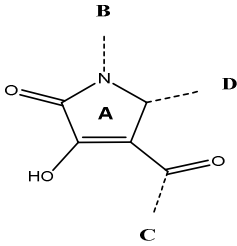
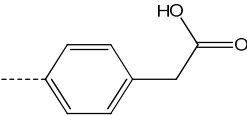
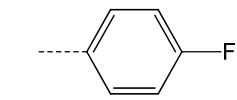
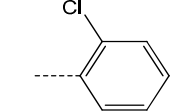
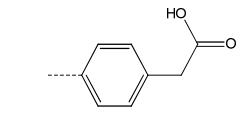
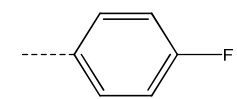
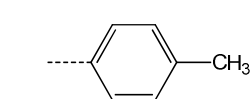
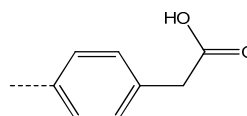
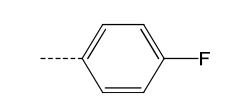
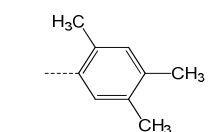
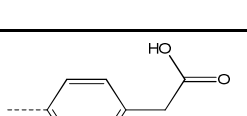
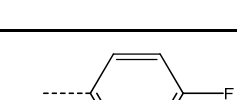
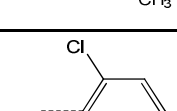
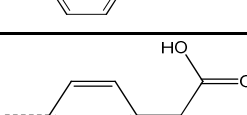
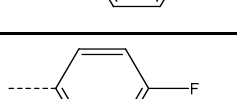
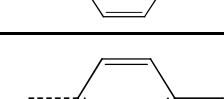
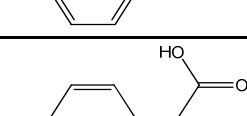
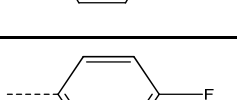
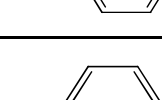
Supplementary Table 2: Substructures by functional groups

Scaffold						
smx	K_D (μM , estimate)	K_D (μM , NMR)	N1 (B)	4-keto (C)	5-aryl (D)	scaffold changes
GA271	836 ± 279					
GA269	876 ± 266					
GA237	889 ± 218					
GA321	924 ± 233					
GA232	1069 ± 193					
GA238	1120 ± 374					

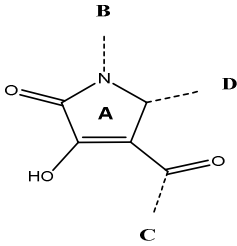
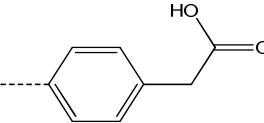
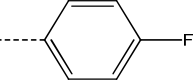
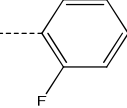
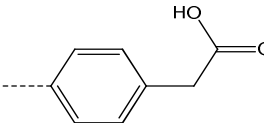
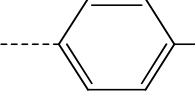
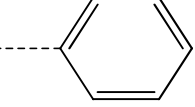
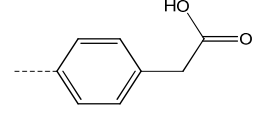
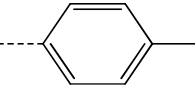
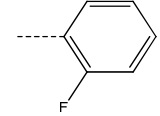
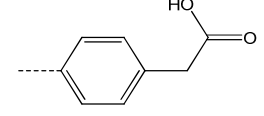
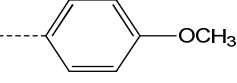
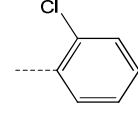
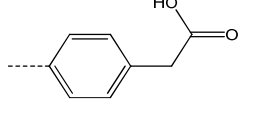
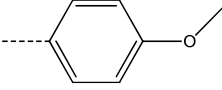
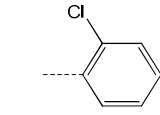
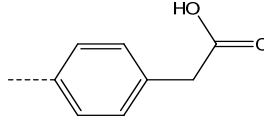
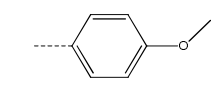
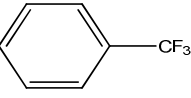
Supplementary Table 2: Substructures by functional groups

Scaffold						
smx	K_D (μM , estimate)	K_D (μM , NMR)	N1 (B)	4-keto (C)	5-aryl (D)	scaffold changes
GA295	1222 ± 144					
GA233	3160 ± 1317					
GA248	3646 ± 1077					
GA296	4595 ± 3288					
GA305	8240 ± 8960					

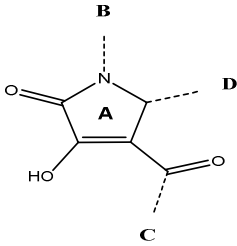
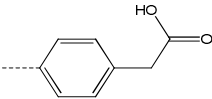
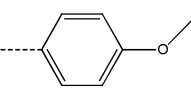
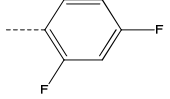
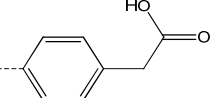
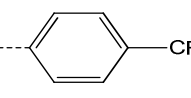
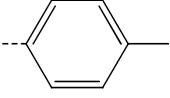
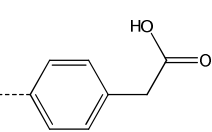
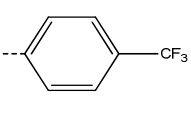
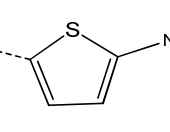
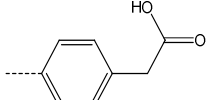
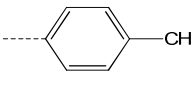
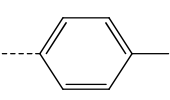
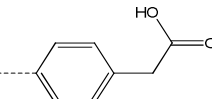
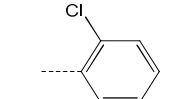
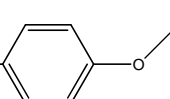
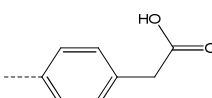
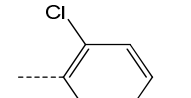
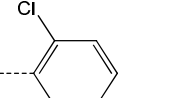
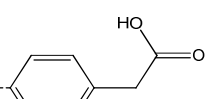
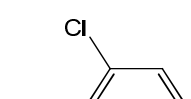
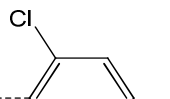
Supplementary Table 2: Substructures by functional groups

Scaffold						
smx	K_D (μM , estimate)	K_D (μM , NMR)	N1 (B)	4-keto (C)	5-aryl (D)	scaffold changes
GA286	238 ± 48					
GA314	313 ± 88					
GA256	330 ± 158					
GA212	331 ± 62					
GA262	504 ± 204					
GA285	626 ± 109					

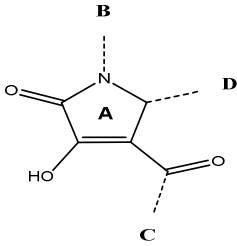
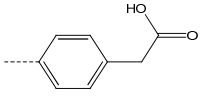
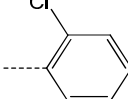
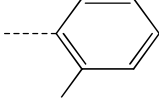
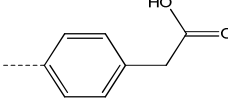
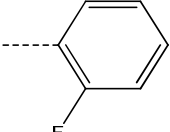
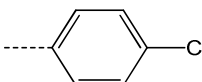
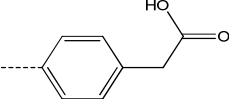
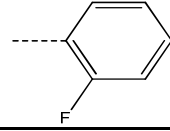
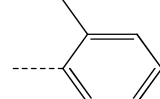
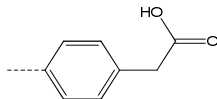
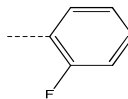
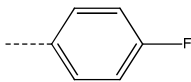
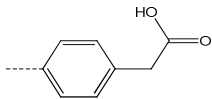
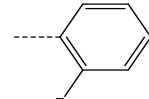
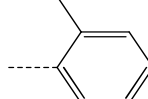
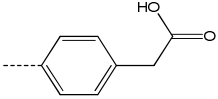
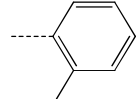
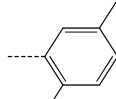
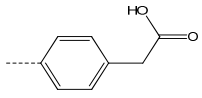
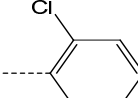
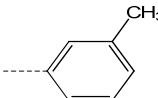
Supplementary Table 2: Substructures by functional groups

Scaffold						
smx	K_D (μM , estimate)	K_D (μM , NMR)	N1 (B)	4-keto (C)	5-aryl (D)	scaffold changes
GA311	690 ± 104					
GA210	752 ± 175					
GA258	760 ± 166					
GA315	260 ± 49					
GA263	417 ± 107					
VPL-26	834 ± 324					

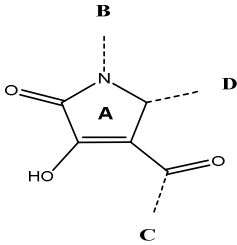
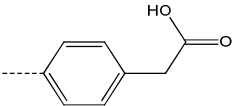
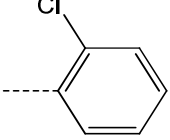
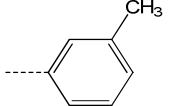
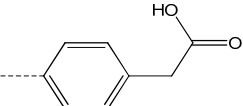
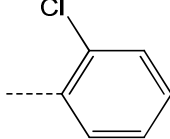
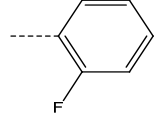
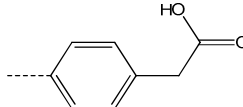
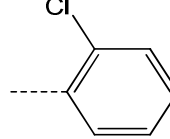
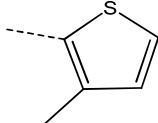
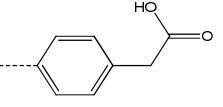
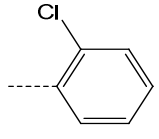
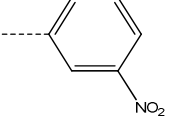
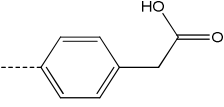
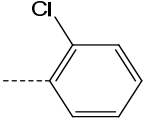
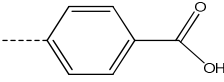
Supplementary Table 2: Substructures by functional groups

Scaffold						
smx	K_D (μM , estimate)	K_D (μM , NMR)	N1 (B)	4-keto (C)	5-aryl (D)	scaffold changes
GA260	988 ± 260					
VPL-21	266 ± 47					
VPL-12	1588 ± 620					
VPL-6	307 ± 51					
GA315	260 ± 49					
GA304	629 ± 98					
GA246	1049 ± 328					

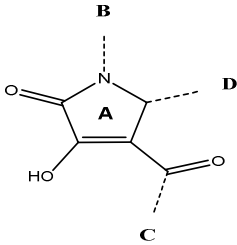
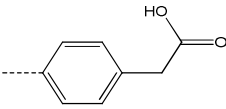
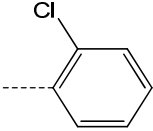
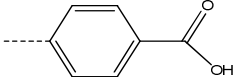
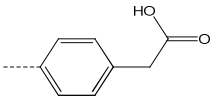
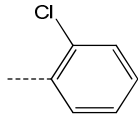
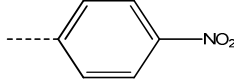
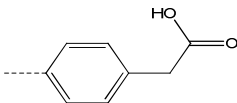
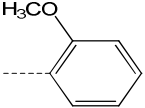
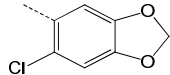
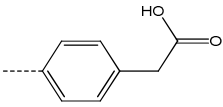
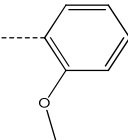
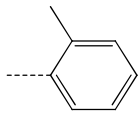
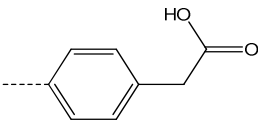
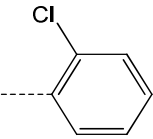
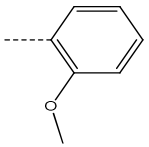
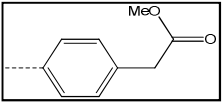
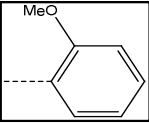
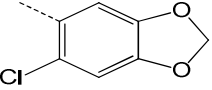
Supplementary Table 2: Substructures by functional groups

Scaffold						
smx	K_D (μM , estimate)	K_D (μM , NMR)	N1 (B)	4-keto (C)	5-aryl (D)	scaffold changes
GA298	1324 ± 402					
GA254=GA310	475 ± 60					
GA267	888 ± 122					
GA252	1472 ± 332					
GA318	1062 ± 49					
GA022	753 ± 74					
GA303	2152 ± 201					

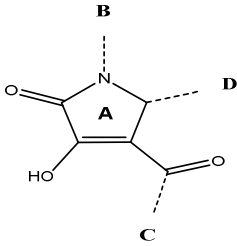
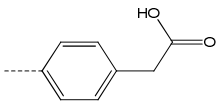
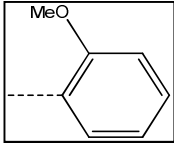
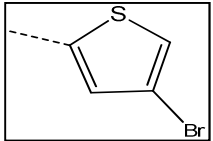
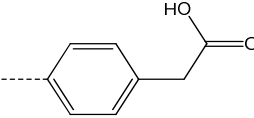
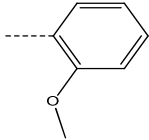
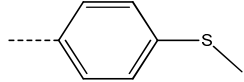
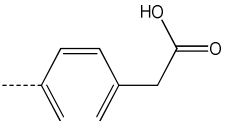
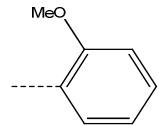
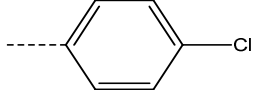
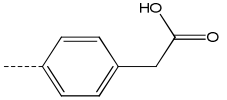
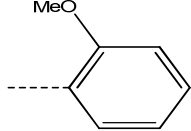
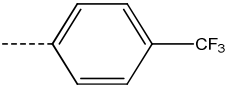
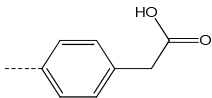
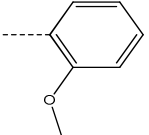
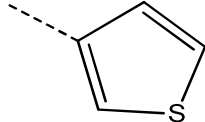
Supplementary Table 2: Substructures by functional groups

Scaffold						
smx	K_D (μM , estimate)	K_D (μM , NMR)	N1 (B)	4-keto (C)	5-aryl (D)	scaffold changes
GA245	2540					
GA236	3060 ± 2222					
GA257	2749 ± 1535					
GA278	4192 ± 1465					
GA220	4501 ± 1785					

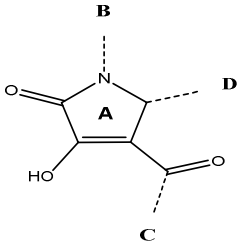
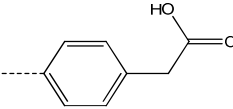
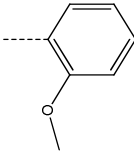
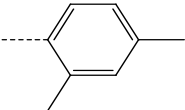
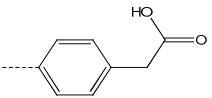
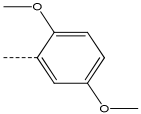
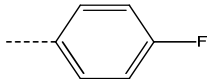
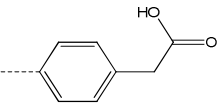
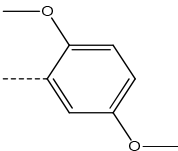
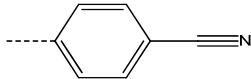
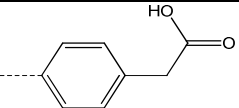
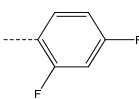
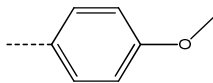
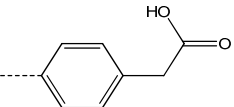
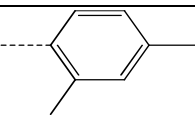
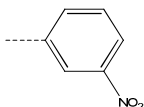
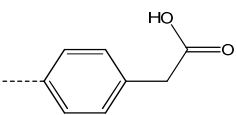
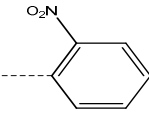
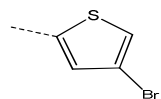
Supplementary Table 2: Substructures by functional groups

Scaffold						
smx	K_D (μM , estimate)	K_D (μM , NMR)	N1 (B)	4-keto (C)	5-aryl (D)	scaffold changes
GA289	4851 ± 3780					
GA277	4860 ± 2405					
VPL-3	361 ± 24					
GA281	4580 ± 1266					
GA323	5477 ± 4894					
VPL-10	1631 ± 1125					cf vpl 3

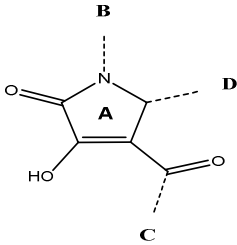
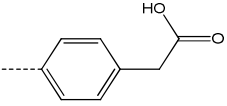
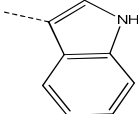
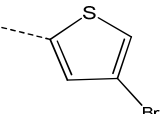
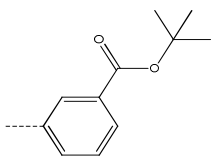
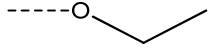
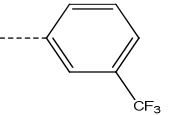
Supplementary Table 2: Substructures by functional groups

Scaffold						
smx	K_D (μM , estimate)	K_D (μM , NMR)	N1 (B)	4-keto (C)	5-aryl (D)	scaffold changes
VPL-15	4044 \pm 1631					
GA021	1283 \pm 138					
VPL-2	3279 \pm 2052					
VPL-18	1537 \pm 514					
GA273	5264 \pm 2274					

Supplementary Table 2: Substructures by functional groups

Scaffold						
smx	K_D (μM , estimate)	K_D (μM , NMR)	N1 (B)	4-keto (C)	5-aryl (D)	scaffold changes
GA279	6340 ± 4469					
GA264=GA316	1256 ± 335					
GA283	5623 ± 5341					
GA313	516 ± 92					
GA019	1177 ± 54					
VPL-16	1436 ± 717					

Supplementary Table 2: Substructures by functional groups

Scaffold						
smx	K_D (μM , estimate)	K_D (μM , NMR)	N1 (B)	4-keto (C)	5-aryl (D)	scaffold changes
VPL-28	458 ± 108					**no carbonyl
VPL-62	-	ND				cf vpl-56